Modelling and optimization of machining processes towards economic and environmental sustainability

Doctoral Dissertation
Doctoral Program in Management, Production and Design (29th Cycle)

Modelling and optimization of machining processes towards economic and environmental sustainability

By

Matteo Robiglio

******

Supervisors:
Prof. Luca Settineri
Dr. Paolo C. Priarone

Doctoral Examination Committee:
Prof. Rosa Di Lorenzo, Referee, University of Palermo (Italy)
Prof. Yusuf Altintas, Referee, University of British Columbia (Canada)
Prof. Luigino Filice, University of Calabria (Italy)
Prof. Pedro Arrazola Arriola, Mondragon Unibertsitatea (Spain)
Prof. Mo Elbestawi, McMaster University (Canada)
Prof. Nikolaos Mikailidis, Aristotle University of Thessaloniki (Greece)

Politecnico di Torino
Discussed in Torino, on the 30th of May, 2017

Declaration

I hereby declare that, the contents and organization of this dissertation constitute my own original work and does not compromise in any way the rights of third parties, including those relating to the security of personal data.

Matteo Robiglio

2017

Author's contact:
Matteo Robiglio
Politecnico di Torino
Department of Management and Production Engineering (DIGEP)
Corso Duca degli Abruzzi 24 - 10129 Torino, Italy
E-mail: matteo_robiglio@polito.it

* This dissertation is presented in partial fulfillment of the requirements for **Ph.D. degree** in the Graduate School of Politecnico di Torino (ScuDo).

I would like to dedicate this thesis to

my parents, Beppe and Grazia,

for making me as I am.

Acknowledgments

First and foremost, I would like to express a special thank to the supervisors of this thesis, Prof. Luca Settineri and Dr. Paolo Claudio Priarone of Politecnico di Torino. My gratitude toward Prof. Luca Settineri is due to his valuable encouragement, advices, and inspirations. Dr. Paolo Claudio Priarone is especially acknowledged for his advice during the thesis preparation and for the numerous technical discussions regarding the research activities.

A significant part of this work was carried out at the National Research Council (CNR), Imamoter, where I had the opportunity to collaborate with Dr. Maria Giulia Faga and Dr. Vincenzo Tebaldo.

A special thanks to my family. Words cannot express how grateful I am to my mother and father for all of the patience paid and sacrifices that you've made on my behalf. Your prayer for me was what sustained me thus far. I would also like to thank all of my friends who supported me in writing, and incented me to strive towards my goal.

The opinions expressed and the conclusions reached in this thesis are only responsibility of the Author.

Abstract

In recent years, the increase in energy demand and carbon emission constraints have forced industry sector to improve the process efficiency with respect to environmental sustainability. Therefore, resource saving has become not only an added value, but a real priority for manufacturing in the Industry 4.0 era. Life-Cycle Assessment (LCA) is a common practice for estimating the environmental impact of products during their life-cycle, and can be used more widely and easily if specific models focusing on each life-cycle phase are available. In this thesis, the manufacturing phase of machined products has been modelled by analyzing different process performance metrics. Both the economic efficiency and the environmental sustainability have been accounted for. The Specific Production Time (SPT) is proposed as indicator of the manufacturing productivity; the Specific Production Cost (SPC) is developed in order to quantify the direct and indirect costs related to the manufacturing process; finally, the Specific Energy Requirement (SER) and the Specific Carbon Emission (SCE) indices are proposed in order to assess the environmental sustainability of the manufacturing phase in terms of primary energy demand and carbon footprint, respectively.

The models have been developed in order to be valid for conventional machining processes in which cutting tools with defined cutting edge are used. The models are also aimed at the identification of optimum process parameters which allow to minimize each specific goal. In particular, optimum tool life values can be computed as a function of the machine tool, the cutting tool, the metalworking fluid, and the workpiece material. As a consequence, optimum process parameters such as cutting speed can be selected with respect to a specific tool life criterion.

The high-efficiency machining range (widely known in literature) has been extended by considering all the four optimal cutting speeds (or tool life values) that minimize each production indicator. Hence, a trade-off criterion is proposed and developed by the introduction of a holistic function which can assign different weights on each optimization target. This advanced optimization method is suggested in order to identify a unique value of cutting speed (or tool life) which can be seen as a compromise among the different criteria of time, cost, and environmental sustainability.

Four case studies have been considered in order to apply the proposed models and are focused on the turning of two titanium-based alloys conventionally used for aerospace applications: a Ti-6Al-4V alloy and a Ti-48Al-2Cr-2Nb intermetallic alloy. A Graziano SAG 101 CNC turning lathe was used in the experiments in order to obtain inventory data to test the models. Various set of process parameters such as depth of cut, feed, and cutting speed have been tested in order to identify the coefficients of the Taylor's tool life equation which plays a key role within the proposed models. Three different cutting tools were used. Finally, four lubrication/cooling conditions were adopted such as dry, wet, Minimum Quantity Lubrication (MQL), and Minimum Quantity Cooling (MQC). Overall, the four case studies are presented in order to assess the influence of (1) process parameters, (2) cutting tool geometries, (3) workpiece materials, and (4) lubrication/cooling conditions onto the machining performance measured by the proposed models.

The wide applicability of the developed models has been proved by the results related to the analyzed case studies. In particular, the results highlighted that the proposed metrics are suitable for a proper selection of machining conditions that enable at the same time resource savings as well as reduced environmental impacts.

Papers related to the Ph.D. research activities

During the preparation of this Ph.D. thesis, some of the results have been published and presented by the Author in national/international journals and conferences. A chronological list of publications and technical presentations (last modified on April 24th, 2017) is given in the following.

Publications

2017 Faga MG, Priarone PC, Robiglio M, Settineri L, Tebaldo V. *Technological and sustainability implications of dry, near-dry, and wet turning of Ti-6Al-4V alloy*. International Journal of Precision Engineering and Manufacturing - Green Technology 4/2 (2017) 129-139.

2016 Priarone PC, Robiglio M, Ingarao G, Settineri L. *Assessment of cost and energy requirements of Electron Beam Melting (EBM) and machining processes*. Proceeding of the 4th International Conference on Sustainable Design and Manufacturing (SDM), Bologna, Italy, 26-28 April 2017. Accepted for publication (December 31st, 2016) in G. Campana et al. (eds.), Sustainable Design and Manufacturing 2017, Smart Innovation, Systems and Technologies 68, Springer International Publishing AG 2017, pp. 723-735, DOI 10.1007/978-3-319-57078-5_65.

2016 Priarone PC, Robiglio M, Settineri L, Tebaldo V. *Modelling of specific energy requirements in machining as a function of tool and lubricoolant usage*. CIRP Annals - Manufacturing Technology 65 (2016) 25-28.

2015 Priarone PC, Robiglio M, Settineri L, Tebaldo V. *Effectiveness of minimizing cutting fluid use when turning difficult-to-cut alloys*. Proceedings of the 22nd CIRP conference on Life Cycle Engineering, Sydney, Australia, 7-9 April 2015. Procedia CIRP 29 (2015) 341-346.

2014 Priarone PC, Robiglio M, Settineri L, Tebaldo V. *Milling and turning of titanium aluminides by using minimum quantity lubrication*. Proceedings of the 5th Machining Innovations Conference (MIC 2014) - New Production Technologies in Aerospace Industry, Garbsen, Germany, 19-20 November 2014. Procedia CIRP 24 (2014) 62-67.

2014 Loglisci G, Robiglio M, Priarone PC, Settineri L. *La sostenibilità di un processo produttivo*. Utensili e Attrezzature (Ed. Tecniche Nuove) Vol. 6 (2014) 18-21.

2014 Loglisci G, Robiglio M, Priarone PC, Settineri L. *Sostenibilità: metodi di analisi e indicatori*. Utensili e Attrezzature (Ed. Tecniche Nuove) Vol. 4 (2014) 16-19.

All the papers published by the Author are cited and referenced in the text and are also listed at the end of the *References* section.

Contents

List of Figures

List of Tables

Nomenclature and abbreviations for the models in Chapter 2

$1/\alpha$; $1/\beta$; $1/\gamma$	exponents in tool-life equation
A	constant in tool-life equation
a_p	depth of cut (mm)
b	specific coefficient of spindle motor (W)
BtF	buy-to-fly ratio
c	specific coefficient of feed motor (W)
C	total production cost (€)
C_1	cost for machine setup (€)
C_2	cost for machining (€)
C_3	cost for tool change (€)
C_4	cost of cutting tool usage (€)
C_5	cost of workpiece material usage (€)
C_6	cost of lubricoolants usage (€)
C_7	cost of cleaning operations (€)
CE	total carbon emission (kg)
CE_1	carbon emission for machine setup (kg)
CE_2	carbon emission for machining (kg)
CE_3	carbon emission for tool change (kg)
CE_4	carbon emission of cutting tool usage (kg)

CE_5	carbon emission of workpiece material usage (kg)
CE_6	carbon emission of lubricoolants usage (kg)
CE_7	carbon emission for swarf and part cleaning (kg)
CES	carbon emission signature (kg/J)
CLF	cooling lubrication fluid
CVD	chemical vapour deposition
D_{avg}	average workpiece diameter (mm)
D_f	final workpiece diameter (mm)
D_i	initial workpiece diameter (mm)
EMCL	emulsion mist cooling lubrication
f	feed (mm/rev)
F_t	tangential cutting force component (N)
h_c	machining cost rate (€/s)
h_c^{MO}	machine operator charge rate (€/s)
h_c^{MT}	machine tool and equipment charge rate (€/s)
k_0	specific cutting energy (J/mm^3)
k_f	specific coefficient of feed motor (W/(mm/min))
k_n	specific coefficient of spindle motor (W/rpm)
k_{SCE}	weighting factor for specific carbon emission
k_{SER}	weighting factor for specific energy requirement
k_{SPC}	weighting factor for specific production cost
k_{SPT}	weighting factor for specific production time
k_t	specific force coefficient (N/mm^2)
LCA	life-cycle assessment

MQC	minimum quantity cooling
MQL	minimum quantity lubrication
MRR	material removal rate (mm^3/s)
n	spindle speed (rpm)
P	total power demand (W)
p; q	exponents in cutting force model
P_{cut}	power demand for material removal (W)
P_{feed}	power demand of feed motor (W)
$P_{lub\ sys}$	power demand of lubrication system (W)
$P_{spindle}$	power demand of spindle motor (W)
$P_{standby}$	power demand of machine tool in standby mode (W)
PVD	physical vapour deposition
q_L	consumption rate of lubricoolant (kg/s)
SCE	specific carbon emission (kg/mm^3)
SER	specific energy requirement (J/mm^3)
SPC	specific production cost (€/mm^3)
SPT	specific production time (s/mm^3)
T	tool-life of a cutting edge (s)
t	total production time (s)
t_1	setup time of machine tool (s)
t_2	actual cutting time (s)
t_3	tool change time (s)
t_4	time for swarf and part cleaning (s)
T_{minSCE}	tool-life for minimum specific carbon emission (s)

T_{minSER}	tool-life for minimum specific energy requirement (s)
T_{minSPC}	tool-life for minimum specific production cost (s)
T_{minSPT}	tool-life for minimum specific production time (s)
$T_{\mathrm{t\text{-}o}}$	tool-life for trade-off criterion (s)
V	volume of material removed at the time t_2 (mm^3)
$v_{\mathrm{c}}^{\mathrm{t\text{-}o}}$	cutting speed for trade-off criterion (m/min)
v_{c}	cutting speed (m/min)
$v_{\mathrm{c}}^{\mathrm{minSCE}}$	cutting speed for minimum specific carbon emission (m/min)
$v_{\mathrm{c}}^{\mathrm{minSER}}$	cutting speed for minimum specific energy requirement (m/min)
$v_{\mathrm{c}}^{\mathrm{minSPC}}$	cutting speed for minimum specific production cost (m/min)
$v_{\mathrm{c}}^{\mathrm{minSPT}}$	cutting speed for minimum specific production time (m/min)
v_{f}	feed rate (mm/min)
V_{P}	volume of the part machined (mm^3)
V_{W}	volume of the workpiece (mm^3)
x_{CL}	cost per volume of material removed for swarf and part cleaning (€/mm^3)
x_{EL}	cost of electricity (€/(W×s))
x_{L}	cost per kilogram of lubricoolant (€/kg)
x_{TE}	cost per cutting edge (€)
x_{W}	cost per volume of workpiece material (€/mm^3)
y_{CL}	primary energy demand per volume of material removed for swarf and part cleaning (J/mm^3)
y_{L}	embodied energy per kilogram of lubricoolant (J/kg)

y_{TE}	embodied energy per cutting edge (J)
y_W	embodied energy per volume of workpiece material (J/mm^3)
z_{CL}	carbon dioxide emission per volume of material removed for swarf and part cleaning (kg/mm^3)
z_L	carbon dioxide emission per kilogram of lubricoolant (kg/kg)
z_{TE}	carbon dioxide emission per cutting edge (kg)
z_W	carbon dioxide emission of per volume of workpiece material (kg/mm^3)
δ_i	*i*-term of the equations of cutting speed and tool life for trade-off criterion (with i = 1, 2, 3, 4)
η	energy conversion coefficient
λ_i	*i*-term of the equations of cutting speed and tool life for trade-off criterion (with i = 1, 2, 3, 4)
τ_{CL}	time per volume of material removed for swarf and part cleaning (s/mm^3)
$\Phi_{t\text{-}o}$	trade-off function

Introduction

The term “Sustainable Manufacturing” is referred to productive processes able to satisfy the current demand for capital and consumer goods by ensuring at the same time the social, environmental, and economic dimensions of human activities. In developed countries, industry is moving towards a fourth stage of industrialization widely defined in literature as Industry 4.0 (e.g., according to Stock and Seliger [2016]). This development of Industry 4.0 is based on the establishment of smart factories, smart products, and smart services achieved through the internet of things and of services applied in the industrial field. The intelligent cross-linked value creation modules introduced by Industry 4.0 can be suited as efficient tools for the allocation of resources in terms of products, materials, energy and water. The holistic resource efficiency approach of Industry 4.0 can be performed by designing appropriate manufacturing process chains or by using new technologies.

The improvement of energy and resource efficiency of manufacturing processes can be carried out at different system levels by means of various methods of analysis and optimization [Duflou et al., 2012]. The unit process level is defined as the smallest unit within a production system, and a typical example is represented by individual machine tools such as lathes, milling centers, grinding machines, etc.

The Life-Cycle Assessment (LCA) is a methodology aimed to study resources consumption, emissions, and their impacts related to the production of goods or the supply of services [Ashby, 2009]. LCA applied in the product manufacture phase takes into account every flow of material, energy and other resource. A full LCA of a product requires to quantify a lot of environmental impacts such as those represented by the Ecopoints, i.e. Land Use, Water Use, Global Warming Potential, Ozone Layer Depletion, Human Toxicity, etc. [Anderson et al., 2009], while the optimization of the manufacturing phase typically involves the minimization of energy requirements and carbon dioxide footprint.

Industry sector was responsible of 30 % on the total annual anthropogenic Green-House Gas (GHG) emissions increase between 2000 and 2010 [IPCC, 2014]. This contribute raises if indirect emissions are taken into account. In

particular, in 2010 industry sector released 21 % of the global GHG emissions and this share is increased to 31 % if emissions from electricity and heat production (i.e., indirect emissions) related to industry demand are included in the estimation.

The reduction of environmental impact of the manufacturing stage should start at the design stage because the majority of the financial and environmental cost of a product is influenced by the decision taken into account during this early stage [Seow et al., 2016]. The design and manufacturing of a product can be developed by identifying where and how energy is effectively used during production. Energy simulation models at the design phase together with empirical and analytical models for the manufacturing phase can be effective tools in order to promote the sustainability of the entire productive process.

Modeling of energy consumption at the machine tool level is the prerequisite for energy-saving in manufacturing. Several models and some comprehensive reviews have been presented in literature to date [Zhou et al., 2016; Moradnazhad and Unver, 2016]. However, the development and comparison of these models still need to be promoted. The estimation of environmental impact related to traditional manufacturing processes, such as machining or forming technologies, requires more attention especially nowadays when additive manufacturing technology is rapidly expanding in industrial sector. In addition, the integration between traditional and additive processes has to be accounted for since performance highlighted by hybrid manufacturing are noticeable [Priarone et al., 2017].

Based on the scenario previously presented, the research activities reported and discussed in the thesis are aimed to the modelling of machining processes in terms of environmental impact (i.e., energy demand and carbon footprint), productivity, and cost. The proposed models are tuned for general cutting operations such as turning, milling, and drilling processes. Moreover, models are deeply focused on the impact of auxiliary equipment (e.g., cooling/lubrication systems) and consumables (e.g., cutting tools and lubricoolants) which are expected to affect the production strategy. The main objects of the present work are to provide indicators of the manufacturing process in order to (I) estimate its time, cost, and environmental impacts, and to (II) select the process parameters which allow to maximize the economic and environmental sustainability. The developed strategy for the minimization of the environmental impact is compared to other strategies such as those for minimizing production time and production cost. In addition, a trade-off criterion is proposed for a rapid and unique

identification of optimum process parameters that allow to achieve a compromise between economic and environmental sustainability targets.

Chapter 1 provides an overview on the sustainable manufacturing and development concepts. The methodology of the Life-Cycle Assessment is briefly presented focusing the attention on its application in the manufacturing sector. A state of the art related to the modelling of machining processes is given with respect to existing models of both economic and environmental sustainability.

The development of four specific models for assessing of machining processes is presented in Chapter 2. The models are referred to (1) production time, (2) production cost, (3) primary energy demand, and (4) carbon dioxide emission. The identification of optimum tool life or process parameters (e.g., cutting speed) are provided by means of analytical and/or empirical approaches. Moreover, an innovative criterion of trade-off between the different goals of efficiency is developed and discussed.

The models are applied to four case studies with the aim of testing the influence of (1) process parameters, (2) tool geometries, (3) workpiece materials, and (4) lubrication/cooling conditions on the economic and environmental sustainability of the manufacturing process. The inventory data is described in Chapter 3 while the discussion of the results is given in Chapter 4.

Chapter 3 includes all the inventory data of time, cost, primary energy demand, and carbon dioxide emission related to each process, equipment and consumable used in the machining scenarios assumed for the case studies. A characterization of the power requirements of a specific machine tool (a turning lathe) has been carefully performed. The cost and environmental impacts of the different cutting tools used as well as the applied lubricoolants are quantified and collected. Workpiece materials such as a titanium aluminide (γ-TiAl) and a conventional titanium alloy (Ti-6Al-4V) are described in terms of their environmental impact during the production phases as well as their purchase cost. Costs and environmental impact due to electricity consumption are analyzed with respect to the specific values characteristic of the Italian grid. Machining cost

rates are quantified according to the specific auxiliary apparatus accounted for when machining.

Lastly, Chapter 4 presents the application of the proposed models on the four selected case studies. Since the results can be influenced by the interaction of several variables (i.e., cutting tools, workpiece materials, lubrication/cooling conditions, and process parameters), each case study is focused only onto the influence of a specific factor. The first case study refers to the influence of process parameters such as cutting speed, feed, and depth of cut on the dry turning of γ-TiAl with a RCMT 0803 cutting tool. The second case study is focused on the comparison of two tool geometries (RCMT 0803 and RCMT 1204) when dry turning of the γ-TiAl intermetallic alloy at varying of cutting speed. The comparison of the machinability performance related to the two workpiece materials (γ-TiAl and Ti-6Al-4V) is presented in the third case study in which a RCMT 1204 cutting tool is used under dry condition for several cutting speeds. The four case study is based on the assessment of four lubrication/cooling conditions namely dry, wet, Minimum Quantity Lubrication (MQL), and Emulsion Mist Cooling Lubrication (EMCL) when turning of Ti-6Al-4V with a RCMT 1204 cutting tool at varying of cutting speed.

The conclusions and outlook section summarizes the whole activity performed in the thesis. Overall, compared to the existing literature, the main outcomes of the research activities presented in the following include the development of specific models of machining processes. The models are structured taking into account a comprehensive approach and are oriented towards a multi-object optimization of the manufacturing process. For these purposes, the models are aimed (I) at quantifying economic and environmental indicators, as well as (II) at the identification of optimized process parameters which allow to satisfy economic and environmental targets. The proposed models are tuned for a general application among material removal process, in which different workpiece materials, machine tools, cutting tools, and metalworking fluids can be used. The application of these models on case studies is based on data collected from experimental activities which enabled and supported the high level of exploitability of such models. As a results, optimization conditions are identified for all the case studies accounted for.

Chapter 1

Sustainable development in Industry 4.0

Industrial revolutions influenced manufacturing enterprises by the introduction of new methods or equipment in order to promote their productivity. The first industrial revolution, which is known as Industry 1.0, refers to a period between 1800 and 1913 that was marked by the use of steam in industrial equipment utilized for manufacturing [Garbie, 2016]. The second industrial revolution (Industry 2.0) is comprised between 1913 and 1970, and was characterized by the development of 'mass production' systems, which were supported by the usage of internal combustion engines and electrical devices. Industry 3.0 was born with the introduction of computers which were the responsible of the third industrial revolutions started in 1970 and endured until 2010. The last industrial revolution (Industry 4.0), recently theorized, have appeared in the last ten years and is characterized by the incorporation of previous advantages introduced by Industries 1.0, 2.0, and 3.0 in smart systems with new notions regarding sustainability. This step forward in industry practices is facilitated by the use of information and communication technologies such as the Internet of Things, Cyber-Physical Systems, and Embedded Systems, which are entered in factories [Gabriel and Pessl, 2016]. Costs and boosting performance are reduced by the rapid advances in underlying technologies that are making knowledge automation more attractive. Computing power is growing exponentially and this can be traced back to the advances provided by data storage systems, big data, and cloud computing [Manyika et al., 2013].

In 2013, the McKinsey Global Institute published a report in which it has been highlighted that economically disruptive technologies, such as 3D Printing, Internet of Things, Mobile Internet, etc., can transform the way we live and work, enabling new business models, and providing an opening for new players to upset the established order [Manyika et al., 2013]. Potentially disruptive technologies should be identified by business leaders and policy makers in order to carefully consider their potential in advance and to prevent their disruptive powers in the economy and society.

Sustainability or sustainable development is conventionally accepted as encompassing the social, economic, and ecological aspects of decision making [Sutherland et al., 2016]. Moreover, sustainability can be defined as a way for improving the quality of life and well-being for present and future generations. Manufacturing enterprises can achieve sustainability by means of a holistic approach that spans the entire supply chain by the inclusion of manufacturing systems across multiple product life cycles [Garbie, 2016]. The three pillars of sustainable manufacturing [Dornfeld, 2013], which addresses impacts on the environment, on the economy, and on the society, have to be merged with the three dimensions (smart, safe and sustainable) of future industrial systems, as recently outlined by Trentesaux et al. [2016] for emerging Information and Communication Technology (ICT) solutions.

The creation of social value, quality of life, wellbeing of the workers and preserving the diversity of the planet are allowed by means of eco-efficiency and eco-effectiveness in material, energy and other resources [Álvarez et al., 2016]. The tasks associated to the development and improvement of the manufacturing technologies should be developed in every life-cycle phase: (1) design, (2) modelling simulation, (3) optimization, and (4) assessment. In order to achieve the environmental sustainability of manufacturing processes, specific metrics must be implemented for quantifying the costs and impacts of existing process strategies. The usage of these designed metrics such that provided by a Life-Cycle Assessment (LCA) can lead to the improvement and optimization of machining processes.

1.1 Life-Cycle Assessment (LCA) approach

In recent years, a growing interest related to environmental protection has been paid by researchers, policy makers, and industry. The Life-Cycle Assessment (LCA) represents one of the techniques used for the identification and quantification of environmental impacts associated with products (in terms of goods or service), both manufactured and consumed. The requirements for conducting an LCA are reported in ISO 14040:2006 (principles and framework) and ISO 14044:2006 (requirements and guidelines).

Every environmental impacts caused by the usage of resources during the entire product's life-cycle (from raw material acquisition through production, use, end-of-life treatment, recycling, and final disposal) are considered in cradle-to-grave life-cycle assessments. An LCA study is composed by four phases such as (1) goal and scope definition, (2) inventory analysis, (3) impact assessment, and (4) interpretation.

The scope definition (1) is focused on the identification of the system boundary and level of detail related to the specific study analyzed. Moreover, the goal of an LCA influences the depth and the breadth of the activity. The Life-Cycle Inventory (LCI) is performed during the inventory analysis phase (2) in which all the input/output data with regard to the system are collected in order to meet the goals of the defined study. The Life-Cycle Impact Assessment (LCIA) phase (3) is aimed to provide additional information in order to assess the environmental significance of a product with respect to LCI results. Finally, the interpretation phase (4) summarizes and discusses results from LCI and/or LCIA phases in order to draw the conclusions, recommendations, and decision-making according to the goal and scope definition.

LCA studies can be conducted by excluding the LCIA phase and in this case they are identified as LCI studies. In addition, the life-cycle approach and methodologies can be suited to assess other aspects of a product. Therefore, Social Life-Cycle Assessment (SLCA) and Life-Cycle Cost (LCC) can be identified as tools for addressing social or economic aspects, respectively [Sala et al., 2015].

The life-cycle of a product can be summarized in four main phases (Figure 1): (1) material production, (2) product manufacture, (3) product use, and (4) product disposal. During the first phase, the material is yielded by mining and processing of ore and feedstock.

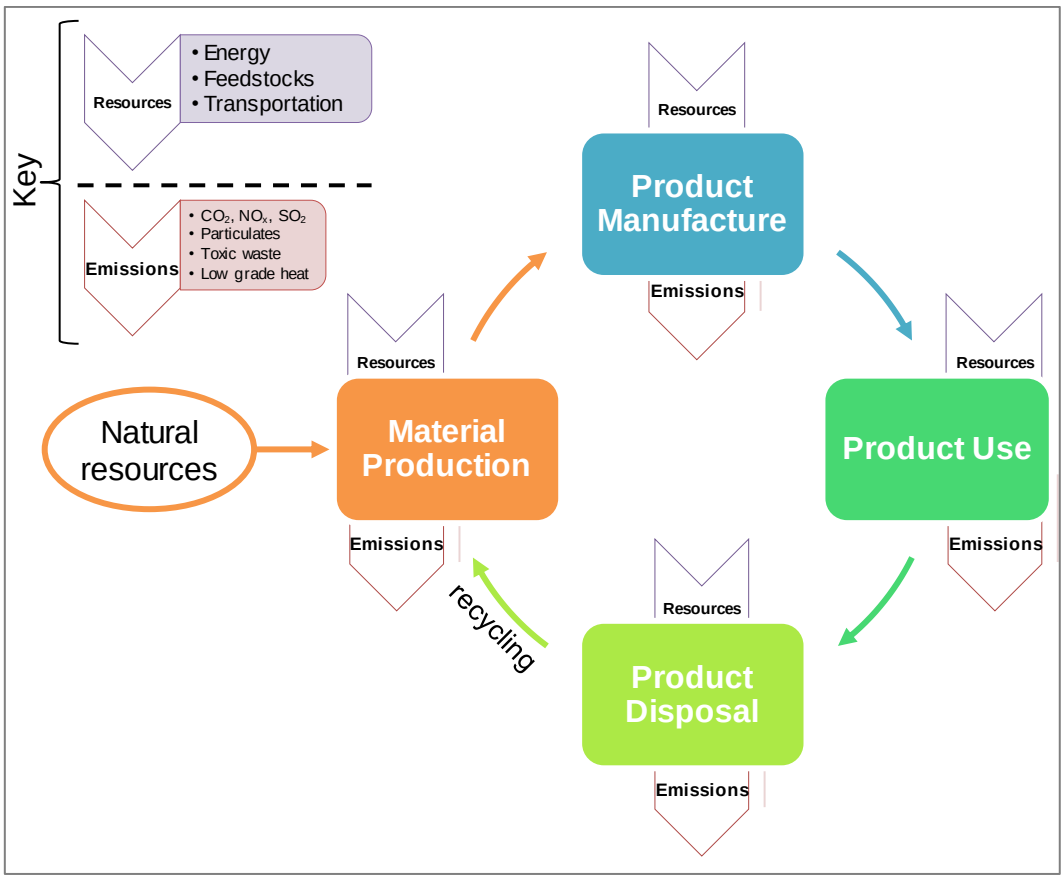

Figure 1. Scheme of material life-cycle (adapted from [Ashby, 2013]).

Then, the final product is obtained by means of the manufacturing phase. After the use phase, the product reaches the end of its life and, consequently, the product disposal can be performed through landfilling, recycling, or refurbishing and reusing operations. Each phase consumes energy and materials as well as generates waste heat and solid, liquid, and gaseous emissions.

The approach proper of the Sustainable Manufacturing is focused on the innovation-based 6R methodology that merges the principles of the Green Manufacturing (3R - Reduce, Reuse and Recycle) with a broader goal concerning the Recover, Redesign, and Remanufacture of products over multiple life-cycles [Jayal et al., 2010].

Intermediate point between two subsequent phases can be identified as "gates" through which inputs pass and outputs emerge. If the scope of an LCA is

limited only to a specific phase of product life-cycle, that LCA is defined as a gate-to-gate study. Such type of study becomes essential when the total resources consumption and emissions during the life-cycle of a product are dominated by a single phase. For example, a part that is manufactured through a material removal process can require more resources (and, consequently, can cause more emissions) during the material production phase with respect to other phases [Aurich et al., 2013]. In addition, components which are installed in an airplane can save more fuels if they are made by additive manufacturing with topology optimization method (in order to reduce the product weight) with respect to the same component made by traditional manufacturing [Tang et al., 2016]. As a consequence, the use phase of this kind of product is the most important during its life-cycle.

1.2 LCA applied in Manufacturing

In this study a cradle-to-gate approach is selected due to the wide interest in the optimization of the product manufacturing phase aimed to the reduction of resources and emissions. The main optimization that industry sector can provide on the life-cycle of a product is related to the sustainable selection of machining processes [Loglisci et al., 2014a-b]. This goal can be achieved through the minimization of resources demand such as energy, metalworking fluids, cutting tools, and other consumables. System boundary 1 (Figure 2) represents the broadest goal when assessing the resource consumption and emissions of a product during its whole life. On the other hand, system boundary 3, which is the most applied in literature concerning LCA of machining, can be suited to consider only the product manufacturing. However, manufacturing processes can be characterized by the production of material scrap, swarf and chips, as a consequence, the consumption of material has to be included also for the environmental assessment of this phase. Therefore, system boundary 2 is selected in this study in order to consider either the material production stage or the product manufacture phase. In addition, the optimization of the production process is assumed to be independent on the application and the disposal of the manufactured product.

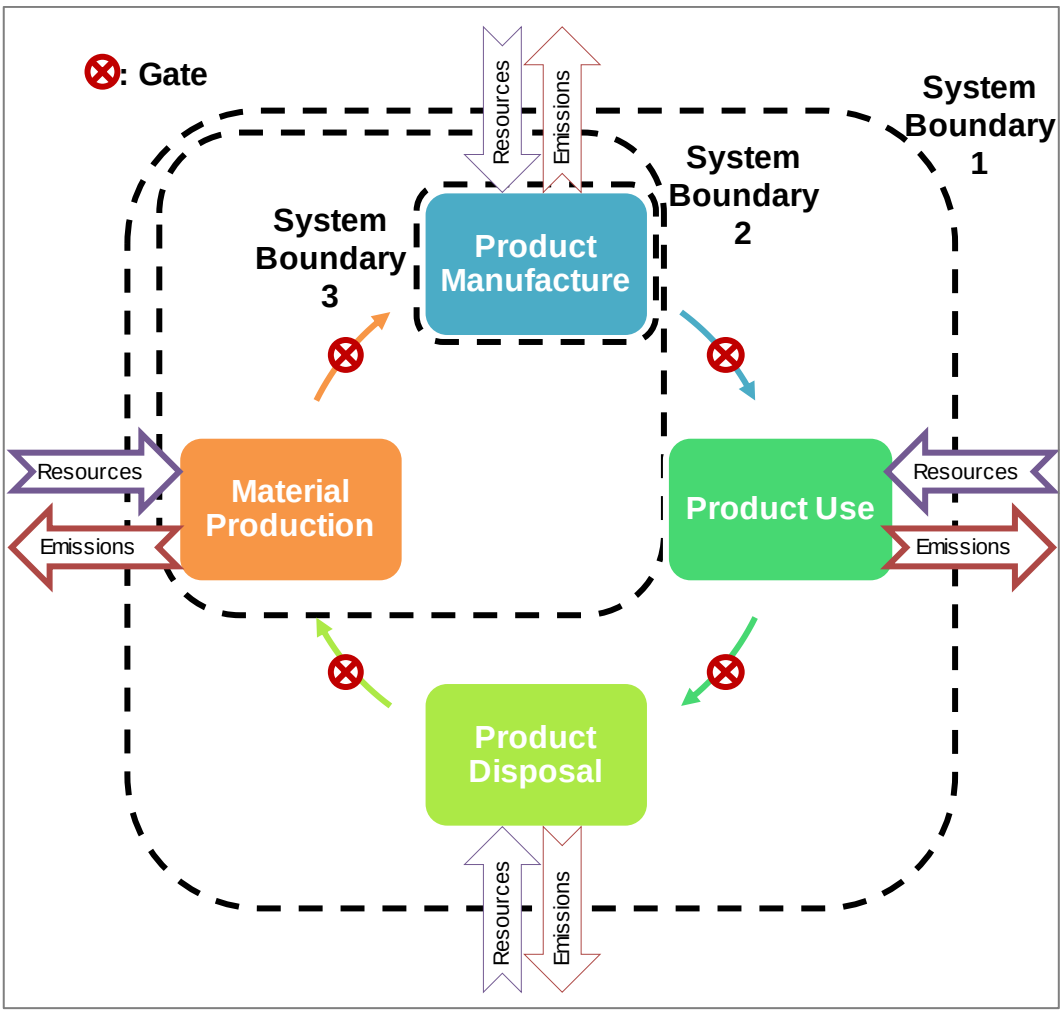

Figure 2. Definition of system boundary (adapted from [Ashby, 2013]).

Dahmus and Gutowski [2004] proposed an analysis of machining by the point of view of environmental sustainability as shown in Figure 3. Their analysis examined qualitatively every processes and all flows shown in dark text, which are included in the shaded region (system boundary) enclosed with a dark dashed line. Others processes and flows shown in grey, which are not included in the shaded region, were examined only to provide an approximate estimation of their environmental impact. Nevertheless, in this thesis all the processes and flows related to the phases of material production and product manufacture are included in the adopted system boundary, as previously discussed. Therefore, Figure 3 presents the flows of resources, energy, and CO_2 (in orange text) in addition to those taken into account by Dahmus and Gutowski [2004].

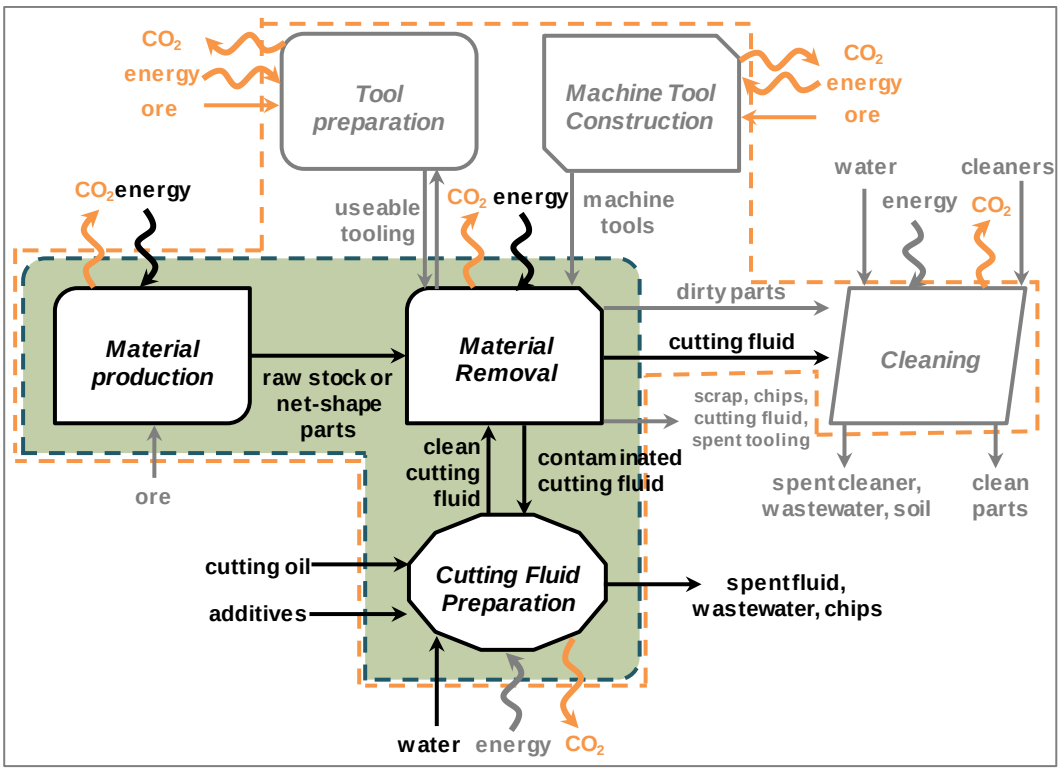

Figure 3. Example of system diagram of machining (adapted from [Dahmus and Gutowski, 2004]).

A material removal process is responsible of most of the environmental impact due to electrical energy use. Dahmus and Gutowski [2004] defined the 'Energy Breakdown' of the total energy consumption of a machine tool as the sum of three contributes which represent various activities performed during the machine use phase. The first contribute is constant and is due to start-up operations such as the energy requirements for computers, fans, and unloaded motors. The second contribute is fixed and is owing to run-time operations which include energy demand to positioning materials and loading tools. Finally, the third contribute is due to material removal operations and refers to the actual energy when cutting (due to the contact between tool and workpiece). Four different machine tools (a production machining center, two automated milling machines, and a manual milling machine) were analyzed and the results highlighted that the material removal can vary from 11.3 to 69.4 % of the total energy demand depending on the machine tool type.

Material production (workpiece) represents a relevant contribute on the product life-cycle: the energy demand for material production could be one order of magnitude higher than the energy requirements of machining. This is due to energy- and resource-intensive processes for the production of metals. For example, titanium requires between 600 and 740 MJ/kg of primary energy when is produced from virgin sources [Ashby, 2013]. Machining is responsible of chips and scrap production which can be estimated in range from 10 % to 60 % [Dahmus and Gutowski, 2004]. Even if chips and scraps can be recycled, a higher amount of pure material is used for machining process with respect to that required for mass conserving or additive processes.

Cutting fluids are often used in machining and are responsible of health issues and environmental impact [Dahmus and Gutowski, 2004]. The presence of mineral oils, emulsifiers, and additives is not the best choice towards sustainable manufacturing although they provide advantages from a technologic point of view. Vegetable oils can replace conventional metalworking fluids even though their embodied energy was quantified to be similar [McManus et al., 2003]. In addition, the disposal of a spent metalworking fluid nowadays requires costs, which are approximately equal to the cost for the replacement of the fluid itself [Dahmus and Gutowski, 2004].

In machining, the environmental impact of a cutting tool can vary considerably depending on the specific cutting process, workpiece, and tool materials. Tool performance is shown in terms of allowable cutting speeds at which the process can be executed and in terms of durability. These features play a key role in machining because the material removal rate is influenced by the level of allowable process parameters, while the tool change replacements are influenced by the tool life. Nowadays, carbide tools are profusely used in most metal cutting operations. The production of carbide tools requires the usage of some energy-intensive materials and processes. Carbide cutters are mainly made of tungsten, which has an embodied energy of approximately 400 MJ/kg [Dahmus and Gutowski, 2004]. In addition, other manufacturing steps such as sintering and coating are involved during the production and of carbide cutters and have been estimated as quite energy intensive processes. The influence of cutting tool material can significantly affect the productivity. For example, High-Speed Steel and Polycrystalline Diamond tool are also used in machining and they show drastic differences in material removal rate. Lower machining energy requirements per unit volume of material removed can be achieved at higher material removal rates. This advantage can be suited in roughing operations in

which the part geometries and surface finish requirements are less important than those for finish machining. The environmental footprint of tools and tool maintenance/cost have to be considered for the specific case of metal cutting operation: when machining soft materials, a tool is typically amortized over numerous products. By contrast, when cutting difficult-to-machine materials the relative low tool life and allowable material removal rate determine a higher influence of tooling during the manufacture of a product.

The impact of machine tool construction has a relative low contribute on the environmental footprint [Dahmus and Gutowski, 2004], while plays a key role when accounting productive costs. Most of literature revealed that the environmental impact due to the consumption of electrical energy during the use stage of a machine tool is in the range between 60 % and 95 % of the total environmental impact [Kellens, 2013]. However, these values are deeply influenced by the intensity of use and the functional life span taken into account for a machine tool. In other words, the long lifetimes of machine tools allow to amortize the environmental impact caused by their construction over numerous products over many years. According to Dahmus and Gutowski [2004], the environmental impact due to the machine tool construction can be overlooked when considering the production of a single final part.

Diaz et al. [2010] performed a life-cycle analysis of machine tools taking into account energy and carbon emission due to manufacturing, transportation, and use phases. They showed that the manufacturing portion of the machine tool is strictly related with the manufacturing facility in which the machine tool is used. The authors analyzed two case study of life-cycle energy assessment performed on two different machine tools. The energies required to manufacture the low- and the high-automation machine tool were 18,000 MJ and 100,000 MJ, respectively. Since the use phase dominates the total environmental impact of the machine tools, the carbon emissions related to the manufacturing phase was estimated to vary between 10 % and 30 % for the low automation type, and between 15 % and 40 % for the high automation type.

Cao et al. [2012] estimated the life-cycle carbon emissions of two gear-hobbing machines and showed that the manufacturing phase (related to material extraction and component preparation) represents only 2.8-4.2 % of the total carbon emission computed for the life-cycle of the machine tools.

Azkarate et al. [2011] performed a life-cycle cost and a life-cycle assessment in order to support the design of sustainable machine tools. They quantified the environmental impact of a milling machine during its life in terms of consumption of electricity, materials, lubricants and working fluids, and transportation. Materials were estimated to determine 25.6 % of the total environmental impact. The same machine tool was analyzed by Gonzalez [2007] who evaluated the impact of production phase around 5 % of the overall environmental impact. Material consumption (around 40 tons in total) has been considered for the production stage, while production processes are not considered since their contribute was assumed to be relatively little. The functional unit was 15 years of work or 60,000 hours. The difference between the study of Azkarate et al. [2011] and that of Gonzalez [2007] is due to the different software used for the life-cycle assessment and the different boundaries accounted for.

A full LCA was performed by Santos et al. [2011] on an all-hydraulic press-brake and the results revealed comparable contributions of the machine-tool structure (40 %) and the electricity consumption during its use (46 %) to the global environmental impact of the equipment. The reduced contribute of the use phase (with respect to previous authors) is due to the energy consumption for the discrete loading character of the bending process, which is not relevant as that of conventional machine tool (e.g., for cutting).

By contrast, when considering productive costs, the cost rate owing to machine tool amortization (excluding the operator) is greater than the cost rate for electricity during the use phase of the machine. Overall, the system boundaries adopted in this thesis take into account the construction of the machine tool only when cost analysis is computed.

Cleaning operations are needed when the machining process is performed with the usage of metalworking fluids especially when the final product has to be finished with additional treatments such as paintings or other coatings [Dahmus and Gutowski, 2004]. A general qualitative analysis of cleaning processes is difficult due to the highly diversified cleaning landscape (single or multiple cleaning steps), both in terms of amount and type of cleaning. Over the years the cleaning methods typically used have been changed. For example, aqueous cleaners have replaced solvent and chemicals cleaners, which were profusely used in metal cleaning up to the early 1990's. In addition to the cleaning of the workpiece, the chips produced have to be centrifugally separated from the

metalworking fluid and drained before the compaction phase needed to facilitate their transportation [Pusavec et al., 2010b].

Overall, since the modelling section (Chapter 2) concerns machining processes, the selected system boundary has to include all the activities previously presented such as material production, material removal, tool preparation, machine tool construction, and cleaning.

1.3 A state-of-the-art in modelling of machining processes

In order to perform an LCA study, the inventory phase is realized by direct measuring of data or by the usage of models able to define a quantitative and qualitative estimation of the variable observed. Machining models were conventionally aimed at the estimation of production time and production cost. Recently, modelling of direct and indirect energy requirements of machining process have been implemented for the assessment of energy demand or environmental stress. Modelling can represent an effective method for obtaining data for LCA especially when are correlated to the variation of process parameters.

The main process parameter considered in machining is the Material Removal Rate (MRR), which defines the performance of a process in terms of average material removal on a workpiece in unit time. The MRR in machining is computed by the product of other variables such as cutting speed, feed rate, depth of cut, tool diameter, etc., depending on the specific machining process taken into account.

In general, modelling of machining processes can be performed by analytical, numerical, empirical, Artificial Intelligence (AI) based, and hybrid modelling techniques [Arrazola et al., 2013]. These models are focused on the prediction of fundamental variables such as stresses, strains, strain-rates, temperatures, etc. Moreover, the knowledge of these fundamental variables can be suited to correlate performance measures such as product quality (accuracy, dimensional tolerances, finish, etc.), surface and subsurface integrity, tool-wear, chip-form/breakability, burr formation, machine stability, etc.

Cost- and productivity-based models are part of the industrial cultural background, therefore a brief overview of these conventional models is presented

in the following paragraphs. Modelling of environmental impact is mainly based on the estimation of direct and indirect energy requirements, or carbon emission. Direct energy requirements concern the electricity consumption of machine tools during their usage [Balogun and Mativenga, 2013]. The indirect energy requirements deal with the usage of consumables such as cutting tools, metalworking fluids and other auxiliary materials [Li et al., 2015]. Overall, a wider review of models concerning the environmental impact assessment of machining is given even if these models have not been fully established yet.

The models presented in the following pages are reported maintaining the nomenclature chosen by the respective author(s). Hence, the nomenclature and abbreviations selected for this thesis is used only for the description of the proposed models, which are included in Chapter 2.

1.3.1 Productivity models

It is known from literature [Kalpakjian and Schmid, 2006; Childs et al., 2000] that the time required to produce one part by using machining operation such as turning, milling, etc., is composed by the following steps: (1) the non-productive time due to loading/unloading the workpiece and to setup the machine tool; (2) the machining time (per piece or per operation); (3) the time required to change or index the insert when its edge is worn out. Non-productive time is generally constant and does not vary for different process rates. Machining time and tool change time are the main factors and they can vary as a function of process rate. Opposite behaviors of these contributes are commonly observed at higher process rate since machining time decreases, whereas the tool change time increases. Tool change time is required every time that a tool reaches its end of life and it can be predicted by using the Taylor's tool life equation and by knowing the process parameters adopted. An increased process rate can be achieved adopting higher cutting speed but this leads to a reduced tool life as determined by the Taylor's tool life equation. Tool change time is more dominant compared to machining, therefore the overall cost increases in terms of process rate. Nevertheless, the process rate value that satisfies the minimum productive time criteria can be identified.

Eskicioğlu A.M. and Eskicioğlu H. [1992] proposed a unit production time model as the sum of five contributes: (1) process adjusting and quick return time, (2) loading and unloading time, (3) set-up time for jigs, fixtures, etc., (4)

machining time, and (5) tool change time. In particular, this model is based on a non-linear mathematical functions and is subject to non-linear constraints. Therefore, three numerical methods were used for solving the optimization problem in order to determine optimal machining condition with respect to the production time target.

Calvanese et al. [2013] estimated the total time required to manufacture a component as basically composed by three contributions: the time due to the workpiece and machine tool setup, the machining time, and the overall time to execute the tool changes. Tool change time includes rapid axis motion time, tool workpiece approach time, and the overall tool replacement time.

Overall, the factors that are most important to keep and estimate accurately in production time models are the machining time and the tool change time. The time for workpiece and machine tool setup is typically assumed to be fixed and cannot be easily optimized. The time for tool rapid movements can be assumed as negligible compared to the machining time. In literature models which take into account a time for post processing operations, such as the time for part and swarf cleaning, still lack. For this reason, a specific time contribute for post processing operations should be included in a production time model.

1.3.2 Production cost models

Generally, direct manufacturing cost comprises various contributions such as workpiece material cost, energy cost, and tool cost. Energy and tool costs are the main factors and can vary as a function of process rate. Energy costs represent 17 % of the total cost of ownership for a production machine while an additional 5 % is due to the costs of compressed air [Yoon et al., 2015]. Since machine purchase costs, maintenance costs, capital commitment cost and space cost are fixed, it is clear that energy efficiency is the only viable solution to reduce total productive cost and, at the same time, to reduce environmental impact.

A productive cost model typically shows a behavior similar to that of a productive time model since the correlation between these two models is obvious. As a consequence, the process rate value that satisfies the minimum cost criteria can be identified. Typically, the optimum process parameters are selected by considering a compromise between productive time and manufacturing cost. The

range between the two criterions is known as the high-efficiency machining range [Kalpakjian and Schmid, 2006]. Some cost models are presented in the following.

In the manufacturing cost model (Equation 1.1) developed by Yoon et al. [2013] the peripheral cost related to cooling and chip inhalation systems has been introduced in addition to the costs for electrical energy consumption and costs for cutting tools usage. Peripheral costs are fixed since they do not vary in function of the process rate selected. The authors computed the optimum process parameters for minimum manufacturing cost (C_{TOTAL}) by means of numerical methods based on empirical data.

$$C_{TOTAL} = C_{TOOL} + C_{ENERGY} + C_{PERIPHERAL} \tag{1.1}$$

In the cost model (Equation 1.2) proposed by Rajemi et al. [2010] the machine cost rate (x) has been introduced in order to include the cost of ownership of the machine tool amortized over its depreciation period. The cost model is made of four contributions such as nonproductive cost (due to machine setup time t_1), actual cutting cost (due to chip removal during time t_2), cost for tool change operation (due to tool change time t_3), and the cost for tooling (y_c). The ratio t_2/T represents the number of cutting tool (edge) and/or tool replacements needed when using a tool having the tool life T. The cost for workpiece material was neglected by the authors since it is independent by process parameters.

$$C = x \cdot \left(t_1 + t_2 + t_3 \cdot \frac{t_2}{T} \right) + y_c \cdot \frac{t_2}{T} \tag{1.2}$$

Pusavec et al. [2010b] estimated the cost per part production (C_{p}, Equation 1.3) as the sum of machining cost (C_{m}), cutting tool cost (C_{t}), lubricoolant fluid cost (C_{CLF}), electrical usage cost (C_{E}), and cost for part and swarf cleaning and/or preparation (C_{cl}). This approach is particular useful for the comparison of processes performed under different lubrication conditions due to the considerations about metalworking fluid usage.

$$C_p = C_m + C_t + C_{CLF} + C_E + C_{cl} \tag{1.3}$$

Manufacturing cost can be deeply influenced by the variation of the required tolerances on the final part produced [Schultheiss et al., 2015]. Appropriate cutting conditions for assuring a specific surface roughness have to be taken into account and, as a consequence, the corresponding cycle time and part cost can be

calculated under this quality constraint. The imposition of a desired surface roughness target directly influences the cycle time and the tool cost during a common turning operation, even when assuming any variation of the workpiece scrap rate. The manufacturing model (k) used by the authors is reported in Equation 1.4 where k_{CP} is the hourly cost of machines during production, k_{CS} is the hourly cost of machines during downtime, k_D is the hourly operator salary, k_t is the cost per cutting edge, q_P is the production rate loss, q_Q is the scrape rate, q_S is the downtime rate, T is the tool life, t_{rem} is the cycle time, and t_i is the tool change time. In the case study analyzed by the authors an increase of the part cost by roughly 20 % was highlighted when the average surface roughness was required to vary from 3.2 μm to 1.6 μm.

$$k = k_t \cdot \frac{t_i}{T} + k_B \cdot \left(\frac{-q_Q}{1-q_Q} \right) + \left[k_{CP} + \frac{1}{1-q_S} \cdot \left(k_{CS} \cdot q_S + k_D \right) \right] \cdot \left[\frac{t_i + t_{rem}}{(1-q_Q) \cdot (1-q_P) \cdot 60} \right] \quad (1.4)$$

Anderberg et al. [2009] proposed a machining cost model composed by traditional and non-traditional cost components (Equation 1.5). Traditional cost components concern several contributes such as machine tool and labour cost (C_m), set-up cost (C_s), idle cost (C_I), direct tool cost (C_T), indirect tool cost - tool change cost (C_c). On the other hand, non-traditional cost components account for direct (C_{ED}) and indirect (C_{EID}) costs due to energy consumption (during cutting and non-cutting time, respectively), and carbon dioxide emission (cap and trade) cost (C_{CO2}). These non-traditional cost components related to energy consumption were found to represent a very small part of the total cost even for different material removal rates. In particular, they contributed to less than one per cent of the total machining cost when accounting for the case characterized by the largest energy cost proportion. The electrical energy cost constitutes a large expenditure for a company only on a larger scale. Consequently, considerable savings can be achieved in real terms when promoting more energy efficient machining strategies.

$$C_p = \overbrace{C_m + C_I + C_s + C_c + C_T}^{\text{Traditional cost components}} + \overbrace{C_{ED} + C_{CO2} + C_{EID}}^{\text{Non-trad. cost comp.}} \quad (1.5)$$

Overall, the most important factors to keep and estimate accurately in production cost models are the machining cost (due to machine tool charge rate) and the costs for tool replacement (due to the tool change operation and the cost for tool itself). The cost due to workpiece material production has to be included

in a production cost model if a system boundary as that presented in Figure 2 (i.e., System Boundary 2) is taken into account. The cost for the usage of cooling lubrication fluids needs to be accounted for as highlighted by the cost model of Equation 1.3. However, in case of MQCL systems, which need compressed air as carrier gas, the indirect power demand for the air compressor is usually neglected in cost models presented in literature. Hence, the taking into account of such contribute can represent a possible area of improvement when proposing a new cost model able to quantify a real productive cost. In addition, the cost for a post processing operation such as the part and swarf cleaning should be accounted for due to the presence of lubricoolants when machining such as that accounted for by Pusavec et al. [2010b] in Equation 1.3.

In conclusion of this subsection, conventional cost and productivity models are still valid in the era of sustainable manufacturing and industry 4.0 even if they cannot be assumed as the only options when selecting a machining strategy. Hence, alternative criteria such as those of energy demand and related carbon footprint have to be considered to enhance the environmental consciousness related to manufacturing strategies. Moreover, a different choice of the level of process parameters which allow to minimize these additional targets could be identified.

1.3.3 Models focused on energy and environmental impact issues

Modelling of energy consumption and environmental factors have emerged over the past half-century, due to the demand for energy conservation in the industrial sector [Yoon et al., 2013]. In this regard, various detailed energy-related studies of machine tools have been proposed in literature.

Machine tools are the key elements in a manufacturing process since they dominate the energy consumption during production [Guo et al., 2015]. As reported previously, the electrical energy consumption of a machine tool typically causes more than 90 % of the environmental impact associated to manufacturing operations. Therefore, a lot of works concern the improvement towards the reduction of the energy consumption of machine tools since this strategy can effectively contribute to reduce both the environmental impact and the production cost of manufacturing. Typically, two types of modelling methods can be identified for machining processes at machine level: the Black-Box Approach (BBA) and the Bottom-Up Approach (BUA). In black-box approaches, the

machine tool is considered as an opaque object, in which machining parameters are input variables while machine energy demand is the output. Models from BBA are made of specific coefficients coming from fitting of experimental energy data. On the other hand, the bottom-up approach requires that the energy consumption of a machine tool is fractionated into various contributes linked to either machine mode (e.g., startup, standby, cutting) or machine device (e.g., spindle motor, axis drives, coolant pump). The total machine energy can be obtained by the sum of the energy of all contributes. In BUA models, the form of the various energy elements cannot be made explicit since requires to be empirically explored. In other words, a single energy element cannot be expressed as a function of process parameters but has to be directly obtained from experimental measurements or simulations. As a consequence, BUA models are more flexible than BBA models due to the detailed energy composition of a machine tool during various operations.

Models were typically used to quantify the total energy demand or the specific energy consumption (i.e., referring to the unit of material removed) of manufacturing processes. The first type of models is useful for quantifying the total energy required to manufacture a particular component and in case of comparison with other technologies such as additive manufacturing [Watson and Taminger, 2016] or mass conserving processes [Ingarao et al., 2015], or with different process chain [Weinert et al., 2011]. This consideration can be traced back to the non-linear relationship between the volume of material processed and the energy consumption related to electricity, tooling, and auxiliary equipment. By contrast, models that express the energy demand with respect to the volume of material removed are able to directly show the influence of the process rate on the energy demand and they can be used to compare various manufacturing processes as reported in Gutowski et al. [2006].

An important aspect of the quantification of the energy required to manufacture a product is related to the level of energy considered. Energy can be assessed either in term of electrical energy requirements (i.e., the direct energy consumption) or by estimating the Cumulated Energy Demand (CED) [Patel, 2003] due to the usage of direct and indirect energies. Indirect energy concerns the usage of tools, cutting fluids, additional processes such as the disposal of metalworking fluids and chips, or cleaning of the part produced. The cumulated energy demand is one of the key indicators conventionally used in the LCA methodology and is based on the calculation of primary energy consumption of products, services or organizations [Frischknecht, 2015]. Primary energy is

defined as the energy directly extracted from nature (e.g., from crude oil or coal). Secondary energy is represented by energy commodities used for different activities such as electricity or fuel. Secondary energy can be quantified from primary energy by introducing the primary-to-secondary energy conversion factor [Arvidsson and Svanström, 2016]. The Global Warming Potential (GWP) is another key indicator of environmental impact commonly adopted in a LCA. The GWP is defined as an emission metric able to expressed in a common unit (so-called 'CO_2-equivalent emissions' or carbon footprint/emission) the emissions of different greenhouse gases (GHGs) and other climate forcing agents [IPCC, 2014]. This metric was introduced to address the needs when comparing components with different physical properties.

The direct energy demand, the cumulated energy demand, and the carbon footprint (or GWP) are used in literature to build machining models able to assess the environmental sustainability of a manufacturing process. A state of the art concerning models of machining process is given in the following subsections where electrical energy models, total energy models, and carbon footprint models are separately presented.

1.3.3.1 Electrical energy models

The models analyzed in this subsection are aimed at the estimation of the electrical energy demand of machining processes, which is directly related to the electricity demand of the machine tool and the auxiliary systems accounted for the specific process analyzed. These are the most common models available in literature since energy can be easily measured and/or monitored with relative precision during the usage of machine tools and other equipment.

Draganescu et al. [2003] determined the (electric) specific consumed energy (E_{cs}) for machining as a function of the machine tool efficiency (η), the cutting power (P_c) and the material removal rate (Z), as shown in Equation 1.6. Machine tool efficiency is defined as the ratio between the cutting power (due to the chip removal mechanism) and the power consumed by the electric motors of a machine tool. It was found that the energy consumption of a machine tool is highly influenced by the machine tool workload, the process parameters, and the tool cutting capacity. Moreover, energy can be minimized with respect to certain conditions such as machine tool and cutting tool constraints.

$$E_{cs} = \frac{P_c}{60 \cdot \eta \cdot Z} \tag{1.6}$$

The specific electrical exergy (B_{elect}) per unit of material processed has been used by Gutowski et al. [2006] to model the electricity demand of various manufacturing processes (Equation 1.7). In general, B_{elect} is a function of a term defined from the ratio between the power consumption (P_0) of equipment that support the process, and the rate of material processing ($\dot{v}$), plus a term (k) owing to the physics of the process. For instance, in machining P_0 is the power consumption due to coolant pump, axis motors, computer console, fans, and other auxiliary equipment, while k is the specific cutting energy characteristic of a specific workpiece material. By observing the structure of the model, it is clear that the minimization of the electrical energy usage can be performed either (1) by the redesign of support equipment or (2) by increasing the rate at which the manufacturing operation is performed. The first strategy is aimed at reducing P_0 by developing more efficient machine tools. The second condition requires to use a higher $\dot{v}$ by adopting cutting tools that allow a reduction of machining times.

$$B_{elect} = \frac{P_0}{\dot{v}} + k \tag{1.7}$$

Mori et al. [2011] defined a model (Equation 1.8) for the estimation of the specific energy consumption (y) of a machine tool during normal operation. Several processes are included in normal operation such as positioning and acceleration the spindle following a tool change, machining, returning the spindle to the tool exchange position after machining, and stopping the spindle. The model is composed by various terms: P_1 is the constant power consumption during the machine operation regardless of the running state; P_2 is the power consumption for cutting by the spindle and servo motor; P_3 is the power consumption to position the work and to accelerate/decelerate the spindle to the specified speed; T_1 is the cycle time during non-cutting state, T_2 is the cycle time during cutting state; T_3 is the time required to position the work and to accelerate the spindle; M_{R} is the material removal volume. The proposed model is useful to evaluate either the machining energy or the setup energy required to accelerate/decelerate the spindle and to position the worktable. This last contribute can be optimized in terms of power consumption by developing new acceleration/deceleration methods.

$$y = \frac{P_1 \times (T_1 + T_1) + P_2 \times T_2 + P_3 \times T_3}{M_R} \tag{1.8}$$

Diaz et al. [2011] quantified the electric energy consumption e of a machine tool as the product between the average power demand p_{avg} and the process time Δt (Equation 1.9). The average power demand can be expressed as the sum of the cutting component p_{cut}, and the air cutting component p_{air}. The authors highlighted that machining time dominates the energy demand especially when high tare machine tools are used. In order to reduce processing time, they suggested to increase the material removal rate even if cutting power increases. Nevertheless, the energy consumption is smaller and this conclusion is according to that reported by previous authors such as Gutowski et al. [2006] by means of their model of specific exergy.

$$e = p_{avg} * \Delta t = (p_{air} + p_{cut}) * \Delta t \tag{1.9}$$

Li and Kara [2011] proposed a BBA empirical model (Equation 1.10) in which the specific energy consumption (*SEC*) of a machine tool can be evaluated through three terms: *i*) the coefficient of the inverse model (C_0), *ii*) the coefficient of the predictor (C_1), and *iii*) the predictor of the inverse model (*MRR*). C_1 was found to depend only on the machine tool, whereas C_0 is a function of workpiece material, tool geometrics and spindle drive characteristics. This empirical model is able to very accurately predict (with an error lower than 10 %) the specific energy consumption for a given set of process parameters.

$$SEC = C_0 + \frac{C_1}{MRR} \tag{1.10}$$

A model for the energy estimation of machine tool during cutting and transient operations was adopted by Kong et al. [2011] as reported in Equation 1.11. The model E is the sum of four contributes such as the energy consumed not related to machining (E_{const}); the energy consumed by spindle, machine axes and tool change when accelerating or decelerating to reach specified values ($E_{run\text{-}time\text{-}transient}$); the energy consumed the by spindle, machine axes and tool change when the spindle motor and the axis drives keep a specified value ($E_{run\text{-}time\text{-}steady}$); and the energy consumed by material removal action (E_{cut}).

$$E = E_{const} + E_{run-time-transient} + E_{run-time-steady} + E_{cut} \tag{1.11}$$

Guo et al. [2012] defined the total specific energy (*TSE*) as the sum of specific process energy (*SPE*) and the specific constant energy (*SCE*) as shown in Equation 1.12. The *TSE* is obtained by a black box approach since is correlated with the process parameters such as cutting speed (v_c), feed (f), depth of cut (a_p), and workpiece diameter (D). The specific process energy is a function of process parameters, which are weighted in the model by exponents (α, β, γ and φ), and a constant term (C_0). The exponents and the constant can be obtained experimentally and they depend on workpiece material, cutting tool and machine tool. *SCE* is expressed similar to the term C_1/MRR as suggested by Li and Kara [2011] when a turning process is considered.

$$TSE = SPE + SCE = C_0 \cdot v_c^{\alpha} \cdot f^{\beta} \cdot a_p^{\gamma} \cdot D^{\varphi} + \frac{C_1}{v_c \cdot f \cdot a_p} \tag{1.12}$$

An improved version of the SEC model was reported by Li et al. [2013] in which the term related to the energy consumption due to spindle rotation and friction has not been disregarded (Equation 1.13). This term highly depends on process parameters (i.e., spindle speed n and material removal rate MRR) and can represent a large portion of the total power demand of a machine tool. The model coefficients k_0, k_1, and k_2 can come from statistic modelling of experimental data or can be calculated by knowing the specific cutting energy, the specific coefficients of spindle motor, and the constant coefficient of machine tools, respectively. The authors highlighted an accuracy of the model greater than 96 % with respect to validation tests.

$$\mathrm{SEC} = k_0 + k_1 \frac{n}{\mathrm{MRR}} + k_2 \frac{1}{\mathrm{MRR}} \tag{1.13}$$

Wang et al. [2013] presented an integrated method of evaluation of the energy efficiency/consumption in machining workshop on different layers such as machine tool layer, manufacturing unit layer, task layer, and workshop layer. For the machine tool layer, they proposed a model (Equation 1.14) for the energy demand in function of three states: the startup energy (E_s), the idle energy (E_u), and the machining energy (E_m). The values of E_s and idle power (P_u) can be determined by regression analyses based on experiments, while t_u is the time at which the machine tool is in idle state. The machining energy E_m can be further computed as a function of several terms such as the additional load loss coefficients a_1, a_2 (due to electrical and mechanical loss in the motor, and the loss of mechanical transmission system generated by the cutting load), idle power P_u,

the cutting power P_c, and the cutting time t_c. In particular, a_1 and a_2 can be identified through experiments while P_c can be calculated by the usage of empirical equations such those reported in various manual of machining.

$$E_{machine} = \overbrace{f_s(n)}^{E_s} + \overbrace{P_u t_u}^{E_u} + \overbrace{\left[P_u + (a_1 + 1)P_c + a_2 P_c^{\,2}\right] t_c}^{E_m} \tag{1.14}$$

Yoon et al. [2013] developed a BUA model (Equation 1.15) for computing the total energy when machining. The total energy (E_{TOTAL}) is obtained multiplying the total power (P_{TOTAL}) for the process time (t). The total power takes into account four contributes: P_{BASIC} represents the basic power consumption of the machine, due to idle energy, axis jog energy, and surrounding energy devices; $P_{SPINDLE}$ is the power consumed by spindle when rotating; P_{STAGE} is the power consumed by moving stage; $P_{MACHINING}$ is the power demand for material removal. $P_{SPINDLE}$ and P_{STAGE} are modelled by means of regression models as function of angular velocity V and in-feed rate f, respectively. Therefore, the specific constants of the models a_1, a_2, b_1, b_2, c_1, and c_2, can be obtained from experiments. For a drilling operation, the machining power is computed as the sum of a term due to the product between thrust force (T) and in-feed rate (f), and another term owing to the product between drilling torque (M) and angular velocity (V).

$$E_{TOTAL} = P_{TOTAL} \times t = \left(P_{BASIC} + \overbrace{a_1 V^{b1} + c_1}^{P_{SPINDLE}} + \overbrace{a_2 f^{b2} + c_2}^{P_{STAGE}} + \overbrace{T \times f + M \times V}^{P_{MACHINING}} \right) \times t \tag{1.15}$$

Balogun and Mativenga [2013] developed an improved energy model (Equation 1.16) which accounts for the energy for tool change. Five different machine states were defined and used in the energy model. E_b is the electrical energy in basic state required to activate machine components and ensure the operational readiness of the machine tool. E_r is the additional electric energy in ready state needed for the drives and spindle movement to bring the tool and workpiece to the correct, about to cut position and to set-up the necessary cutting velocity. During tool change state the energy consumption is expressed as the product between P_{tc} and t_{tc}, which represent the power demand and time, respectively, for tool change. The contribute due to tool change is corrected by considering the number of cutting tool consumed (i.e., cutting tool which have reached the tool life T and are considered worn) over the total cutting time t_c. The

energy demand during the air state is modelled as the product between P_{air} and t_{air}, which represent the average power requirement and the total time duration, respectively, for a non-cutting approach and for retract moves over the component. In cutting state the energy requirement is due to the additional power demands by the spindle (P_s), the lubricating system (P_{cool}), and the material removal ($k\dot{v}$). The spindle power was modelled as linear function of spindle speed (N) through the spindle speed coefficient (m) and a constant (C). The power demand for material removal is modelled as proposed by Gutowski et al. [2006].

$$E_{total} = E_b + E_r + P_{tc} t_{tc} \left[INT\left(\frac{t_c}{T}\right) + 1 \right] + P_{air} t_{air} + \left(\overbrace{mN + C}^{P_s} + P_{cool} + k\dot{v} \right) t_c \quad (1.16)$$

The model of Velchev et al. [2014] was aimed at the optimization of cutting parameters for the minimization of the specific energy consumption when turning. The determination of the direct energy consumption E_{ec} (Equation 1.17) in single pass turning operations is modelled as the sum of the energy consumed during cutting E_{ecc} plus the energy consumed during tool change $E_{ect\ c}$. E_{ecc} is estimated by using a model of specific machining energy consumption e_{ecc} similar to that of Gutowski et al. [2006]: the term k of Equation 1.7 was replaced by $B_0 Q^{B1}$ in Equation 1.17 where Q is the material removal rate, and B_0 and B_1 are specific machine coefficients (to be determined experimentally) depending on process parameters, workpiece, and cutting tool. $E_{ect\ c}$ is estimated by the product between the electrical power P_0, which is required by machine tool with motionless spindle, and the tool change time t_m, and the number of tool replacements. This number can be expressed by the ratio between the machining time t_m and the tool life T of a cutting edge. The proposed model can be used to determine the optimum cutting speed for minimum energy consumption. A comparison between three different criteria, related to cost, energy, and productivity optimization targets, revealed that the cutting speed for minimum energy criterion was found to be greater than that for maximum production rate and, as a consequence, than that for minimum production cost.

$$E_{ec} = E_{ecc} + E_{ect\ c} = e_{ecc} Q t_m + P_0 t_c \frac{t_m}{T} = \left(\frac{P_0}{Q} + B_0 Q^{B_1} \right) Q t_m + P_0 t_c \frac{t_m}{T} \quad (1.17)$$

Liu F. et al. [2015] proposed a new method for predicting the energy consumption of the main driving system of a machine tool. Three types of periods

were defined for a machining process and were namely as start-up periods, idle periods and cutting periods. The total energy consumption prediction model E (Equation 1.18) was given as the sum of prediction models characteristic of each type of period. The start-up energy is modelled as a quadratic function of spindle speed (n). In particular, x_1, x_2, and x_3 are the coefficients of the j-th regression model of each start-up period. The idle energy is obtained by the sum of the energy consumption of idle periods, which can be calculated by multiplying the j-th idle power (P_{uj}) by the j-th idle time (t_{uj}). The energy demand related to cutting periods is the sum of each j-th energy consumption. In particular, the energy consumption of the cutting periods can be calculated by the integral of power over time. α_1, α_2 are the additional loss coefficients characteristic of each transmission chain of machine tools, which can be obtained empirically. P_{c} is the cutting power and can be calculated by referring to cutting manuals.

$$E = \overbrace{\sum_{j=1}^{Q_s}\left(x_1 n_j^{\,2} + x_2 n_j + x_3\right)}^{start\ -up} + \overbrace{\sum_{j=1}^{Q_u}\left(P_{uj} \times t_{uj}\right)}^{idle} + \overbrace{\sum_{j=1}^{Q_c}\left[\int_0^{t_{cj}}\left(\alpha_{2\mathrm{j}} P_c^{\,2} + \left(1+\alpha_{1\mathrm{j}}\right)P_c + P_{uj}\right)\mathrm{d}t\right]}^{cutting} \tag{1.18}$$

An empirical power consumption model was developed by Yoon et al. [2014] with respect to process parameters and tool wear. The model (Equation 1.19) is able to predict accurately the material-removal power taking into account the variation due to tool-flank wear (VB) progression. This peculiarity accounts for the influence of tool wear that is typically observed to increase over time when higher values of feed, spindle rotational speed, and depth of cut are selected. However, the constructed model is based on empirical data and cannot be directly suitable because more research needs to be performed. This research requires additional measurement and standardization of energy consumption at various scales, with several types of machine tools and workpiece materials. As a result, the material-removal power can be found more accurately. However, this contribute is only a small part of the total power consumption.

$$E_{TOTAL} = \int \left\{ f_1\left(n,\, f,\, a_p\right) + f_2\left(n,\, f,\, a_p\right) \cdot \overline{VB}\,(t) \right\} \mathrm{d}t \tag{1.19}$$

Campatelli et al. [2014] presented a study aimed to analyze the effect of simultaneous variations of four cutting parameters (cutting speed, feed rate, and radial and axial depth of cut) on energy consumption. The model E (Equation 1.20) considers n variables ($x_{\mathrm{i}}\ldots x_{\mathrm{n}}$) whereas a_{ij}, b_{i} and c are the constants of the equation to be determined using a regression approach. Response Surface Method

(RSM) was utilized as regression (quadratic) function in order to correlate the experimental data of energy consumption with cutting parameters. A lower energy demand was found by using the developed model when the MRR was set higher as far as possible. This results can be achieved by choosing a cutting speed, feed rate, and chip section that are as large as possible while remaining compatible with the feasible working parameters of the tool.

$$E = \sum_{i=1}^{n} \sum_{j=1}^{i} a_{ij} \cdot x_i \cdot x_j + \sum_{i=1}^{n} b_i \cdot x_i + c \tag{1.20}$$

Liu N. et al. [2015] developed a hybrid energy consumption model based on cutting power. Either analytical methods (for the estimation of the average cutting power at the tool tip, P_{cutting}) or empirical methods (for obtaining coefficients C_0 and C_1) are considered in this hybrid model (Equation 1.21). Cutting power at the tool tip is more accurately estimated with this model due to the better description of the nature of material removal (especially for interrupted cutting processes such as milling). The hybrid model is able to provide valuable information regarding the impact of specific cutting parameters on power consumption. Moreover, the hybrid model is able to explain the phenomenon related to the different power consumption when machining under the same MRR and spindle speed, which represents one major limitation of the existing models, such as those of Li and Kara [2011] and Li et al. [2013].

$$SEC^* = \frac{C_0}{MRR} + C_1 \frac{\overline{P_{cutting}}}{MRR} \tag{1.21}$$

He et al. [2015] extended the model of Gutowski et al. [2006] by considering several time periods in which a machine tool is turned on and consumes energy. In the energy model E (Equation 1.22) additional time steps have been accounted besides the cutting time (t_c) such as the idle (wait) time for the next operation (t_w), the time for tool and workpiece setup (t_s), and the switching time (t_g) for multiple-function machine tools. The improved model and is useful to identify the best strategy of operation sequence of jobs in order to reduce of the idle energy of machine tools for non-machining operations.

$$E = P_0 \cdot \left(t_w + t_s + t_g + t_c\right) + k\dot{v} \cdot t_c \tag{1.22}$$

Guo et al. [2015] proposed an energy model based on an operation-mode approach, which incorporates material removal simulations to predict the energy

consumption of machining processes. The total energy model (E_{TOT}) reported in Equation 1.23 was obtained by adding up the energy consumption of three different modes: the Rapid Traverse Mode energy (E_{RTM}), the Material Removal Mode energy (E_{MRM}), and the Process Transition Mode energy (E_{PTM}). Each energy is computed as the integral of the power consumption characteristic of each mode for the respective time period. The power consumption of a machine tool during RTM is attributed to the machine axes motion (P_{ax}), the spindle rotation (P_{sp}), and the auxiliary components (P_{aux}). The power demand in the MRM is the aggregation of the effective cutting energy (P_{mr}) and the consumption of all the activated machine components as observed in RTM. During PTM, the power demand is only due to the auxiliary components of the machine tool.

$$E_{TOT} = \overbrace{\int_0^t \left(P_{sp} + P_{ax} + P_{aux}\right) \mathrm{d}t}^{E_{RTM}} + \overbrace{\int_0^t \left(P_{mr} + P_{sp} + P_{ax} + P_{aux}\right) \mathrm{d}t}^{E_{MRM}} + \overbrace{\int_0^t P_{aux}\, \mathrm{d}t}^{E_{PTM}} \tag{1.23}$$

In conclusion to this subsection, electric energy models characterized by a bottom up approach, such as that proposed by Balogun and Mativenga [2013] in Equation 1.16, can be suited for a detailed estimation of the electricity demand required by machine tool and auxiliary equipment. However, the presence of consumables such as cutting tool and metalworking fluids, as well as the workpiece material need to be included in the estimation of total energy demand due to their product manufacture phase. As a consequences, an electric energy model is seen as a limit and a total energy model has to be considered in order to provide a comprehensive estimation of the global energy requirements related a machining operation as that represented in Figure 3.

1.3.3.2 Total energy models

The models analyzed in this section are aimed at the estimation of the total energy demand of machining processes. The total energy demand is obtained as the sum of the direct energy demand, which is related to the electricity demand of a machine tool and auxiliary systems, and the indirect energy demand, which is required for the material extraction and production of consumables (e.g., tools and cutting fluids). Since the sum of direct and indirect energies should be referred to the same energy level, the models are assumed to be computed as the sum of only primary energy (i.e., the energy that is extracted from nature) or only secondary

energy (i.e., energy commodities used for different activities such as electricity or fuel) [Arvidsson and Svanström, 2015].

Rajemi et al. [2010] developed a BUA model (Equation 1.24) for the calculation of the total energy when machining a component by the turning process. The total energy (E) is the sum of the machine setup energy (E_1), the machining energy (E_2), the energy consumed during tool change operations (E_3), and the embodied energy due to the production a cutting tool (E_4). E_1 and E_3 are estimated multiplying the power consumption of the machine tool in the idle state (P_0) for the setup time t_1 and for the tool change time t_3, respectively. E_2 comes from Gutowski et al. [2006] and is the electrical energy consumed during the cutting time t_2. E_4 is calculated by using the embodied energy y_E of a specific material for cutting tools. The ratio between t_2 and the tool life of a cutting edge (T) is required in E_3 and E_4 contributes in order to estimate the number of cutting edge and, then, the number of tool replacements. This linear energy model can be suited for the estimation of the optimized tool life (or the corresponding values of process parameters) which satisfies the minimum energy footprint criterion.

$$E = E_1 + E_2 + E_3 + E_4 = P_0 t_1 + (P_0 + k\dot{v})t_2 + P_0 t_3\left(\frac{t_2}{T}\right) + y_E\left(\frac{t_2}{T}\right) \qquad (1.24)$$

The BBA model proposed by Li and Kara [2011] was extended by Liu et al. [2016] considering the tool embodied energy in addition at the machine tool energy consumption (Equation 1.25). The fitted data used for the determination of coefficients C_1 and C_0 were recorded with respect to the tool wear progression. The machine tool specific energy (U_{ME}) was observed to be a function of the electrical energy for auxiliary equipment, spindle motor (U_s), and net cutting (U_{nc}), and was found to be higher when tool wear increased. The tool embodied energy (U_w) was calculated considering the specific energy of tungsten carbide (U_{wc}), the volume of one insert (V_{insert}), the flank wear limit (w_c), the tool wear rate (α), and the material removal rate (MRR). Generally, the tool wear rate is not constant during cutting time and varies among wear regions (e.g., initial, stable, accelerating). When a cutting tool is near to its end of life determines an increase both on the electrical energy consumption of the machine tool during cutting and on its own consumption (in terms of embodied energy). The curve fitting parameters (C_1 and C_0) for U_t were estimated for various tool wear progression and the authors suggested that the tool wear progression should not be omitted during the assessment of the specific energy footprint of a cutting process.

$$U_t = \overbrace{f\left(aux.equip.;U_s;U_{nc}\right)}^{U_{ME}} + \overbrace{\frac{U_{wc}V_{insert}}{w_c}\frac{\alpha}{\text{MRR}}}^{U_w} = \frac{C_1}{\text{MRR}} + C_0 \qquad (1.25)$$

Overall, among the reviewed energy models, those developed by implementing a bottom-up approach can be identified as the most efficient even when considering calibration and uncertainties. This is due to the better knowledge of each term which composes the model since is come from experimental characterization tests. The total energy type has to be accounted for in order to consider indirect energy demand related to the consumables used during the product manufacture phase.

More in detail, the most important factors to keep and estimate accurately in a total energy model are the primary energy demand of the machine tool and auxiliary equipment during machining and tool replacement operations, and the embodied energy of the cutting tool(s) used. The embodied energy related to the workpiece material extraction and production must be considered when the system boundary selected accounts for this contribute. The embodied energy for the CLF production and usage has to be considered especially for mineral oils which present a high embodied energy. The post processing operations such as those for part and swarf cleaning should be accounted for according to the system boundary selected.

1.3.3.3 Carbon footprint models

This subsection includes some models proposed in literature for the assessment of the carbon dioxide emission caused by machining processes. Typically, the analysis of the carbon footprint is conducted together with the estimation of the (primary) energy demand since this last can be used as a proxy for CO_2. However, the amount of carbon emission depends on the specific primary energy source used. Most of the carbon emissions are due to fossil fuels since these primary energy sources require steps of combustion [Jeswiet and Kara, 2008].

Liu et al. [2016] estimated the total carbon emission (CO_2) when machining as the sum of emissions due to the energy consumption of the machine tool plus the emissions owing to the embodied energy of the cutting tool. As reported for the total specific energy proposed by the same authors (Equation 1.25), the influence of tool wear rate on the carbon emission due to the usage of cutting

tools was taken into account for the calculation of the CO_2 model (Equation 1.26). Therefore, several coefficients of the inverse BBA model (β_0 and β_1) were obtained for different value of tool wear.

$$\mathrm{CO}_2 = \frac{\beta_1}{\mathrm{MRR}} + \beta_0 \tag{1.26}$$

Yi et al. [2013] proposed an optimization model in which the carbon emission caused by a machining process (CE_p) can be calculated as the sum of the three terms (Equation 1.27): the carbon emission due to electricity consumption of the machine tool (CE_{elec}), the carbon emission due to cutting tool usage (CE_{tool}), and the carbon emission for coolants consumption ($CE_{coolant}$). The carbon footprint for electricity is estimated by the product of the electricity carbon emission factor (CEF_{elec}) with the energy consumption of the CNC machine tool ($EC_{process}$) during process cutting time. The carbon emission due to cutting tool usage is obtained multiplying the carbon emission factor of cutting tools (CEF_{tool}) by the mass of the tool (W_{tool}) and by the number of tool used that is expressed as the ratio between cutting time (t_m) and tool life (T_{tool}). $CE_{coolant}$ comprises two terms: the carbon emissions due to production of cutting oil (CE_{oil}), and the carbon emissions concerned the disposal phase of cutting fluid (CE_{wc}). In addition, the ratio between process time (T_p) and the replacement cycle of cutting fluid ($T_{coolant}$) is introduced to restrict the footprint of the cutting fluid only for the process time instead of the entire period of fluid usage inside the coolant system. The obtained model was used by the authors for a multi-objective optimization of cutting parameters by means of a fast non-dominating Genetic Algorithm (GA) based on experimental data.

$$CE_p = \overbrace{CEF_{elec} \cdot EC_{process}}^{CE_{elec}} + \overbrace{\frac{t_m}{T_{tool}} \cdot CEF_{tool} \cdot W_{tool}}^{CE_{tool}} + \overbrace{\frac{T_p}{T_{coolant}} \cdot (CE_{oil} + CE_{wc})}^{CE_{coolant}} \tag{1.27}$$

An extend version of the previous model was presented by Li et al. [2015] in which the carbon footprint related to workpiece material was taken into account (Equation 1.28). The carbon emission of the workpiece is related to the production phase (CE_m) and the recycling phase (CE_{chip}) of the amount of removed material that is transformed into chips. CE_m refers to the embodied energy of new workpiece material, whereas CE_{chip} is due to the generation of electricity necessary to support the process of metal recycling (i.e., in case of electric furnace).

$$CE_{p} = CE_{elec} + CE_{tool} + CE_{coolant} + CE_{m} + CE_{chip} \quad (1.28)$$

Lin et al. [2016] accounted for the carbon emission during a machining operation in wet cut environment by using a model that comprises three terms: (CE_{elec}, CE_{tool}, and $CE_{coolant}$) as that of Yi et al. [2013] reported in Equation 1.27. The model of carbon emissions was used together with models concerning operation time and machining cost in order to perform a multi-objective optimization of machining parameters in multi-pass turning operations. A MOTLBO algorithm [Lin et al., [2015] was used to implement the multi-objective teaching–learning-based optimization, in which the construction of non-dominated set and crowding distance assignment method were also used. Their results highlighted that the use of cutting fluids can significantly reduce the total carbon emissions, cutting time, and production cost even though it implies additional carbon emissions and machining cost (owing to the usage of cutting fluids itself) which have been quantified to be little.

The approach used in the last model analyzed can be assumed a reference for the development of a new carbon footprint model since it encompasses all the material and operations identified within the system boundary selected for the development of new models within the thesis. However, the usage of advance optimization algorithms in order to perform a machining optimization can be seen as a limiting factor when process parameters have to be directly and rapidly selected. As a consequence, this limitation can be overcome by adopting a linear model for carbon emission in order to perform a simplified optimization without affecting the accuracy of the results.

1.4 Evidences from literature review

As reported in the previous paragraphs, several machining models focused on the production time/cost, the specific energy consumption, the total direct energy requirements, or the carbon footprint of manufacturing processes have been presented to date. However, there remains a need for comprehensive models which consider the carbon emission caused by machining process in terms of direct and indirect energy demands, and materials consumption. Moreover, the comparison between sustainability models and conventional model (e.g., model for estimating productive time or productive cost) have not been proposed following a holistic view accounting for all the requirements of a manufacturing

operation. The thesis is aimed at the development of sustainable models for the estimation of environmental stress, cost and productivity caused by machining operations. However, the scope of the work does not want to limit their efforts only by providing other models aimed to extend or refine those found in the literature. In particular, the approach implemented onto the models is that to obtain straightforward equations that can be used for the identification of process parameters which satisfy the minimization of environmental impact, process time, or productive costs. In addition, there is a need of comprehensive metrics aimed at suggest a trade-off solution when optimization targets could be conflicting. As a consequence, a solution for the proposed multi-objective optimization is developed in order to provide a comprehensive and accurate decision support tool for the selection of the most sustainable strategy concerning machining processes.

Chapter 2

Modelling of specific production indicators for machining

After having highlighted the limitations of the models presented in the literature, new models are introduced in the following sub-sections. The models are developed by a hybrid technique in which analytical and empirical methods are merged together. The proposed models are applied for quantifying (1) the production time, (2) the production cost, (3) the energy requirement, and (4) the carbon emission. The boundaries for the system-level analysis are chosen as suggested by Dahmus and Gutowski [2004] and discussed in section 1.2. All the activities related to workpiece material production, chip removal, tool preparation, machine tool construction, cutting fluid production/usage, and part cleaning are included in the overall approach. The models of production time, production cost, primary energy requirement, and carbon emission are referred to the specific volume unit of material removed. Such models are used to derive the process parameters (by means of the material removal rate) in order to minimize each of the four considered outputs. Therefore, all the factors either constant or independent of cutting parameters are streamlined in the model development. The contributions from literature, where available, are highlighted in the text. All the terms in the equations are listed in Nomenclature and abbreviations. The equations provide the correct results when using the measurement units assigned per each parameter in Nomenclature and abbreviations.

2.1 Modelling of Specific Production Time

According to Kalpakjian and Schmid [2006], the total process time (t) when machining can be computed as the sum of the time for the machine tool setup (t_1), the actual cutting time (t_2), the time for tool change (t_3). In addition, the time for lubricoolant replacement or refilling and cleaning operations (t_4) is introduced with respect to the selected system boundary. As shown in Equation 2.1, the ratio of actual cutting time t_2 to tool life T defines the number of tool changes. In the present dissertation, T is referring to the tool life of a single cutting edge, and can be computed from the extended Taylor's tool life equation as reported in Equation 2.2 [Mativenga and Rajemi, 2011].

$$t = t_1 + t_2 + t_3 \cdot \left(\frac{t_2}{T} \right) + t_4 \tag{2.1}$$

$$T = \frac{A}{v_c^{\,1/\alpha} \cdot f^{\,1/\beta} \cdot a_p^{\,1/\gamma}} \tag{2.2}$$

The time for the machine tool setup (t_1) can be quantified as a constant value, which is not dependent on the process parameters or lubrication/cooling strategy. The time for lubricoolant replacement or refilling and cleaning operations (t_4) is needed in presence of lubrication. The additional time for lubricoolant replacement or refilling can be neglected, assuming such contribute to be negligible when is shared in proportion to the cutting time required to make a single component. By contrast, the time for swarf and part cleaning operation can be assumed (for simplicity) to be directly proportional to the volume of material removed V (i.e., $t_4 = \tau_{CL} \times V$). This assumption can be traced back to the time needed for the swarf disposal preparation process as suggested by Pusavec et al. [2010b], where chips have to be separated from the oil and shredded if needed.

The Specific Production Time (SPT) has been obtained by dividing the total process time t by the volume of material removed V at the actual cutting time t_2 (Equation 2.3). The contribute of t_1 on the total production time is as lower as higher is the volume of material removed V. The ratio of V to t_2 is the Material Removal Rate (MRR). The MRR for longitudinal turning operations is recalled in Equation 2.4, where the depth of cut a_p is written as $(D_i - D_f)/2$ and the average workpiece diameter D_{avg} is $(D_i + D_f)/2$.

$$\mathrm{SPT} = \frac{t}{V} = \frac{t_1 + t_2 + t_3 \cdot \left(\frac{t_2}{T}\right) + t_4}{V} = \frac{t_1}{V} + \frac{1}{\mathrm{MRR}} + \frac{t_3 \cdot \left(\frac{1}{T}\right)}{\mathrm{MRR}} + \tau_{CL} \tag{2.3}$$

$$\mathrm{MRR} = \pi \cdot \frac{D_i^{\,2} - D_f^{\,2}}{4} \cdot \frac{f \cdot v_c}{\pi \cdot D_{avg}} \cdot \frac{1000}{60} = a_p \cdot f \cdot v_c \cdot \frac{1000}{60} \tag{2.4}$$

Equations 2.2 and 2.4 can be both applied in Equation 2.3, in order to express the specific production time as a function of cutting conditions. The resultant equation is suitable to identify the process parameters aimed to minimize the specific production time (i.e., to maximize the production rate). For instance, the cutting speed corresponding to the minimum production time is computed by differentiating SPT with respect to cutting speed and equating it to zero (Equation 2.5). Equation 2.5 can be further simplified to Equation 2.6 and the final result is given in Equation 2.7. The value of v_c^{minSPT} is affected mostly by the factors used to model the tool life, by the tool change time t_3, and by the selection of depth of cut and feed.

$$\frac{\partial \mathrm{SPT}}{\partial v_c} = \frac{60}{1000} \cdot \left(\frac{t_3}{a_p^{\,(1-1/\gamma)} \cdot f^{\,(1-1/\beta)} \cdot v_c^{\,(2-1/\alpha)}} \cdot \frac{1-\alpha}{\alpha} \cdot \frac{1}{A} - \frac{1}{a_p \cdot f \cdot v_c^{\,2}} \right) = 0 \tag{2.5}$$

$$a_p^{\,1/\gamma} \cdot f^{\,1/\beta} \cdot v_c^{\,1/\alpha} \cdot t_3 \cdot \frac{1-\alpha}{\alpha} \cdot \frac{1}{A} - 1 = 0 \tag{2.6}$$

$$v_c^{\,\mathrm{min\ SPT}} = \left(\frac{A}{a_p^{\,1/\gamma} \cdot f^{\,1/\beta} \cdot t_3} \cdot \frac{\alpha}{1-\alpha} \right)^{\alpha} \tag{2.7}$$

Moreover, the optimum tool life for minimizing the production time T_{minSPT} (Equation 2.8) is obtained by substituting the Taylor's tool life equation (Equation 2.2) into Equation 2.7. T_{minSPT} is independent by process parameters because is only function of the tool change time t_3 and the exponent $1/\alpha$ related to cutting speed used in the tool life equation.

$$T_{\mathrm{min\ SPT}} = t_3 \cdot \left(\frac{1-\alpha}{\alpha} \right) \tag{2.8}$$

2.2 Modelling of Specific Production Cost

The total production cost (C, in Equation 2.9) is directly related with the costs due to machine tool use during the setup time (C_1), the machining time (C_2), and the tool change time (C_3). In addition, the costs for acquiring cutting tool(s) (C_4), workpiece material (C_5), and cutting fluid(s) (C_6) have to be accounted for, together with the costs for post-machining operations as swarf and part cleaning (C_7).

$$C = \sum_{i=1}^{n} C_i = C_1 + C_2 + C_3 + C_4 + C_5 + C_6 + C_7 \tag{2.9}$$

In Equation 2.10, the costs for machine tool use (C_1, C_2, and C_3) are usually computed by considering a machining cost rate (h_c), which comprises the amortization of the equipment cost h_c^{MT} (including the machine tool and all the auxiliaries, as the lubricoolant supply systems) and the labour charge rate h_c^{MO}, as shown in Equation 2.11. The cost for the electric energy is generally assumed to be negligible (with reference to Childs et al. [2000]). Some authors (as Schultheiss et al. [2015]) impliedly account for the power demand by applying different hourly rates for the various operational modes of the machine tool (i.e., during production mode or downtime mode). In the present thesis, the cost model introduced in Equation 2.9 has been extended by taking into account also the cost for the direct electric energy consumption x_{EL} (as suggested by Pusavec et al. [2010b]).

$$C = \overbrace{\underbrace{\left(h_c + x_{EL} \cdot P_{standby}\right) \cdot t_1}_{C_1} + \underbrace{\left(h_c + x_{EL} \cdot P\right) \cdot t_2}_{C_2} + \underbrace{\left(h_c + x_{EL} \cdot P_{standby}\right) \cdot t_3 \cdot \left(\frac{t_2}{T}\right)}_{C_3}}^{Machine\ \ tool\ \ use} + \underbrace{x_{TE} \cdot \left(\frac{t_2}{T}\right)}_{C_4} + \underbrace{x_W \cdot V_W}_{C_5} + \underbrace{x_L \cdot q_L \cdot t_2}_{C_6} + \underbrace{x_{CL} \cdot V}_{C_7} \tag{2.10}$$

$$h_c = h_c^{MT} + h_c^{MO} \tag{2.11}$$

The cost for the direct electric energy consumption is defined multiplying the electricity cost x_{EL} by the power required during the respective process step time, and by the step time itself. During the times for setup or tool change operations the power consumption is equal to the standby power of the machine tool

($P_{standby}$), which is assumed to be constant. The power consumed during transitory phases was neglected in the model because is assumed to be negligible (i.e., the transitory period is negligible with respect to the total production time). The power consumption of the machine tool during machining time is evaluated as reported in Equation 2.12. The model of P is focused on single-pass turning operations.

$$P = P_{standby} + P_{spindle} + P_{feed} + P_{cut} + P_{lub\ sys} \tag{2.12}$$

In addition to the standby power of the machine tool ($P_{standby}$), the operational power for the spindle rotation ($P_{spindle}$) and for the feed motor (P_{feed}), as well as the cutting power (P_{cut}) are always present. The operational power for the spindle rotation ($P_{spindle}$) and for the feed motor (P_{feed}) are typically assumed to increase almost linearly when spindle speed (n) and feed rate ($v_f = f \times n$) increase, respectively. In this study, the specific coefficients of spindle (k_n and b) and feed (k_f and c) motors have been used to model $P_{spindle}$ and P_{feed} as suggested by Li et al. [2013]. The cutting power P_{cut}, owing to the removal of the workpiece material in the form of chips, is modelled multiplying the specific cutting energy k_0 (which is a characteristic of the given workpiece material) with the material removal rate, as indicated by Gutowski et al. [2006]. In presence of metalworking fluids, the power demand for the lubrication/cooling system ($P_{lub\ sys}$) has to be accounted for. This contribute is assumed constant because is expected to be independent from the variation of process parameters. Consequently, Equation 2.12 can be rewritten as Equation 2.13.

$$P = P_{standby} + (k_n \cdot n + b) + (k_f \cdot f \cdot n + c) + k_0 \cdot \mathrm{MRR} + P_{lub\ sys} \tag{2.13}$$

The costs for acquiring cutting tools C_4 is estimated by the product of the cost per cutting edge x_{TE} and the number of cutting edges required up to the actual time t_2. The number of required cutting edges is defined by the ratio of the actual cutting time t_2 to the tool life T, as reported previously (Section 2.1). The cost for the workpiece materials C_5 is quantified multiplying the cost per volume of workpiece material x_W for its total volume V_W, before the pass turning operation. C_6 represents the cost for cutting fluids usage and disposal and is defined by the product between the cost per kilogram of lubricoolant x_L and its consumption rate q_L (in kg/s), and for the actual cutting time t_2. The costs for post-machining

operations as swarf and part cleaning are incorporated in C_7, which is calculated multiplying the cleaning cost x_{CL} for the volume of the material removed V.

The specific production cost SPC has been obtained by dividing the total production cost C by the volume of material removed V, as detailed in Equation 2.14. The contribute on SPC related to the setup operation (C_1/V), the workpiece material (C_5/V), and the cleaning operations (C_7/V), are quantified to be independent on process parameters and inversely proportional to the volume of material removed V.

$$\begin{aligned} \mathrm{SPC} = \frac{C}{V} = \frac{\left(h_c + x_{EL} \cdot P_{\mathrm{standby}}\right) \cdot t_1}{V} + \frac{h_c + x_{EL} \cdot P}{\mathrm{MRR}} + \\ + \frac{\left(h_c + x_{EL} \cdot P_{\mathrm{standby}}\right) \cdot t_3 \cdot \left(\frac{1}{T}\right)}{\mathrm{MRR}} + \frac{x_{TE} \cdot \left(\frac{1}{T}\right)}{\mathrm{MRR}} + \frac{x_W \cdot V_W}{V} + \frac{x_L \cdot q_L}{\mathrm{MRR}} + x_{CL} \end{aligned} \tag{2.14}$$

Both Equation 2.1 and Equation 2.2 can be applied in Equation 2.14 in order to express the specific production cost SPC as a function of process parameters. The equation obtained can be used to identify the cutting parameters that satisfy the minimum production cost. For instance, the cutting speed for minimum production cost is computed by differentiating SPC with respect to the cutting speed and equating it to zero (Equation 2.15). Equation 2.15 can be further simplified to Equation 2.16 and the final result is given in Equation 2.17. v_c^{minSPC} is influenced by the majority of parameters used to model the tool life, the cost for energy consumption of equipment, the cost for lubricoolant usage, and the tool change time t_3.

$$\begin{aligned} \frac{\partial\,\mathrm{SPC}}{\partial\, v_c} = \frac{60}{1000} \cdot \left[\frac{\left(h_c + x_{EL} \cdot P_{\mathrm{standby}}\right) \cdot t_3 + x_{TE}}{a_p^{(1-1/\gamma)} \cdot f^{(1-1/\beta)} \cdot v_c^{(2-1/\alpha)}} \cdot \frac{1-\alpha}{\alpha} \cdot \frac{1}{A} + \right. \\ \left. - \frac{h_c + x_{EL} \cdot \left(P_{\mathrm{standby}} + b + c + P_{\mathrm{lub\ sys}}\right) + x_L \cdot q_L}{a_p \cdot f \cdot v_c^{\,2}} \right] = 0 \end{aligned} \tag{2.15}$$

$$\begin{aligned} a_p^{1/\gamma} \cdot f^{1/\beta} \cdot v_c^{1/\alpha} \cdot \left[\left(h_c + x_{EL} \cdot P_{\mathrm{standby}}\right) \cdot t_3 + x_{TE}\right] \cdot \frac{1-\alpha}{\alpha} \cdot \frac{1}{A} + \\ - \left[h_c + x_{EL} \cdot \left(P_{\mathrm{standby}} + b + c + P_{\mathrm{lub\ sys}}\right) + x_L \cdot q_L\right] = 0 \end{aligned} \tag{2.16}$$

$$v_c^{\min SPC} = \left\{ \frac{A \cdot \left[h_c + x_{EL} \cdot \left(P_{standby} + b + c + P_{lub\ sys} \right) + x_L \cdot q_L \right]}{a_p^{1/\gamma} \cdot f^{1/\beta} \cdot \left[\left(h_c + x_{EL} \cdot P_{standby} \right) \cdot t_3 + x_{TE} \right]} \cdot \frac{\alpha}{1-\alpha} \right\}^{\alpha} \quad (2.17)$$

Then, the optimum tool life for minimizing production cost T_{minSPC} is given in Equation 2.18 by substituting the Taylor's tool life equation (Equation 2.2) into Equation 2.17. T_{minSPC} is independent by the process parameters because is only function of constant values which are not affected by the level of process parameters.

$$T_{\min SPC} = \frac{\left(h_c + x_{EL} \cdot P_{standby} \right) \cdot t_3 + x_{TE}}{h_c + x_{EL} \cdot \left(P_{standby} + b + c + P_{lub\ sys} \right) + x_L \cdot q_L} \cdot \left(\frac{1-\alpha}{\alpha} \right) \quad (2.18)$$

2.3 Modelling of Specific Energy Requirement

A model of Specific Energy Requirement has been published by the author in [Priarone et al., 2016] and was presented at the 66th CIRP General Assembly hold in Guimarães (Portugal) on August 2016. However, the model of Specific Energy Requirement introduced in this thesis presents some minor differences with respect to that previous version. In particular, the cleaning operations are now accounted for according to the system boundary selected in Section 1.2. Moreover, the abbreviation selected for the new version of the Specific Energy Requirement is SER in place of *U* in order to keep the same style as adopted for SPT and SPC indicators.

The total energy demand (*E*) for machining was computed according to the model proposed by Rajemi et al. [2010] and Mativenga and Rajemi [2011] by adding the various *i*-th contributions (E_i), as shown in Equation 2.19. E_1 accounts for the energy consumed by the machine tool during setup operations, E_2 is the energy demand of the machine tool during cutting, whereas E_3 is the energy consumption of the machine tool due to tool change. Indirect energy demands have been included in the model and are referred to E_4, E_5, and E_6 contributes. E_4 is due to the energy to produce cutting tool(s), E_5 is the embedded energy in the workpiece material(s), and E_6 accounts for the energy for producing metalworking fluid(s). In addition, the contribute E_7 is introduced in order to estimate the energy demand during cleaning operations. According to the approach of Dahmus and

Gutowski [2004], the energy for producing the machine tool has been overlooked, since its contribution allocated to each manufactured unit is quantified to be negligible.

$$E = \sum_{i=1}^{n} E_i = E_1 + E_2 + E_3 + E_4 + E_5 + E_6 + E_7 \tag{2.19}$$

E_1 is a constant value, while E_2 is evaluated by multiplying the power consumed during normal operation (Equation 2.13) by the machining time t_2. The energy demand due to tool change (E_3) was computed as reported by Rajemi et al. [2010] and Mativenga and Rajemi [2011]. In particular, E_3 is obtained by the product of the standby power for the tool change time (t_3) and for the number of tool replacements (t_2/T). The model of total energy requirement works properly if all the terms (E_i) are referred to their primary energy source. As a consequence, the energy conversion coefficient η has been introduced in order to estimate the amount of primary energy, as used by Jeswiet and Kara [2008]. This efficiency coefficient comprises the energy losses occurring at the various steps during the production of electricity.

The energy footprint due to the cutting tool usage is represented by E_4 contribute. This contribute is computed by multiplying the embodied (primary) energy of the tool (including material production and tool manufacturing), normalized per cutting edge (y_{TE}), by the number of cutting edge used during the cutting time. E_5 is the energy due to workpiece material and is computed as the product between the workpiece volume V_W and the embodied energy y_W (for primary or secondary production) of the workpiece material. E_6 represents the energy footprint for the usage of lubricoolants and is determined similarly to E_5, i.e. by multiplying the embodied energy per unit mass of the cooling/lubrication fluid (y_L) by its consumption rate (q_L) during cutting time (t_2). E_7 is computed by the product between the primary energy demand for cleaning operation (y_{CL}) and the material removed volume (V) at the cutting time (t_2). Finally, the model of E was obtained based on the previous assumptions and is shown in Equation 2.20.

$$E = \overbrace{\frac{P_{\text{standby}} \cdot t_1}{\eta}}^{E_1} + \overbrace{\frac{P \cdot t_2}{\eta}}^{E_2} + \overbrace{\frac{P_{\text{standby}} \cdot t_3}{\eta} \cdot \left(\frac{t_2}{T}\right)}^{E_3} + \\ + \underbrace{y_{TE} \cdot \left(\frac{t_2}{T}\right)}_{E_4} + \underbrace{y_W \cdot V_W}_{E_5} + \underbrace{y_L \cdot q_L \cdot t_2}_{E_6} + \underbrace{y_{CL} \cdot V}_{E_7} \tag{2.20}$$

Therefore, the complete model of Equation 2.20 is used to define the Specific Energy Requirement SER as reported in Equation 2.21, by dividing E for the material removed volume V. Furthermore, the SER is expressed as a function of MRR (V/t_2).

$$\text{SER} = \frac{E}{V} = \frac{P_{\text{standby}} \cdot t_1}{\eta \cdot V} + \frac{P}{\eta \cdot \text{MRR}} + \frac{P_{\text{standby}} \cdot t_3 \cdot \left(\frac{1}{T}\right)}{\eta \cdot \text{MRR}} + \\ + \frac{y_{TE} \cdot \left(\frac{1}{T}\right)}{\text{MRR}} + \frac{y_W \cdot V_W}{V} + \frac{y_L \cdot q_L}{\text{MRR}} + y_{CL} \tag{2.21}$$

The Specific Energy Requirement SER can be further expressed as a function of process parameters by applying both Equation 2.2 and Equation 2.4 in Equation 2.21. The identification of the cutting parameters that satisfy the minimum specific energy criterion can be obtained by differentiating SER with respect to a cutting variable (v_c, f, or a_p) and equating it to zero. For instance, Equation 2.22 is proposed for computing the cutting speed for minimum energy requirement (v_c^{minSER}). Equation 2.22 can be further simplified to Equation 2.23 and the final result of v_c^{minSER} is given in Equation 2.24. v_c^{minSER} is influenced by the majority of parameters used to model the total energy demand and is a function of the other two process parameters (a_p and f).

$$\frac{\partial \mathrm{SER}}{\partial v_c} = \frac{60}{1000} \cdot \left(\frac{\frac{1}{\eta} \cdot P_{\mathrm{standby}} \cdot t_3 + y_{TE}}{a_p^{\,1-(1/\gamma)} \cdot f^{\,1-(1/\beta)} \cdot v_c^{\,2-(1/\alpha)}} \cdot \frac{1-\alpha}{\alpha} \cdot \frac{1}{A} + \right.$$
$$\left. - \frac{\frac{1}{\eta}\left(P_{\mathrm{standby}} + b + c + P_{\mathrm{lub\ sys}}\right) + y_L \cdot q_L}{a_p \cdot f \cdot v_c^{\,2}} \right) = 0 \tag{2.22}$$

$$a_p^{\,1/\gamma} \cdot f^{\,1/\beta} \cdot v_c^{\,1/\alpha} \cdot \left(\frac{1}{\eta} \cdot P_{\mathrm{standby}} \cdot t_3 + y_{TE} \right) \cdot \frac{1-\alpha}{\alpha} \cdot \frac{1}{A} +$$
$$- \left[\frac{1}{\eta}\left(P_{\mathrm{standby}} + b + c + P_{\mathrm{lub\ sys}}\right) + y_L \cdot q_L \right] = 0 \tag{2.23}$$

$$v_c^{\,\mathrm{min\ SER}} = \left\{ \frac{A \cdot \left[\frac{1}{\eta} \cdot \left(P_{\mathrm{standby}} + b + c + P_{\mathrm{lub\ sys}}\right) + y_L \cdot q_L \right]}{\left(a_p^{\,1/\gamma} \cdot f^{\,1/\beta}\right) \cdot \left(\frac{1}{\eta} \cdot P_{\mathrm{standby}} \cdot t_3 + y_{TE} \right)} \cdot \left(\frac{\alpha}{1-\alpha} \right) \right\}^{\alpha} \tag{2.24}$$

The optimum tool life for minimizing specific energy demand T_{minSER} is given in Equation 2.25 by applying the Taylor's tool life formula (Equation 2.2) into Equation 2.24. T_{minSER} is independent by the process parameters v_c, f, and a_p.

$$T_{\mathrm{min\ SER}} = \frac{\left(\frac{1}{\eta} \cdot P_{\mathrm{standby}} \cdot t_3 + y_{TE} \right) \cdot \left(\frac{1-\alpha}{\alpha} \right)}{\frac{1}{\eta} \cdot \left(P_{\mathrm{standby}} + b + c + P_{\mathrm{lub\ sys}}\right) + y_L \cdot q_L} \tag{2.25}$$

2.4 Modelling of Specific Carbon Emission

The total carbon emission *CE* for machining is computed according to the approach used on previous cost and energy models, by adding the various *i*-th contributions (CE_i), as shown in Equation 2.26. The carbon emission due to the electric consumption of the machine tool during setup time, machining time, and

tool change time are represented by CE_1, CE_2, and CE_3, respectively. CE_4 accounts for the carbon emission due to the usage of cutting tools. CE_5 considers the carbon emission owing to the production of the workpiece. CE_6 represents the carbon emission due to the production and usage of lubricoolants. Finally, the carbon emission related to cleaning operations are accounted for by means of CE_7.

$$CE = \sum_{i=1}^{n} CE_i = CE_1 + CE_2 + CE_3 + CE_4 + CE_5 + CE_6 + CE_7 \tag{2.26}$$

CE_1, CE_2, and CE_3, can be quantified by the product between CES^{TM} [Jeswiet and Kara, 2008] and the electric energy consumption characteristic of each operation, as shown in Section 2.2. CE_5 is computed as the product between the specific carbon footprint of the workpiece z_W (due to primary or secondary production) and its volume V_W. CE_6 is obtained by multiplying the carbon footprint per unit mass of the cooling/lubrication fluid (z_L) and its consumption when machining. The carbon emission due to cleaning operation CE_7 is referred to the energy usage during part and swarf cleaning. Therefore, CE_7 is computed by multiplying the specific carbon emission z_{CL} (owing to the cleaning operation) for the volume of material removed V. Finally, the model of CE is obtained based on the previous assumptions and is reported in Equation 2.27.

$$\begin{aligned} CE = {} & \overbrace{\text{CES} \cdot P_{standby} \cdot t_1}^{CE_1} + \overbrace{\text{CES} \cdot P \cdot t_2}^{CE_2} + \overbrace{\text{CES} \cdot P_{standby} \cdot t_3 \cdot \left(\frac{t_2}{T}\right)}^{CE_3} + \\ & + \overbrace{z_{TE} \cdot \left(\frac{t_2}{T}\right)}^{CE_4} + \overbrace{z_W \cdot V_W}^{CE_5} + \overbrace{z_L \cdot q_L \cdot t_2}^{CE_6} + \overbrace{z_{CL} \cdot V}^{CE_7} \end{aligned} \tag{2.27}$$

The Specific Carbon Emission (SCE) can be obtained by dividing the total carbon emission CE by the volume of material removed V at the actual cutting time t_2 (Equation 2.28). Hence, the SCE can be written as dependent on the MRR (V/t_2).

$$\mathrm{SCE} = \frac{CE}{V} = \frac{\mathrm{CES} \cdot P_{\mathrm{standby}} \cdot t_1}{V} + \frac{\mathrm{CES} \cdot P}{\mathrm{MRR}} + \frac{\mathrm{CES} \cdot P_{\mathrm{standby}} \cdot t_3 \cdot \left(\frac{1}{T}\right)}{\mathrm{MRR}} + \\ + \frac{z_{TE} \cdot \left(\frac{1}{T}\right)}{\mathrm{MRR}} + \frac{z_W \cdot V_W}{V} + \frac{z_L \cdot q_L}{\mathrm{MRR}} + z_{CL} \tag{2.28}$$

Both Equation 2.2 and Equation 2.4 can be applied in Equation 2.28 in order to express the specific carbon emission as a function of process parameters. The obtained equation can be used to identify the cutting parameters that satisfy the minimum specific carbon emission. For instance, the cutting speed for minimum carbon emission (v_c^{minSCE}) is computed by differentiating SCE with respect to the cutting speed and equating it to zero (Equation 2.29). Equation 2.29 can be further simplified to Equation 2.30 and the final result is given in Equation 2.31. v_c^{minSCE} is influenced by the carbon emission owing to the electricity consumption during tool change and machining, and by the carbon emission due to the production and usage of cutting tools and lubricoolants. It is worth to remark that v_c^{minSCE} is a function of a_p and f.

$$\frac{\partial \mathrm{SCE}}{\partial v_c} = \frac{60}{1000} \cdot \left[\frac{\mathrm{CES} \cdot P_{\mathrm{standby}} \cdot t_3 + z_{TE}}{a_p^{(1-1/\gamma)} \cdot f^{(1-1/\beta)} \cdot v_c^{(2-1/\alpha)}} \cdot \frac{1-\alpha}{\alpha} \cdot \frac{1}{A} + \right. \\ \left. - \frac{\mathrm{CES} \cdot \left(P_{\mathrm{standby}} + b + c + P_{\mathrm{lub\ sys}}\right) + z_L \cdot q_L}{a_p \cdot f \cdot v_c^{\,2}} \right] = 0 \tag{2.29}$$

$$a_p^{1/\gamma} \cdot f^{1/\beta} \cdot v_c^{1/\alpha} \cdot \left(\mathrm{CES} \cdot P_{\mathrm{standby}} \cdot t_3 + z_{TE}\right) \cdot \frac{1-\alpha}{\alpha} \cdot \frac{1}{A} + \\ - \left[\mathrm{CES} \cdot \left(P_{\mathrm{standby}} + b + c + P_{\mathrm{lub\ sys}}\right) + z_L \cdot q_L\right] = 0 \tag{2.30}$$

$$v_c^{\mathrm{min\ SCE}} = \left\{ \frac{A \cdot \left[\mathrm{CES} \cdot \left(P_{\mathrm{standby}} + b + c + P_{\mathrm{lub\ sys}}\right) + z_L \cdot q_L\right]}{a_p^{1/\gamma} \cdot f^{1/\beta} \cdot \left(\mathrm{CES} \cdot P_{\mathrm{standby}} \cdot t_3 + z_{TE}\right)} \cdot \left(\frac{\alpha}{1-\alpha}\right) \right\}^{\alpha} \tag{2.31}$$

In addition, the optimum tool life for minimizing carbon emission T_{minSCE} is given in Equation 2.32 by using the Taylor's tool life formula (Equation 2.2) into Equation 2.24. T_{minSCE} is independent by a_p and f since it is only a function of constant values, which are not affected by the process parameters.

$$T_{\min\ SCE} = \left(\frac{CES \cdot P_{standby} \cdot t_3 + z_{TE}}{CES \cdot \left(P_{standby} + b + c + P_{lub\ sys}\right) + z_L \cdot q_L} \right) \cdot \left(\frac{1-\alpha}{\alpha} \right) \quad (2.32)$$

2.5 Optimization method with trade-off criterion

Each specific production indicator (SPT, SPC, SER, and SCE) can be represented as a continuous function of cutting speed or material removal rate. The curves of these indicators are expected to be similar to parables whose minimum point falls into the range of cutting speed (or material removal rate) that are allowed when machining a specific workpiece material under technological constraints. In literature, the high-efficiency machining range is defined between the cutting speed for minimum cost and the cutting speed for maximum productivity (i.e., minimum production time) [Kalpakjian and Schmid, 2006]. Since sustainable indicators are introduced (i.e., the SER and SCE indices) in addition to productivity (SPT) and economic (SPC) indicators, the high-efficiency machining range has to be reconsidered and extended by including, for example, the cutting speed for minimum energy requirements (v_c^{minSER}) and the cutting speed for minimum carbon emission (v_c^{minSCE}).

The cutting speeds or tool life values which minimize a specific production indicator (SPT, SPC, SER, and SCE) can vary among the optimization targets. Since an optimum condition cannot simultaneously satisfy all the four optimization criterions presented above, there is a need to estimate the optimum cutting speed (or optimum tool life) that represents the trade-off among the four criteria accounted for. This trade-off condition can be computed as shown in Equation 2.33 by the introduction of the trade-off function ($\Phi_{t\text{-}o}$). This function is developed in order to minimizes the sum of the distances d_i (with i = 1, 2, 3, 4) plotted in Figure 4. Each distance is computed as the difference between the value of the curve of a specific production indicator computed for the trade-off cutting speed, which is still unknown (i.e., is equal to the unknown variable v_c), and the minimum value of the same curve. The minimum value of a curve is obtained by computing the specific indicator for the respective optimum cutting speed, as identified in the previous paragraphs (Equations 2.7, 2.17, 2.24, and 2.31). Since the distances are still expressed in their unit of measure, they cannot be added together. In order to solve this problem, each distance d_i is divided by the minimum value of the indicator of which is referred. As a consequence, the four

terms of the trade-off indicator are positive and dimensionless values that can be added together.

$$\Phi_{t-o} = \overbrace{\frac{SPT(v_c) - SPT\left(v_c^{\min SPT}\right)}{SPT\left(v_c^{\min SPT}\right)}}^{d_1} + \overbrace{\frac{SER(v_c) - SER\left(v_c^{\min SER}\right)}{SER\left(v_c^{\min SER}\right)}}^{d_2} + \underbrace{\frac{SPC(v_c) - SPC\left(v_c^{\min SPC}\right)}{SPC\left(v_c^{\min SPC}\right)}}_{d_3} + \underbrace{\frac{SCE(v_c) - SCE\left(v_c^{\min SCE}\right)}{SCE\left(v_c^{\min SCE}\right)}}_{d_4} = \tag{2.33}$$

$$= \frac{SPT(v_c)}{SPT\left(v_c^{\min SPT}\right)} + \frac{SER(v_c)}{SER\left(v_c^{\min SER}\right)} + \frac{SPC(v_c)}{SPC\left(v_c^{\min SPC}\right)} + \frac{SCE(v_c)}{SCE\left(v_c^{\min SCE}\right)} - 4$$

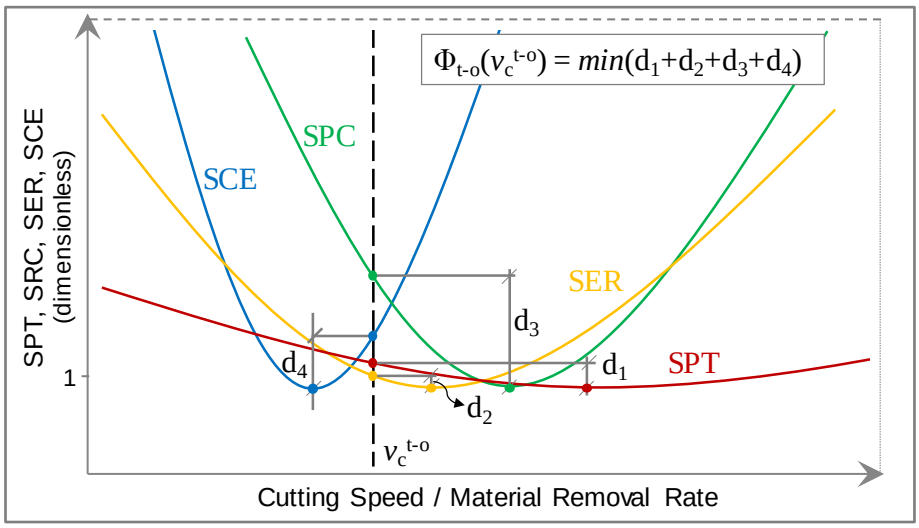

Figure 4. Trade-off optimization criterion. Note: SPT, SPC, SER, and SCE indices are plotted on the same graph since are dimensionless due to the normalization with respect to their minimum point.

The minimum value of the trade-off function can be computed by differentiating $\Phi_{t\text{-}o}$ with respect to the cutting speed and equating it to zero (Equation 2.34).

$$\frac{\partial \Phi_{t-o}}{\partial v_c} = \frac{\partial}{\partial v_c}\left(\frac{\mathrm{SPT}\left(v_c\right)}{\mathrm{SPT}\left(v_c^{\min \mathrm{SPT}}\right)} + \frac{\mathrm{SPC}\left(v_c\right)}{\mathrm{SPC}\left(v_c^{\min \mathrm{SPC}}\right)} + \right.$$
$$\left. + \frac{\mathrm{SER}\left(v_c\right)}{\mathrm{SER}\left(v_c^{\min \mathrm{SER}}\right)} + \frac{\mathrm{SCE}\left(v_c\right)}{\mathrm{SCE}\left(v_c^{\min \mathrm{SCE}}\right)} - 4 \right) = 0 \qquad (2.34)$$

Hence, the final equation for the identification of the trade-off cutting speed ($v_c^{t\text{-}o}$) can be obtained in a compact form as reported in Equation 2.35.

$$v_c^{t-o} = \left[\frac{A}{a_p^{1/\gamma} \cdot f^{1/\beta}} \cdot \left(\frac{\delta_1 + \delta_2 + \delta_3 + \delta_4}{\lambda_1 + \lambda_2 + \lambda_3 + \lambda_4} \right) \cdot \left(\frac{\alpha}{\alpha - 1} \right) \right]^{\alpha} \qquad (2.35)$$

Where:

$$\lambda_1 = \mathrm{SPC}\left(v_c^{\min \mathrm{SPC}}\right) \cdot \mathrm{SER}\left(v_c^{\min \mathrm{SER}}\right) \cdot \mathrm{SCE}\left(v_c^{\min \mathrm{SCE}}\right) \cdot t_3$$

$$\lambda_2 = \mathrm{SPT}\left(v_c^{\min \mathrm{SPT}}\right) \cdot \mathrm{SER}\left(v_c^{\min \mathrm{SER}}\right) \cdot \mathrm{SCE}\left(v_c^{\min \mathrm{SCE}}\right) \cdot \left[\left(h_c + x_{EL} \cdot P_{\mathrm{standby}}\right) \cdot t_3 + x_{TE} \right]$$

$$\lambda_3 = \mathrm{SPT}\left(v_c^{\min \mathrm{SPT}}\right) \cdot \mathrm{SPC}\left(v_c^{\min \mathrm{SPC}}\right) \cdot \mathrm{SCE}\left(v_c^{\min \mathrm{SCE}}\right) \cdot \left(\frac{1}{\eta} \cdot P_{\mathrm{standby}} \cdot t_3 + y_{TE} \right)$$

$$\lambda_4 = \mathrm{SPT}\left(v_c^{\min \mathrm{SPT}}\right) \cdot \mathrm{SPC}\left(v_c^{\min \mathrm{SPC}}\right) \cdot \mathrm{SER}\left(v_c^{\min \mathrm{SER}}\right) \cdot \left(\mathrm{CES} \cdot P_{\mathrm{standby}} \cdot t_3 + z_{TE}\right)$$

$$\delta_1 = \mathrm{SPC}\left(v_c^{\min \mathrm{SPC}}\right) \cdot \mathrm{SER}\left(v_c^{\min \mathrm{SER}}\right) \cdot \mathrm{SCE}\left(v_c^{\min \mathrm{SCE}}\right)$$

$$\delta_2 = \mathrm{SPT}\left(v_c^{\min \mathrm{SPT}}\right) \cdot \mathrm{SER}\left(v_c^{\min \mathrm{SER}}\right) \cdot \mathrm{SCE}\left(v_c^{\min \mathrm{SCE}}\right) \cdot$$
$$\cdot \left[h_c + x_{EL} \cdot \left(P_{\mathrm{standby}} + b + c + P_{\mathrm{lub\ sys}} \right) + x_L \cdot q_L \right]$$

$$\delta_3 = \mathrm{SPT}\left(v_c^{\min \mathrm{SPT}}\right) \cdot \mathrm{SPC}\left(v_c^{\min \mathrm{SPC}}\right) \cdot \mathrm{SCE}\left(v_c^{\min \mathrm{SCE}}\right) \cdot$$
$$\cdot \left(\frac{1}{\eta} \cdot \left(P_{\mathrm{standby}} + b + c + P_{\mathrm{lub\ sys}} \right) + y_L \cdot q_L \right)$$

$$\delta_4 = \mathrm{SPT}\left(v_c^{\min \mathrm{SPT}}\right) \cdot \mathrm{SPC}\left(v_c^{\min \mathrm{SPC}}\right) \cdot \mathrm{SER}\left(v_c^{\min \mathrm{SER}}\right) \cdot$$
$$\cdot \left[\mathrm{CES} \cdot \left(P_{\mathrm{standby}} + b + c + P_{\mathrm{lub\ sys}} \right) + z_L \cdot q_L \right]$$

Moreover, the tool life for trade-off criterion ($T_{t\text{-}o}$), which is independent by the process parameters, can be expressed as shown in Equation 2.36 by substituting the Taylor's tool life formula (Equation 2.2) into Equation 2.35.

$$T_{t-o} = \left(\frac{\lambda_1 + \lambda_2 + \lambda_3 + \lambda_4}{\delta_1 + \delta_2 + \delta_3 + \delta_4} \right) \cdot \left(\frac{1-\alpha}{\alpha} \right) \tag{2.36}$$

The trade-off function is tuned in order to account for the different shape of the curve related to each specific production indicator. In particular, the concavity of a curve can lead to a different distance between the values related to the trade-off cutting speed and the minimum point of the same curve. As a consequence, an indicator with a higher concavity of its curve has a greater influence on the identification of the cutting speed for trade-off condition. The simple average performed on the four values of optimum cutting speed (i.e., v_c^{minSPT}, v_c^{minSPC}, v_c^{minSER}, and v_c^{minSCE}) cannot lead to the same result provided by the trade-off optimization because the average does not consider the shape of each curve. Although the trade-off function is self-balanced with respect to the shape of every curve accounted for, weighting factors can be introduced in order to attribute different weights among the four indicators included in the trade-off function. Hence, k_{SPT}, k_{SPC}, k_{SER} and k_{SCE} are the selected weighting factors to be apply in the equations of $v_c^{\text{t-o}}$ and $T_{\text{t-o}}$, which can be rewritten as reported in Equation 2.37 and Equation 2.38, respectively. These factors have been formulated in such a way that their value can vary between 0 and 1 and their sum has to be equal to 1 (Equation 2.39). When a k_i-th (i = SPT, SPC, SER, or SCE) factor assumes the maximum value (i.e., 1), the others are set to zero and the computed $v_c^{\text{t-o}}$ and $T_{\text{t-o}}$ are equal to the optimum cutting speed/tool life proper of that indicator set to 1. Therefore, the trade-off can be achieved by considering from a minimum of one to a maximum of four criterions, also with different weights among them.

$$v_c^{t-o} = \left[\frac{A}{a_p^{1/\gamma} \cdot f^{1/\beta}} \cdot \left(\frac{k_{\text{SPT}} \cdot \delta_1 + k_{\text{SPC}} \cdot \delta_2 + k_{\text{SER}} \cdot \delta_3 + k_{\text{SCE}} \cdot \delta_4}{k_{\text{SPT}} \cdot \lambda_1 + k_{\text{SPC}} \cdot \lambda_2 + k_{\text{SER}} \cdot \lambda_3 + k_{\text{SCE}} \cdot \lambda_4} \right) \cdot \left(\frac{\alpha}{\alpha - 1} \right) \right]^{\alpha} \tag{2.37}$$

$$T_{t-o} = \left(\frac{k_{\text{SPT}} \cdot \lambda_1 + k_{\text{SPC}} \cdot \lambda_2 + k_{\text{SER}} \cdot \lambda_3 + k_{\text{SCE}} \cdot \lambda_4}{k_{\text{SPT}} \cdot \delta_1 + k_{\text{SPC}} \cdot \delta_2 + k_{\text{SER}} \cdot \delta_3 + k_{\text{SCE}} \cdot \delta_4} \right) \cdot \left(\frac{1-\alpha}{\alpha} \right) \tag{2.38}$$

$$k_{SPT} + k_{SPC} + k_{SER} + k_{SCE} = 1 \tag{2.39}$$

2.6 Optimization targets and main evidences

In literature, it is known that the cutting speed for minimum time is greater than the cutting speed for minimum cost or the ratio of the relevant optimum tool lives is $T_{minTime} < T_{minCost}$. Since the high-efficiency machining range is now reconsidered and extended by including the cutting speeds for minimum energy requirements (v_c^{minSER}) and minimum carbon emission (v_c^{minSCE}), a different ratio of the relevant optimum cutting speeds (or optimum tool life values) can be found. This sentence is explained by considering (for convenience) the form of optimum tool life (T_{minSPT}, T_{minSPC}, T_{minSER}, or T_{minSCE}) such as that reported in Equation 2.40. Coefficients χ_1, χ_2, and χ_3 are positive and vary as a function of the specific production indicator accounted for. In particular, the coefficients χ_1, χ_2, and χ_3 for SPT indicator are equal to 1, 0, and 1, respectively. For SPC, SER, and SCE indicators, each optimum tool life is higher than that of SPT if the condition $\chi_2 > (\chi_3 - \chi_1) \times t_3$ is satisfied. This condition is satisfied for conventional models [Arsecularatne et al., 1992; Kalpakjian and Schmid, 2006; Rajemi et al., 2010] in which χ_3 is equal to χ_1. Within the models proposed in this thesis, χ_3 is greater or equal to χ_1, whereas χ_2 has to be evaluated according to inventory data related to cutting tool cost, primary energy demand, and carbon footprint. Hence, the condition when the tool life for minimum production time is always the lowest has to be evaluated only when the inventory data are used for computing coefficients χ_1, χ_2, and χ_3 for all the models proposed here. For example, the model adopted by Velchev et al. [2014] for computing the specific energy consumption revealed that the cutting speed for minimum energy was greater than the cutting speed for maximum production rate.

$$T_{opt} = \left(\frac{\chi_1 \cdot t_3 + \chi_2}{\chi_3} \right) \cdot \left(\frac{1 - \alpha}{\alpha} \right) \tag{2.40}$$

In addition, the optimization target of this thesis is not aimed only at the optimization of the cutting speed, but wants to provide the optimum values of all the process parameters which allow to minimize each specific production indicator. The formulas for the optimum cutting speed have been provided in the previous sections and such kind of equations needs to know the values of feed and

depth of cut. The selection of feed and depth of cut could be performed with a multi-object mathematical optimization. However, this strategy may lead to the identification of a set of process parameters (v_c, f, and a_p) which cannot be adopted when machining due to the violation of mechanical constraints and workpiece surface quality requirements. For this reason, the Author preferred to provide a dedicated optimization procedure in order to obtain the values of the process parameters which allow to minimize a specific single target (among SPT, SPC, SER, or SCE) or the trade-off condition presented above. This procedure is reported in Section 4.1 within the case study related to the influence of process parameters on the production indicators. In such way, the procedure is presented and discussed by means of the direct application on a case study which is based on experimental data.

Chapter 3

Inventory data

The models developed in Chapter 2 are applied to four case studies in order to compare different machining scenarios. For each case study, the data used in the models are referred to the variation of (1) process parameters, (2) cutting tools, (3) workpiece materials, and (4) lubrication/cooling conditions. In this chapter, the inventory data is given in details in order to quantify each contribute of the proposed models related to time, cost, primary energy, and carbon emission.

The following sections report the data which are referred to the machine tool characterization, the properties of workpiece materials, cutting tools, and lubrication/cooling conditions, as well as other data inventory concerning machining cost rates, cleaning operations, electricity, setup time of machine tool, and tool change time.

The data related to the material eco-properties are referred to the average value of a range provided by literature. Sensibility analysis of the proposed indicators has not been carried out considering the variation of inventory data. This choice is motivated by the fact that the approach adopted in this thesis is aimed at the evaluation of the main factors that make influence on the global scenario related to manufacturing processes. In addition, the needed data have been extracted from the most recent literature in order to account for reliable values contextualized to the present time.

Therefore, it is difficult to generalize the achieved outcomes, which are extremely case-specific due to the dependence on the numerical values applied in

the models. However, future works should focus onto the sensibility analysis of the indicator when varying inventory data.

3.1 Machine tool characterization

Every experimental data reported in the thesis are referred to longitudinal external turning operations which were carried out by using a Graziano 101 SAG slant bed CNC lathe (Figure 5). The electrical power demand of the machine tool was measured during the characterization tests and during the cutting tests by using a Fluke 435-II power analyzer. The main specifications of the power analyzer and its current probes are listed in Table 1. The power analyzer was clamped onto the electricity supply wires to the Graziano lathe. The characterization tests were conducted according to the standardized test procedure proposed by Behrendt et al. [2012].

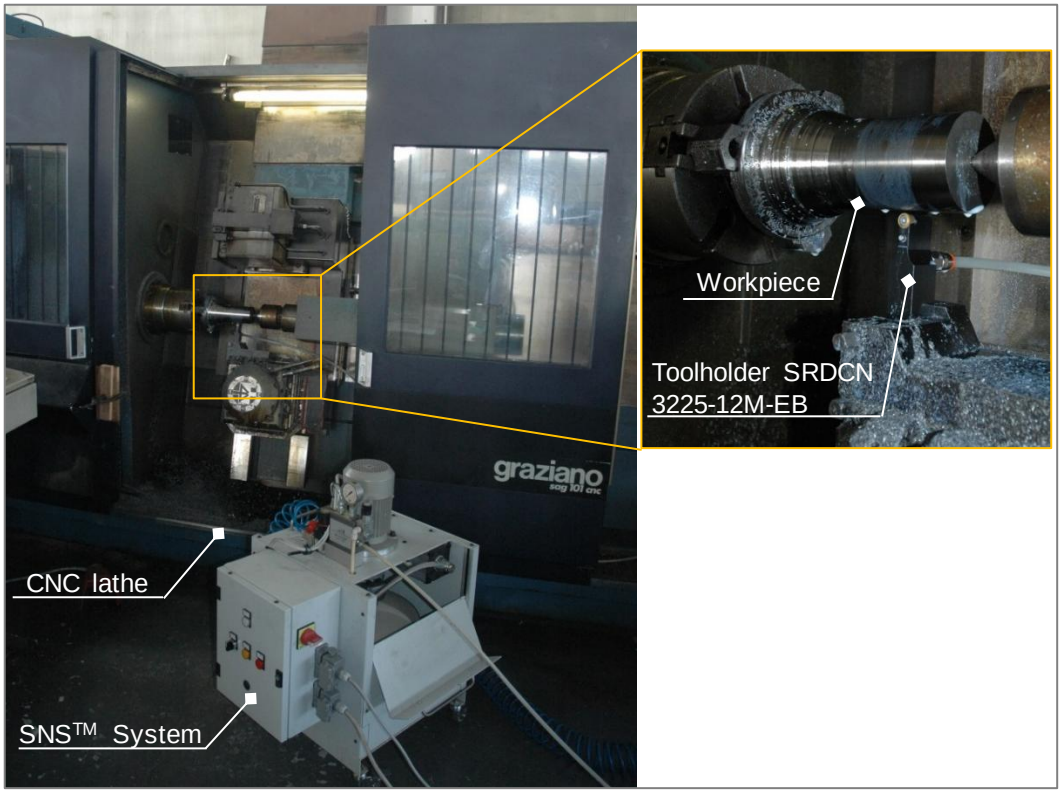

Figure 5. Experimental set-up for cutting tests.

Table 1. Technical specifications for the power analyzer Fluke 435-II.

Voltage inputs	
Number of inputs	4 (3 phase + neutral) dc-coupled
Maximum input voltage	1000 Vrms
Nominal voltage range	Selectable 1 V to 1000 V
Max. peak measurement voltage	6 kV (transient mode only)
Input impedance	4 MΩ//5 pF
Bandwidth	> 10 kHz, up to 100 kHz for transient mode
Scaling	1:1, 10:1, 100:1, 1,000:1 10,000:1 and variable
Current inputs	
Number of inputs	4 (3 phase + neutral) dc- or ac-coupled
Type	Clamp or current transformer with mV output or i430flex-TF
Range	0.5 Arms to 600 Arms with i430flex-TF (with sensitivity 10x) 5 Arms to 6000 Arms with i430flex-TF (with sensitivity 1x) 0.1 mV/A to 1 V/A and custom
Input impedance	1 MΩ
Bandwidth	> 10 kHz
Scaling	1:1, 10:1, 100:1, 1,000:1 10,000:1 and variable
Sampling system	
Resolution	16 bit analog to digital converter on 8 channels
Maximum sampling speed	200 kS/s on each channel simultaneously
RMS sampling	5000 samples on 10/12 cycles according to IEC61000-4-30
PLL synchronization	4096 samples on 10/12 cycles according to IEC61000-4-7
Nominal frequency	50 Hz and 60 Hz
Flexible Current Probe i430 Flexi-TF specification	
Current range	6000 A AC RMS
Voltage output (@1000 ARMS, 50 Hz)	86.6 mV
Accuracy	± 1 % of reading (@ 25 °C, 50 Hz)
Linearity (10 % to 100 % of range)	± 0.2 % of reading
Noise (10 Hz - 7 kHz)	1.0 mV ACRMS
Output impedance	82 Ω min
Load impedance	50 MΩ
Internal Resistance per 100 mm probe length	10.5Ω ± 5 %
Bandwidth (-3dB)	10 Hz to 7 kHz
Phase error (45 Hz - 65 Hz)	± 1°
Position sensitivity	± 2 % of reading max.
Temperature coefficient	± 0.08 % max of reading per °C
Working voltage	1000 V AC RMS or DC (head); 30 V max. (output)

The $P_{standby}$ was measured after switching on the lathe and it includes the constant power demand due to several components such as the control unit, fans, the operation panel, and other auxiliary equipment. The spindle motor was assessed separately because is not included in the standby mode of the machine tool. Therefore, the coefficients of the model for the spindle power demand were obtained following the procedure hereinafter. The spindle was set into rotation at various angular speeds ($100 < n < 1000$ rpm) without any workpiece load. The power demand of spindle motor was experimentally found to be a linear function of spindle speed n. Hence, a linear regression model (with $R^2 = 0.99$) was

computed and the slope (k_n) and the intercept (b) of the model were obtained as result (Figure 6).

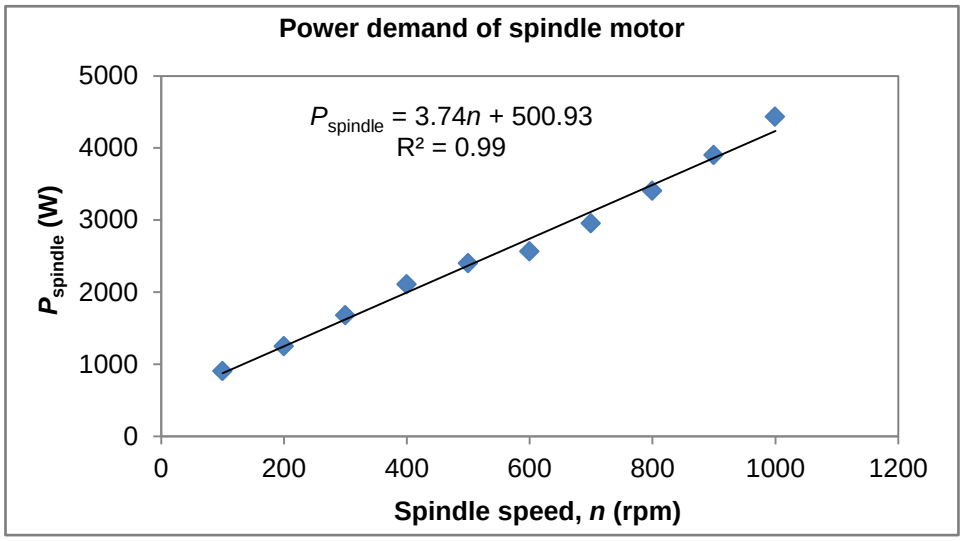

Figure 6. Power demand of spindle motor vs. spindle speed.

Similarly, another model was developed for the feed motor, which was observed to be much less power demanding. The feed motor power varied linearly with the feed rate (Figure 7), so the coefficients k_f and c of the regression model (R^2 = 0.98) were computed.

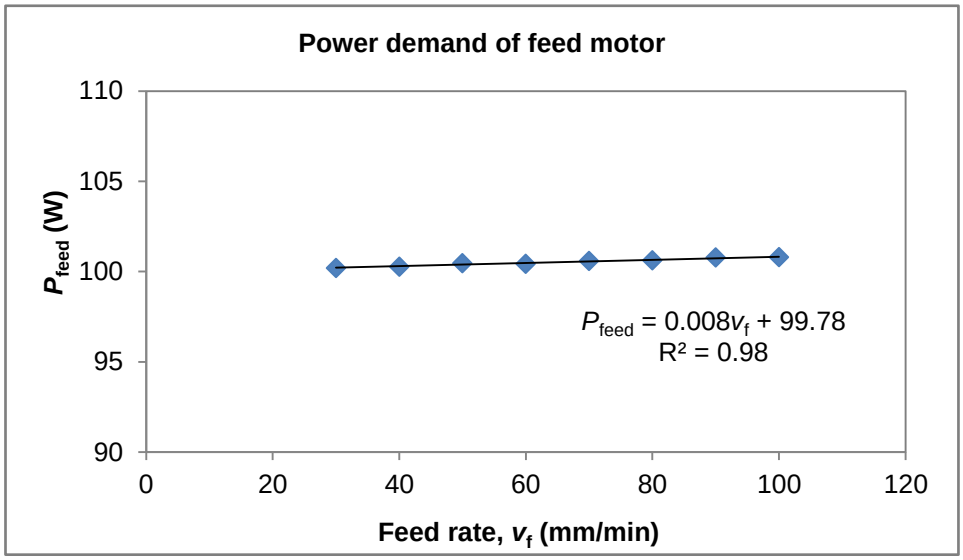

Figure 7. Power demand of feed motor vs. feed rate.

The collected data related to the machine tool characterization are reported in Table 2.

Table 2. Power demands of the machine tool.

System	Variable	Value
CNC lathe	$P_{standby}$ (W)	4500
Spindle motor	k_n (W/rpm)	3.74
	b (W)	500
Feed motor	k_f (W/(mm/min))	0.008
	c (W)	100

The power demand for material removal (P_{cut}) was computed according to [Li et al., 2013] as the difference between the power acquired during air cutting (i.e., when the tool moves toward the workpiece without being in contact with the latter yet) and the power measured during normal cutting. P_{cut} values are used for the identification of the specific cutting energy k_0, which is characteristic of each experimental trial executed under different cutting conditions.

In addition, the specific cutting energy k_0 was estimated also considering data of tangential cutting force (F_t), as suggested by Zhong et al. [2016]. Therefore, k_0 is modelled as reported in Equation 3.1. Cutting forces were acquired by using a three-component piezoelectric quartz Kistler 9263 SN dynamometer equipped with a Kistler 5110 B10 multi-channel charge amplifier. The data of k_0 are reported in Section 4 according to each case study considered.

$$k_0 = \frac{P_{cut}}{MRR} = \frac{F_t \cdot v_c / 60}{a_p \cdot f \cdot v_c \cdot 1000 / 60} = \frac{F_t}{a_p \cdot f \cdot 1000} \quad (3.1)$$

As discussed in Chapter 1, the environmental impact related to the machine tool production is assumed to be negligible when fractionated to the volume unit of material removed. Therefore, the primary energy demand and carbon footprint related to the turning lathe are considered negligible in the computation of the proposed indicators.

3.2 Workpiece materials

Titanium alloys have been considered as important candidates for structural applications in the aerospace and automotive sectors due to their attractive combination of properties [Pramanik, 2014]. For instance, these alloys are heat-resistant materials characterized by a lower density in comparison to that of nickel-based superalloys. Moreover, they exhibit high strength/weight ratio, high temperature strength, and good oxidation and fatigue resistance. On the other hand, titanium alloys are known as difficult-to-machine materials, due to their high hardness and brittleness, high chemical reactivity, low thermal conductivity, and strong tendency to hardening. The limited application of such materials is due to their poor machinability which negatively affects the manufacturing costs. In addition, a higher environmental impact is expected when machining these alloys. Hence, titanium alloys are selected as workpiece materials in order to obtain an overall optimization of their manufacturing phase by applying the proposed models.

In particular, the workpiece materials were a Ti-6Al-4V alloy and a Ti-48Al-2Cr-2Nb (at. %) intermetallic alloy (namely, γ-TiAl). After the preparatory cast skin removal, the bar diameters were 140 mm and the lengths were approximately 200 mm. The production phase related to workpiece material has to be assessed when system boundary 2 (Figure 2) is chosen. However, this phase cannot be neglected even when system boundary 3 is chosen due to the production of metal scrap (i.e., chips). In this case, the total volume of the workpiece (V_W) has to be replaced by the volume of material removed (V) in the contributes of the proposed models which are related to workpiece consumption (Equations 2.10, 2.20, and 2.27).

Workpiece material has an embodied energy and carbon emission that could be one order of magnitude greater than the energy requirements and carbon footprint caused by the manufacturing process. The embodied energy and the carbon footprint for primary production of titanium alloys have been estimated to be 600-740 $\times 10^6$ J/kg and 38-44 $kgCO_2/kg$, respectively [Ashby 2009]. In addition, a workpiece produced by casting and rolling processes requires an energy demand of 9.73-11.47 $\times 10^6$ J/kg and causes a carbon footprint of 0.678-0.802 $kgCO_2/kg$. The density of Ti-6Al-4V and Ti-48Al-2Cr-2Nb are equal to 4.42 and 4.00 $\times 10^{-6}$ kg/mm^3, respectively. The data of embodied energy (y_W) and carbon emission (z_W) for Ti-6Al-4V and Ti-48Al-2Cr-2Nb are computed by accounting for the minimum and maximum values, respectively, of the ranges

previously reported. The choice to consider the highest values for Ti-48Al-2Cr-2Nb can be trace back to the higher complexity of its production process with respect to that for Ti-6Al-4V, which is the most studied and produced titanium alloy.

The price of cylindrical ingots made of titanium aluminide and Ti-6Al-4V are around 90 €/kg (3.60×10^{-4} €/mm^3) and 30 €/kg (1.32×10^{-4} €/mm^3), respectively. The high extraction costs and high processing costs are responsible of the high prize of titanium compared to aluminum and steel [Qian and Froes, 2015]. High processing costs are due to the relatively low processing temperatures used for titanium and the conditioning of surface regions (due to processing temperatures and by the presence of surface cracks) which have to be removed prior to further fabrication.

The impact related to material production and material consumption due to the production of chips during machining is hypothesized to be the same for the different cutting conditions analyzed (i.e., no differences in material losses have been assumed). Furthermore, no improvement related to the workpiece material can be actuated by the selection of different process parameters during machining process. It is difficult to consider the contribute related to the workpiece material especially when the proposed indicators are expressed in function of the volume of material removed. This is due to the fact that the contribute of workpiece material depends also on the volume of the finished part produced. As a consequence, the data related to cost, energy, and carbon footprint related to the workpiece material are not included in the computation of specific production indicators. However, a separated subsection (Section 4.3.1) is proposed in Chapter 4 in order to consider the machining process and the workpiece material as two independent contributes on the total production cost, primary energy demand and carbon dioxide emission.

All the data related to the cost and environmental impact of the two workpiece materials are listed in Table 3.

Table 3. Inventory data for workpiece materials.

Workpiece material	Cost x_W (€/mm^3)	Embodied energy y_W (J/mm^3)	Carbon footprint z_W (kgCO$_2$/mm^3)
Ti-6Al-4V	1.32×10^{-4}	2695	1.71×10^{-4}
Ti-48Al-2Cr-2Nb	3.60×10^{-4}	3006	1.79×10^{-4}

3.3 Cutting tools

Three different tungsten carbide cutting tools (made by Sandvik Coromant) were used in the experiments. The tool inserts were RCMT 1204 M0-SM H13A, RCMT 1204 M0-SM S05F, and RCMT 0803 M0-SM S05F. The inserts coded with S05F were coated by Chemical Vapour Deposition (CVD) of a 4-μm multilayer coating (inner layer: Ti(C,N), intermediate layer: Al_2O_3, outer layer: TiN). The inserts were clamped on Seco SRDCN 2525 M08 or Mircona SRDCN 3225-12M-EB tool holders, according to tool diameters (i.e., 8 or 12-mm).

For carbide cutters, an embodied energy of 400 MJ/kg was reported by Dahmus and Gutowski [2004], and the tool manufacturing step (as sintering and coating) was estimated to be around 1.5 MJ. Therefore, the insert having 12-mm diameter, 4 cutting edges, and weighting 9.5 g was assumed to have an embodied energy per each cutting edge (y_{TE}) of 1.33×10^6 J. This value is according to that reported by Rajemi and Mativenga [2010]. According to Liu et al. [2016] the carbon emission due the production of tungsten carbide tool is comprised between 645 and 727 gCO_2/cm^3. Assuming the average value of 686 gCO_2/cm^3 and the density of tungsten carbide equal to 14.5 g/cm^3, the insert having 12-mm diameter determines a carbon footprint per cutting edge (z_{TE}) of 0.11 $kgCO_2$. The values of y_{TE} and z_{TE} for the insert having 8-mm diameter were estimated to be 0.69×10^6 J and 0.06 $kgCO_2$, respectively. These data for the smaller tool are computed by considering the volume difference with respect to the insert having 12-mm diameter. The difference in terms of primary energy demand and carbon footprint for cutting tools with and without coating materials (by Physical Vapour Deposition (PVD) or Chemical Vapour Deposition (CVD)) was neglected since the manufacturing efforts for bigger tools (i.e., having diameter equal or greater than 12 mm) was proved to be poorly influenced by the coating process [Klocke et al., 2013a]. As a consequence, the differences in terms of y_{TE} and z_{TE} for the tools with 12-mm diameter and S05F and H13A codes (i.e., with or without CVD coating layers) have been neglected.

The cost per unit for the inserts 1204 H13A, 0803 S05F, and 1203 S05F were 5.44, 5.85, and 7.42 €, respectively. Each insert can be indexed four time (i.e., four cutting edge can be used) before being replaced with a new one. Therefore, the costs per cutting edge (x_{TE}) are equal to 1.36, 1.46 and 1.86 €, respectively.

All the data related to the cost and environmental impact of the three cutting tools are listed in Table 4.

Table 4. Inventory data for cutting tools.

Cutting tool	Cost, x_{TE} (€/cutting edge)	Embodied energy, y_{TE} (J/cutting edge)	Carbon footprint, z_{TE} ($kgCO_2$/cutting edge)
RCMT 1204 M0-SM H13A	1.36	1.33×10^6	0.11
RCMT 1204 M0-SM S05F	1.86	1.33×10^6	0.11
RCMT 0803 M0-SM S05F	1.46	0.69×10^6	0.06

3.4 Lubrication/cooling conditions

A lot of phenomenological studies have been presented up to now focusing on the improvement that metalworking fluids can provide in terms of performance of manufacturing processes [Brinksmeier et al., 2015]. The process productivity as well as energy- and resource efficiency are deeply influenced by the application of cutting fluids. The type of metalworking fluid as well as the parameters used in the supply systems used are key factors for the result of manufacturing processes. The case study referred to the influence of lubrication/cooling conditions is based on the data provided in this section, which refer to the working conditions adopted during cutting tests.

Four different lubrication/cooling conditions were adopted in the machining tests. The description of each lubrication system is reported in the following paragraphs together with all data collected in terms of power demand, embodied energy, carbon footprint, and cost related to the usage of cutting fluids. The power demand ($P_{lub\ sys}$) of each lubrication system was directly measured by using the Fluke 435-II power analyzer. Other inventory data have been either experimentally measured or extracted from literature. The costs related to each coolant delivery system investment are not considered in this subsection but are reported in the paragraph '*Machine-tool usage cost rate*', which covers operation and labor costs.

- *Dry cutting*

Since dry cutting does not require the consumption of metalworking fluid as well as the presence of a lubrication system that need of additional power demand,

null values of inventory data (x_L, y_L, and z_L) are considered for such lubrication condition.

- *Conventional flood cooling system (Wet)*

For wet cutting, a 6.7 % CLF-in-water emulsion was supplied by the flood cooling system (i.e., the lubricoolant pump) of the lathe. The emulsion was conveyed through an external nozzle, with a flow rate of 10 l/min. The pump installed inside the lathe was used for supplying the emulsion in the cutting zone. The power demand of the internal pump was found to be constant during cutting operations. For the production of the cutting fluid, the same values of primary energy consumption applied by Pusavec et al. [2010a] are assumed for the emulsion used, due to the comparable lubrication condition. In particular, the emulsion was made of 6.7 % of CLF and 93.3 % of water. The CLF used was composed by mineral oil (20 %), anionic surfactant (9 %), non-ionic surfactant (11 %), and water (60 %). The embodied energies for the production of mineral oil, anionic surfactant, and non-ionic surfactant are 46.7, 60.2, and 51.5 MJ/kg, respectively. As a consequence, the embodied energy for the emulsion (y_L) was computed to be 1.37×10^6 J/kg [Priarone et al., 2016]. The production of mineral oil, anionic surfactant, and non-ionic surfactant are estimated to have a carbon footprint equal to 3.6, 3.0, and 5.6 $kgCO_2/kg$, respectively. As a result, the carbon emission for the wet emulsion (z_L) was computed to be 0.11 $kgCO_2/kg$. The consumption of the emulsion was hypothesized to be 1.32×10^{-4} kg/s, since approximately 1000 liters per year of CLF are used over its duration life time, which is assumed equal to 2112 hours per year. The price of the concentrated CLF used for the emulsion is 10.00 €/l. An additional cost of 0.20 €/l for CLF disposal with phase separation, as well as, a cost of 60 € due to labour for CLF maintenance (i.e., during the duration life time of the emulsion) are accounted for as adopted by Pusavec et al. [2010b]. For the duration life time, the overall usage cost of 1000 liters of CLF is quantified to be 930 €. Then, assuming the density of the emulsion equal to 1.0 kg/l, the CLF usage cost rate x_L is 0.93 €/kg. A detailed calculation of the cost rate of cutting fluid usage is reported in Table 5.

Table 5. Calculation of the cutting fluid (CLF) usage cost rates (adapted from Pusavec et al., [2010b]).

item	Wet	MQL	EMCL
CLF concentrate (volumetric) price (€/l)	10	/	11
CLF disposal with phase separation price (€/l)	0.2	/	0.2
CLF volume fraction (%)	6.7	/	5
CLF volume (needed) (l)	1000	/	/
CLF concentrate volume (needed) (l)	67	/	/
CLF concentrate cost (€)	670	/	/
CLF disposal cost (€)	200	/	1.38 (€/h)
CLF maintenance labor costs (€)	60	/	/
Overall CLF costs (€)	930	/	/
Duration life time (h)	2112	/	/
Non-returnable CLF usage mass flow rate (kg/h)	/	0.016	6.9
Non-returnable CLF specific usage costs (€/kg)	/	55.04	0.55
CLF concentrate density (kg/l)	/	0.90	1.00
CLF usage cost rate (€/h)	0.44	0.89	5.18
CLF usage cost, x_L (€/kg)	**0.93**	**55.04**	**0.75**

- *Minimum Quantity Lubrication (MQL)*

The typical characteristics of Minimum Quantity Lubrication (MQL) systems refer to the application of very small amounts of metalworking fluids (e.g., less than 50 ml/h) [Brinksmeier et al., 2015]. MQL is typically implemented by using pure oil-based fluids, having lubrication power as main effect, with or without the presence of compressed air as carrier gas. The presence of compressed air is conventionally performed by using compressors that require energy consumption. The application of MQL is aimed at the reduction of friction between tool and workpiece material as well as the prevention of chips adhesion onto the tool [Priarone et al., 2014]. MQL is mainly applied in cutting and forming processes. However, the use of the MQL-technique can be critical for manufacturing processes that require a higher cooling effect since the low quantity of metalworking fluid used by this technique. The choice to investigate the performance of an MQL system is aimed at providing a comprehensive evaluation of such system taking into account economic and environmental aspects since many studies are focused only on the technological assessment of MQL conditions.

Concerning the experiments performed by the Author, an Accu-Lube Minimum Quantity Lubrication system (Figure 8) equipped the machine tool during cutting under MQL condition.

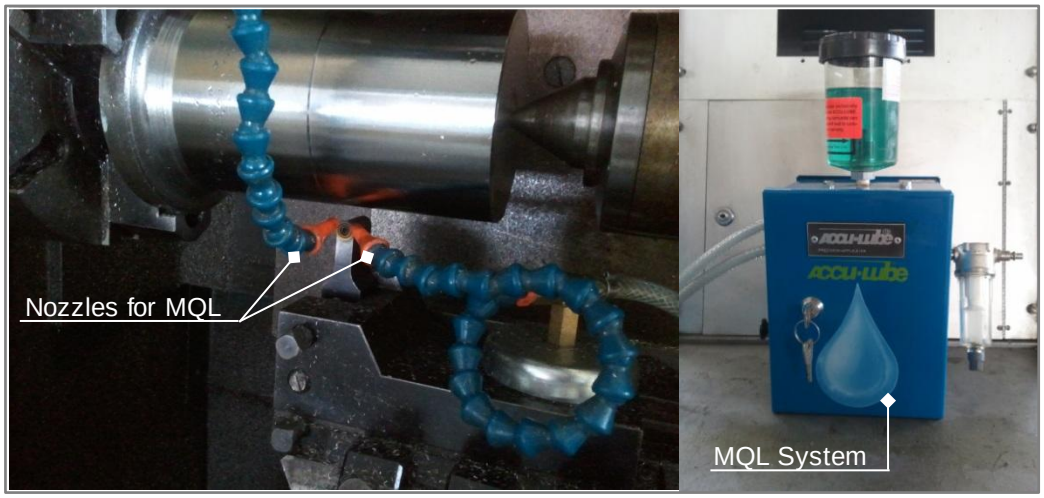

Figure 8. Set up of the MQL system.

An aerosol of a vegetable-based oil conveyed by compressed air (at a pressure of 5.5 bar) was applied to the cutting area. The oil consumption was measured to be 0.3 ml/min. For the MQL system, a reciprocating air compressor (of 3 kW power, 10 bar maximum air pressure) was used to supply the compressed air. Therefore, the electricity demand of the compressor was accounted for and its average power demand was estimated by using Equation 3.2. according to that proposed by Dindorf [2012].

$$P_{\text{lub sys}} = \frac{1}{1000} \cdot P_A = \frac{1}{1000} \cdot \frac{P_L \times t_L}{t_L + t_{UL}} \tag{3.2}$$

where: P_A (kW) is the average power draw, P_L (kW) is the power consumption during loading, t_L (hrs) is the total time while loaded, and t_{UL} (hrs) is the total time unloaded Dindorf [2012]. Equation 3.2 computes the average power draw for on/off control of an air compressor. The compressor type and its wear conditions can influence the specific energy consumption of air compressors.

For MQL conditions, the embodied energy y_L of the cutting fluid was assumed as that of a vegetable (rapeseed) oil. This assumption can be traced back

to the fact that vegetable-based oils are conventionally produced by using soybean, sunflower and rapeseed [Shashidhara and Jayaram, 2010]. McManus et al. [2003] estimated the embodied energy (y_L) and the carbon footprint (z_L) of rapeseed oil to be around 6.18×10^6 J/kg and 0.30 $kgCO_2$/kg, respectively. These values are estimated by considering all the production phases of the vegetable oil, starting from the seedbed preparation up to the rapeseed crushing and refining. The cost of the vegetable oil used in MQL system is 55.04 €/kg. The density of the rapeseed oil was 0.9 kg/l, while the oil consumption for MQL condition was computed to be 4.50×10^{-6} kg/s. Additional costs for disposal or for maintenance labour are not considered for this lubrication condition. This choice is due to the fact that the flow rate of MQL used in the experiments allowed to keep both chips and workpiece in a "near-dry" condition [Weinert et al., 2004]. A detailed cost calculation of the MQL condition is given in Table 5.

- *Emulsion Mist Cooling Lubrication (EMCL)*

The application of small amounts of water-based metalworking fluids can be performed by Minimum Quantity Cooling (MQC) systems [Weinert et al., 2004]. A MQC system allows a better heat exchange compared to that of a MQL system due to the higher specific heat capacity of water (4.18 kJ/kgK versus 1.92 kJ/kgK for the oil). Therefore, MQC is more suitable for continuous cutting processes as well as for machining difficult-to-cut materials characterized by low thermal conductivity [Priarone et al., 2015]. The flow rate conventionally used is lower than 2,000 ml/h [Brinksmeier et al., 2015] and can be applied with or without the presence of compressed air as carrier gas (as for a MQL system).

The fourth lubrication condition used in the experiments is similar a MQC system, however, the consumption of metalworking fluid computed for this condition exceeds the limit of 2,000 ml/h established by literature [Brinksmeier et al., 2015]. As a consequence, the Author preferred to not adopt the acronyms MQC for this last cooling/lubrication condition which is renamed as Emulsion Mist Cooling Lubrication (EMCL) [Faga et al, 2017].

EMCL condition was performed by equipping the machine tool with a SNS^{TM} system - model SNS03IDR (Figure 5) provided by Auges S.r.l. (Italy). Such apparatus nebulizes the cutting fluid (an ester-based oil) stored in a tank by using compressed air. The lubricoolant micro-mist is formed into the internal SNS

mixer, and then supplied to the tool and the cutting area by means of the two nozzles integrated into the Mircona SRDCN 3225-12M-EB tool holder. The lubricoolant flow is directed on both flank and rake faces of the tool. The air supply pressure was fixed to 3 bar, while the cutting fluid flow rate was adjusted by setting the flow regulator of the SNS system. A consumption equal to 115 ml/min of emulsion was used in the cutting trials under EMCL.

The SNS03IDR machine for Emulsion Mist Cooling Lubrication requires direct power consumption due to the electric pump for lubricant and indirect power consumption due to the usage of compressed air. The power requirement of the pump was experimentally measured to be 500 W and the average power demand of the compressor was computed to be 2300 W by following the same procedure adopted for MQL as proposed by Dindorf [2012].

The emulsion used for EMCL condition is composed by 5 % of ester oil and 95 % of water. Since the ester oil is produced from vegetable oils, its environmental impact is assumed equal to that of the rapeseed oil accounted for MQL. Therefore, the emulsion for EMCL has an embodied energy (y_L) and carbon footprint (z_L) are computed to be 0.31×10^6 J/kg and 0.02 $kgCO_2/kg$, respectively (i.e., 5 % of those of the neat rapeseed oil). The emulsion had density of 1.0 kg/l and its consumption (q_L) was computed to be 1.92×10^{-3} kg/s. The cost x_L of the ester-based emulsion used in SNS system is 0.75 €/kg and includes the cost of for CLF disposal with phase separation since the consumption of this cutting fluid cannot be classified as minimal (i.e., the chips and workpiece are not kept in a "near-dry" condition after machining). The cost calculation for EMCL condition is reported in Table 5.

Overall, the data collected for each lubrication system used in the experiments are listed in Table 6.

Table 6. Inventory data for lubrication systems.

Lubrication condition	Power demand $P_{lub\ sys}$ (W)	CLF usage q_L (kg/s)	CLF Cost x_L (€/kg)	Embodied energy y_L (J/kg)	Carbon footprint z_L ($kgCO_2/kg$)
Wet	600	1.32×10^{-4}	0.93	1.37×10^6	0.11
MQL	2550	4.50×10^{-6}	55.04	6.18×10^6	0.30
EMCL	2800	1.92×10^{-3}	0.75	0.31×10^6	0.02

3.5 Other data inventory

In this section, data related to electricity, machining cost rate, cleaning operations, tool change time, and machine setup operation are collected and discussed. Moreover, some considerations are reported concerning the selection of process parameters and tool wear measurements.

- *Electricity*

The cost for electric energy x_{EL} is assumed equal to 2.61×10^{-8} €/(W×s) which represents the average electricity prices commonly paid by Italian medium size industries in 2015 [Eurostat database, 2016]. The concept of the Carbon Emissions Signature (CES^{TM}) has been introduced by Jeswiet and Kara [2008] in order to provide a tool for computing the carbon emitted when consuming energy coming from a specific electrical energy grid. Several primary energy sources supply an electrical power grid and are characterized by different carbon emissions. Coal (C), Natural Gas (NG), and Petroleum (P) are primary sources commonly used in electrical power grids and are responsible of carbon emission during energy production due to their combustion. The amount of carbon emitted per heat released for coal, natural gas, and petroleum are assumed to be 112, 66, and 49 $kgCO_2/GJ$, respectively. Equation 3.3 was proposed by Jeswiet and Kara [2008] for computing the carbon emission related to electricity consumption as the sum of fractions of the primary sources (C, NG, and P) multiplied by the conversion efficiency η for each energy source. This equation is used for the computation of the CES related to the Italian electricity by assuming a conversion efficiency equal to 0.34.

$$CES = \eta \cdot (112 \cdot \%C + 49 \cdot \%NG + 66 \cdot \%P) \tag{3.3}$$

The environmental impact caused by the electricity consumption is computed with reference to the data of the final electricity balance of 2014 provided by the main Italian electricity supplier [Terna, 2014]. In 2014, the electrical energy from Italian power grid was 86 % internally produced, 14.9 % imported and (-)1.0 % exported, as listed in Table 7. Considering only the data for the internal production (and assuming this value as 100 %), electricity was produced by primary sources with contributes of 14.6 % by carbon, 33.8 % by natural gas, and 1.6 % by petroleum. Using Equation 3.3, the CES for Italian grid in 2014 is

computed to be 100.1×10^{-9} $kgCO_2/J$. This values overestimates the real CES since the imported energy has not been accounted for. In particular, electricity for Italy was mainly imported from Austria, France, Slovenia, and Switzerland which were characterized by lower CESs with respect to that of Italy (with the exception of Slovenia) due to the large contribution of nuclear source in their electricity production.

It is worth to underline that the computation of CES can be influenced by other aspects such as the reference year and the inclusion of transmission and distribution losses. The reference year play a key role in the computation of CES since the contribute of each primary source varies for year-by-year. For example, in 2010, Brander et al. [2010] estimated the carbon emission per unit energy of electricity consumed in Italy around 120.91×10^{-9} $kgCO_2/J$. These authors computed the total carbon emission by considering the total electricity consumed as the sum of the generated energy plus the amount of transmission and distribution losses. The differences between this estimated value and the proposed value (used in this thesis) can be due to the trend in renewable energy sources that has been growth over the years, and in particular for 2014. In addition, the transmission and distribution losses contribute can determine a different value of the CES of the same year.

Table 7. Data of electricity grid for Italy in 2014 (adapted from Terna [2014]).

	Data for 2014	GWh	% TOTAL	% Partial
Produced	Electricity internal production	269,147.9	86.0%	(100.0%)
	Carbon (C)	39,428.6		14.6%
	Natural Gas (NG)	91,066.8		33.8%
	Oil (P)	4,271.8		1.6%
	Other Thermoelectric	32,313.1		12.0%
	Nuclear	0.0		0.0%
	Hydroelectric	59,574.9		22.1%
	Other Renewables	42,492.7		15.8%
	IMPORT	46,747.5	14.9%	
	EXPORT	(-)3,031.1	(-)1.0%	
	TOTAL Electricity Demand	**312,864.3**	**100.0%**	
Consumed	Pumped storage hydro	2,329.1	0.7%	
	Total internal demand	310,535.2	99.3%	(100.0%)
	Agriculture	5,372.1		1.7%
	Industry	122,505.0		39.4%
	Tertiary	98,951.4		31.9%
	Domestic	64,255.0		20.7%
	Grid loss	19,451.7		6.3%

- *Machining cost rate*

The labour charge rate h_c^{MO} for machining is assumed equal to 23.25 €/h. The amortization rate of the equipment cost h_c^{MT} is 30.66 €/h for dry and wet conditions, which are equal because the internal lubricating pump is inclusive in the machine tool investment. MQL and EMCL equipment require additional investment which are accounted for their amortization rates. Therefore, h_c^{MT} for machining under MQL and EMCL are estimated to be 30.86 and 31.35 €/h, respectively. Finally, the hourly cost for the machine tool (h_c) is computed to be 14.98×10^{-3} €/s for dry and wet cutting conditions, 15.03×10^{-3} €/s for MQL condition, and 15.17×10^{-3} €/s when cutting under EMCL. The detailed calculation of the total machining cost rates for each machining condition are reported in Table 8. The depreciation period of the machine tool and other equipment are assumed according to Pusavec et al. [2010b].

Table 8. Calculation of total machining cost rates (adapted from Pusavec et al., [2010b]).

item	Dry	Wet	MQL	EMCL
Machine-tool investment (€) [a]	350,000	350,000	350,000	350,000
Tooling investment (10% of [a]) (€) [b]	35,000	35,000	35,000	35,000
Coolant delivery system investment (€) [c]	/	(inclusive)	2,500	9,000
Machine-tool installation investment (€) [d]	10,000	10,000	10,000	10,000
Machine-tool investment as installed (€) [a+b+c+d]	395,000	395,000	397,500	404,000
Depreciation period (year)	7	7	7	7
Maintenance cost rate (1.5% of [a+b+c]) (€/year)	5,775	5,775	5,813	5,910
Insurance/taxes cost rate (0.4% of [a+b+c]) (€/year)	1,540	1,540	1,550	1,576
Tool holder costs (12 x 85 €) (€)	1,020	1,020	1,020	1,020
Time fraction of machine-tool usage (h/year)	2,640	2,640	2,640	2,640
Down time fraction (%)	20	20	20	20
Time fraction of actual machine-tool usage (h/a)	2,112	2,112	2,112	2,112
Machine-Tool usage cost rate (€/h) [e]	30.66	30.66	30.86	31.35
Machine-Tool usage cost rate, h_c^{MT} ($\times10^{-3}$ €/s)	**8.52**	**8.52**	**8.57**	**8.71**
Labor costs Direct labor cost rate (€/h) [f]	15.00	15.00	15.00	15.00
Indirect labor cost rate (10% of [f]) (€/h)	1.50	1.50	1.50	1.50
Supervision cost rate (12% of [f]) (€/h)	1.80	1.80	1.80	1.80
Fringe benefits cost rate (33% of [f]) (€/h)	4.95	4.95	4.95	4.95
Machine-tool Operator cost rate (€/h) [g]	23.25	23.25	23.25	23.25
Machine-tool Operator cost rate, h_c^{MO} ($\times10^{-3}$ €/s)	**6.46**	**6.46**	**6.46**	**6.46**
Overall machining cost rate (€/h) [e+g]	53.91	53.91	54.11	54.60
Overall machining cost rate, h_c ($\times10^{-3}$ €/s) [$h_c^{MT}+h_c^{MO}$]	**14.98**	**14.98**	**15.03**	**15.17**

- *Cleaning operations*

It is worth to point out that cleaning operations have to be considered for the comparison of the cost, energy demand, and carbon emission when machining under different lubrication conditions. These contribute can be considered negligible only in case of MQL or dry cutting conditions. On the contrary, the cost for cleaning operation after wet cutting cannot be omitted since it can be estimated to be up to 4 % of the total productive cost as highlighted by Pusavec et al. [2010b].

The cleaning cost per volume of material removed x_{CL} is assumed equal to 5.17×10^{-6} €/mm^3. Such value is according to the study of Pusavec et al. [2010b] in which the cleaning cost per part for a single pass turning operation performed on Inconel 718 bars was quantified to be 0.078 € for a volume of material removed equal to 15.08 cm^3. The total cost for cleaning operation considered either the cost for part cleaning or the cost for swarf preparation (i.e., due to swarf shredding operation). The x_{CL} cost was applied in case of turning under wet and emulsion mist conditions. The environmental impact (per volume of material removed) in terms of primary energy (y_{CL}) and carbon footprint (z_{CL}) due to electricity usage for cleaning operations is assumed equal to 18.72 J/mm^3 and 6.37×10^{-7} kgCO_2/mm^3, respectively. The specific time required for cleaning operation (τ_{CL}) is assumed equal to 3.21×10^{-4} s/mm^3.

- *Tool change time*

It is known from literature (Kalpakjian and Schmid, 2006; Childs et al., 2000) that the shape of the curve related to production time (or cost) versus MRR is mainly obtained by the sum of two contributes characterized by opposite trend (Figure 9). For example, the production time is typically computed by the summation of times due to machining (or cutting) and non-machining (or tool indexing/change) operations. The contribute related to the machining process becomes lower when material removal rate is increased. By contrast, the contribute due to non-machining operations (i.e., related to cutting tool) becomes relevant at higher material removal rates.

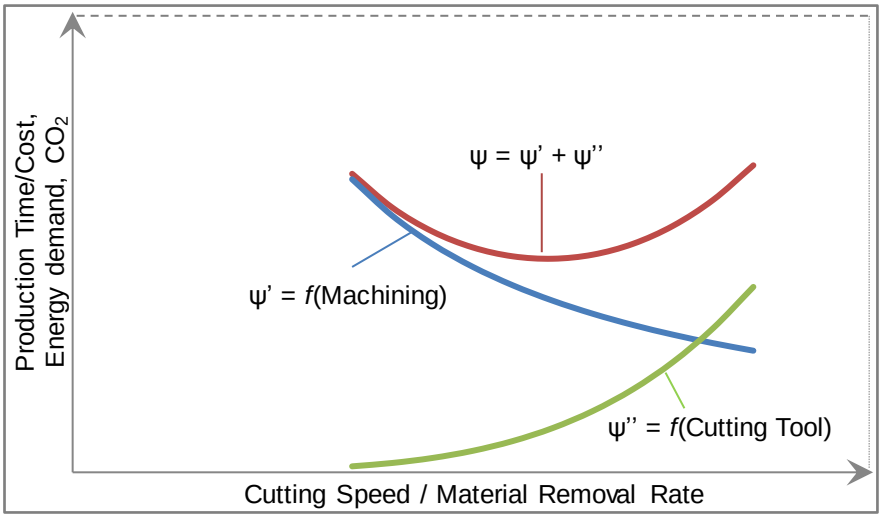

Figure 9. Typical curve profile (in qualitative terms) of a production indicator (ψ) at varying of cutting speed and/or material removal rate.

The same trend can be observed for the energy demand and carbon emission [Li et al., 2015] in which the embodied energy/carbon footprint of cutting tool (due to its production phase) are added in addition to the environmental impact for tool change operation.

As a consequence, the time required for tool change (t_3) plays a key role in the curve behavior of production indicators and, therefore, in the determination of optimal cutting conditions. Rajemi and Mativenga [2008] used a tool change time equal to 2 minutes in their optimization model. This value can represent the average time for tool replacement when using CNC machines without automatic tool change equipment. Kwon and Fischer [2003] considered tool indexing time of 2 min, tool change time of 3 min, and tool inspection time of 2 min for a CNC turning centre. A tool change time of 5 min was adopted by Velchev et al. [2014] in their empirical model for specific energy consumption. By contrast, automatic machining centers generally contain an Automatic Tool Changer (ATC) for holding multiple cutting tools. In those machines the unit tool switching time can require few seconds [Baykasoğlu and Ozsoydan, 2016] and this reduced makespan can considerably enhance the machine productivity. A sensitivity analysis (in qualitative terms) of the influence of tool change time (t_3) on production indicators at varying of cutting speed and/or material removal rate is represented in Figure 10.

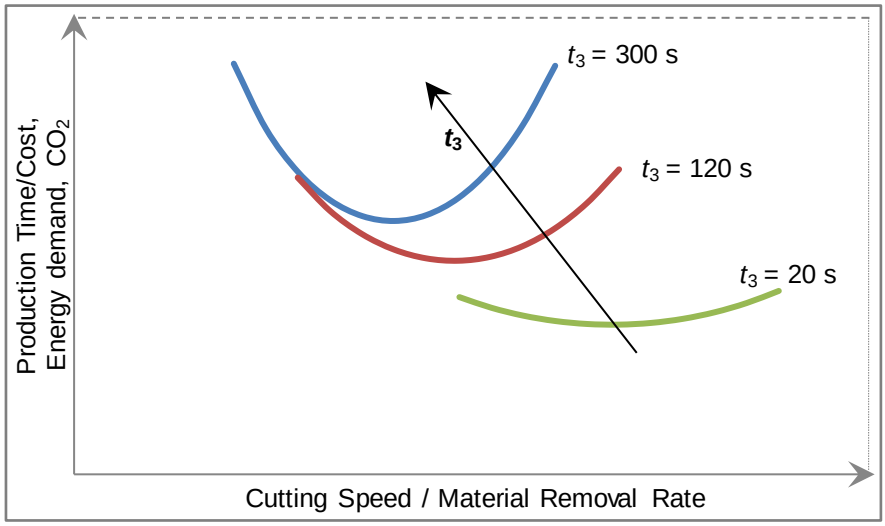

Figure 10. Influence of tool change time (t_3) on production indicators (in qualitative terms) at varying of cutting speed and/or material removal rate.

Each indicator (i.e., production time, production cost, energy demand and carbon dioxide emission) can be represented (in qualitative terms) by one of the three curves showed in Figure 10 since they are affected in the same way by the variation of t_3 evaluated. Production indicators show increased values when a higher tool change time is accounted for. Moreover, the differences within an interval of MRR are more pronounced and the minimum of the curve is shifted toward lower MRRs. Overall, the tool change time chosen for the computation of specific production indicators in the case studies is t_3 = 120 s.

- *Machine setup operation*

The machine setup operation requires time for tool and workpiece setup/handling. In this thesis, the setup operation is assumed to represent a negligible portion of time with respect to the time needed for cutting (i.e., the ratio between t_1 and t_2 is negligible). The graph of Figure 11 shows (in a double logarithmic scale) a comparison between the specific time for cutting and specific time for setup operation at varying of volume of material removed.

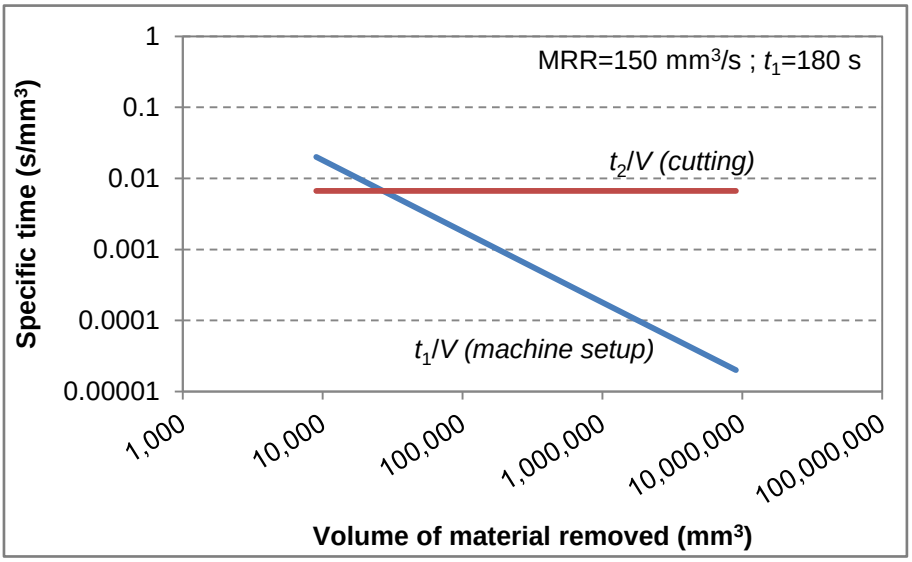

Figure 11. Comparison of specific time for machine setup and cutting operations.

The greater is the volume of material removed, the lower is the specific time required for machine setup. The same observation can be applied when computing the specific production cost, specific energy requirement, and specific carbon emission. Therefore, the contributes of machine setup is neglected also for these production indicators.

- *Selection of process parameters and tool wear measurements*

The values of the process parameters such as cutting speed, feed, depth of cut, and material removal rate are chosen according to each case study and reported in the respective sections of Chapter 4. All the preliminary tests used for the identification of allowable working conditions were executed three times maintaining the same level of the process parameters. The variation of process parameters was used for the identification of the coefficients in the Taylor tool life's equation (Equation 2.2). The results are discussed assuming that all the surfaces machined under the different conditions comply with the same specifications (in terms of both surface quality/integrity and dimensional accuracy).

Several measurements of the tool wear were executed for obtaining the coefficients needed for the Taylor's tool life equations. Therefore, for each cutting test, the wear of the cutting edge was measured at regular time-steps by using an optical microscope (at 50× magnification). The maximum flank wear $VB_B max = 0.2$ mm was assumed as tool wear limit to estimate the tool life T. In addition, the tool wear was monitored since the specific cutting energy (k_0) was observed to increase for higher values of the tool wear. This can be traced back to the energy requirements of the machine tool during cutting which were observed to be affected by tool wear. Three tool wear conditions are considered for the computation of k_0: $VB_B max \cong 0.0$ mm (i.e., unworn tool), $VB_B max \cong 0.1$ mm, and $VB_B max \cong 0.2$ mm (i.e., worn tool).

Chapter 4

Application of developed models on case studies

The four machining models described in Chapter 2 are applied in case studies where the influence of several variables are taken into account. Such models are used (I) to quantify the time, cost, energy demand, and carbon dioxide emission related to a turning operation, and (II) to identify optimum values of process parameters in order to minimize each target previously quantified. In particular, the selected variables are related to (1) process parameters, (2) cutting tool, (3) workpiece material, and (4) lubrication/cooling condition. Each case study focuses on the variation of one variable at a time. As a consequence, there are four case studies, one for each variable accounted for. In particular, cutting speed v_c, feed f, and depth of cut a_p are the selected process parameters conventionally used in a turning process. The influence of cutting tool is referred to the usage of two different tool diameter (i.e., RCMT 0803 S05F and RCMT 1204 S05F). The workpiece materials investigated in the third case study are the two titanium alloys presented in Section 3.2 (i.e., Ti-48Al-2Cr-2Nb and Ti-6Al-4V). The influence of lubrication/cooling condition is evaluated considering turning passes under EMCL, wet, MQL, and dry cutting conditions. Table 9 presents the four case study which are reported in the following sections. Dry cutting condition is adopted in all the case studies since it represents a sustainable choice for minimizing the environmental impact of machining. All the data collected in Chapter 3 are used for the application of the developed models in the case studies.

Table 9. Variables considered in the case studies.

Section	Case study	Variable			
		Process Parameter	**Cutting Tool**	**Workpiece Material**	**Lubrication/cooling condition**
4.1	Influence of **process parameters**	v_c; f; a_p	RCMT 0803 S05F	Ti-48Al-2Cr-2Nb	Dry
4.2	Influence of **cutting tool**	v_c	**RCMT 0803 S05F; RCMT 1204 S05F**	Ti-48Al-2Cr-2Nb	Dry
4.3	Influence of **workpiece material**	v_c	RCMT 1204 S05F; RCMT 1204 H13A	**Ti-48Al-2Cr-2Nb; Ti-6Al-4V**	Dry
4.4	Influence of **lubrication/cooling condition**	v_c	RCMT 1204 H13A	Ti-6Al-4V	**Dry; Wet; MQL; EMCL**

4.1 Influence of process parameters

The aim of the present case study is to apply the developed machining models of Chapter 2 in an optimization procedure in order to (I) directly obtain optimum value of process parameters, and (II) to quantify the impact of turning operation (by using the previous optimized parameters) in terms of time, cost, energy demand and CO_2 emission.

In turning, the process parameters that are usually optimized are cutting speed, depth of cut, and feed rate. Typically, the optimum cutting conditions are identified in order to satisfy an economic criterion (i.e., minimum cost or maximum production rate) without violating any of the constraints which may be applied on the process. Based on the proposed approach, environmental targets such as the minimization of energy demand and/or carbon footprint should be considered in addition to the economic criterion. Constraints that have to be taken into account when determining the cutting conditions include: (1) the type of operation (i.e., roughing or finishing); (2) the machine tool parameters (i.e., available power, speed and feed ranges and rigidity of the spindle bearing system); (3) the cutting tool parameters (i.e., tool material, geometry and the tool cost); (4) the workpiece characteristics (i.e., work material properties, geometry, tolerances and surface finish requirements) [Meng et al., 2000].

Hinduja et al. [1985] developed a procedure for obtain the optimized cutting condition for roughing operation which considers several constraints such as chip-

breaking control, maximum allowable tool force, component instability, torque and power characteristics of the machine, workholding limitations, axial spindle loading, allowable process parameters for cutting tool, range of machine speed, and tool deflection. In addition, surface finish and workpiece accuracy need to be accounted for finishing operations.

Arsecularatne et al. [1992] improved the study of Hinduja et al. [1985] in order to apply this procedure in a technologically orientated numerically controlled (NC) system for various machining processes.

Meng et al. [2000] proposed a method for the calculation of optimum cutting conditions using a machining theory. The method uses to check process constraints such as machine power, tool plastic deformation and built-up edge formation.

With respect to the works described above, a simplified method is proposed in the following for the identification of optimum process parameters that allow to reduce production time, cost and environmental stress. Technological constraints, such as those previously reported according to Hinduja et al. [1985], were satisfied during the executed turning trials, which were aimed at the collection of inventory data used for the computation of specific production indicators presented within this thesis.

The procedure determined for the identification of process parameters is composed by the following steps:

a. Selection of cutting tool;

b. Definition of a grid point by depth of cut and feed ($a_{p,i}$, f_j);

c. Calculation of optimum cutting speed that satisfies the optimum tool life calculated using the appropriate objective criterion (i.e., minimum production time, minimum production cost, minimum energy requirements, or minimum carbon emission). For example, the optimal cutting speed $v_{c,\ opt}(i,j)$ can be obtained as in Equation 4.1 by using a rearranged form of the extended Taylor's tool life equation (Equation 2.2):

$$v_{c,opt}(i,j) = \left(\frac{A}{T_{opt} \cdot (f_i)^{1/\beta} \cdot (a_{p,j})^{1/\gamma}} \right)^{\alpha} \tag{4.1}$$

In which T_{opt} has to be chosen between the optimum tool life that satisfy a specific criterion of time/cost/energy/CO_2 (i.e., T_{minSPT}, T_{minSPC}, T_{minSER}, or T_{minSCE}).

d. Verification of constraints related to machine tool, tool, and surface quality of the machined part. If the verification is not satisfied, the grid point could not be feasible (e.g., the working condition exceed machine power or surface quality constraint) or require a different selection of the cutting speed (e.g., due to cutting tool constraints or chatter vibrations). In this last case, the grid point determines a tool life that differs from the optimum values suggested by the implementation of the proposed methodology;

e. Computation of specific production indicators (SPT, SPC, SER, and SCE) for each set of process parameters verified;

f. Identification of the optimum combination of depth of cut, feed and cutting speed which provides the absolute minimum value of specific production time/cost, energy requirements and carbon emission. Since the cutting speed varies among the four criteria (for a given pair of a_p and f), $T_{t\text{-}o}$ can be used in Equation 4.1 in order to provide a unique value of cutting speed. The verification of the constraints when adopting $T_{t\text{-}o}$ should be always positive since the working parameters related to this condition are comprised within those identified for the four optimum tool life related to SPT, SPC, SER, and SCE.

The flow chart of Figure 12 shows the procedure previous discussed for the identification of optimum process parameters. The tables reported near the flow chart are presented as examples.

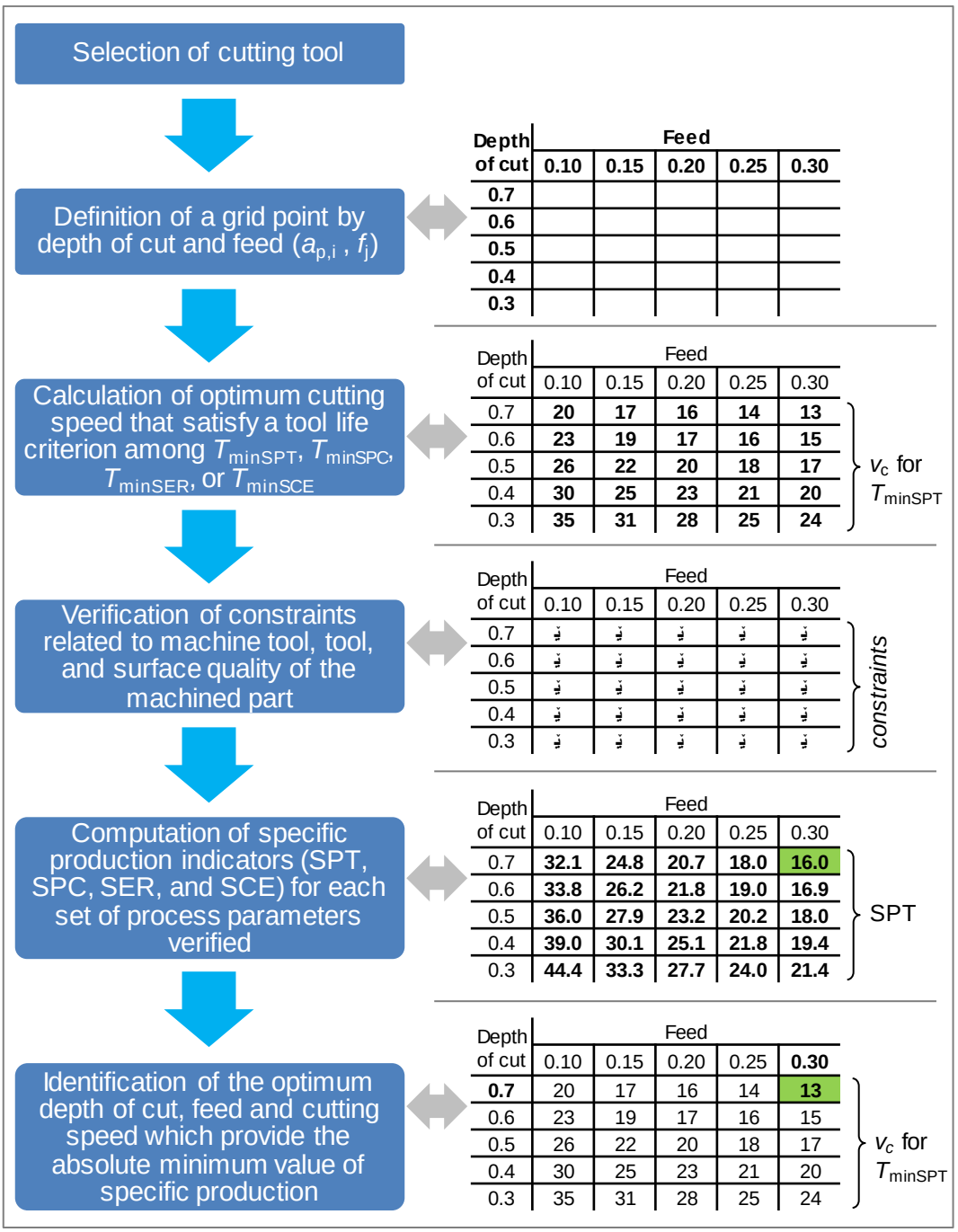

Figure 12. Procedure for the identification of optimum process parameters (flow chart on the left). Example of implementation of the procedure (tables on the right).

The case study analyzed in this section refers to dry turning of Ti-48Al-2Cr-2Nb at varying of process parameters (a_p, f, and v_c). Based on the procedure presented above, each point is now examined:

a. The cutting tool selected is the RCMT 0803 M0-SM S05F round insert with 8-mm diameter;

b. The grid point by depth of cut and feed selected according to the tool geometry is reported in Table 10;

Table 10. Values of depth of cut and feed used for the grid point.

Process Parameter	**Values**				
a_p (mm)	0.3	0.4	0.5	0.6	0.7
f (mm/rev)	0.10	0.15	0.20	0.25	0.30

c. The optimum tool life values which satisfy the minimum specific production time/cost, energy requirement, carbon emission criterions are computed by using Equations 2.7, 2.16, 2.22, and 2.28, respectively. These values of optimum tool life can be calculated by the knowledge of the exponent α used in Taylor's tool life equation (Equation 2.2), which is obtained through experimental cutting tests. The turning trials for the identification of the constant and the exponents of the Taylor's tool life equation have been performed at cutting speed v_c that ranged from 25 to 40 m/min, at feed f from 0.1 to 0.3 mm/rev, and at depth of cut a_p from 0.3 to 0.7 mm. Typical tool wear curves are plotted in Figure 13. Then, the constant and exponents identified for the generalized form of Taylor's tool life equation are computed and reported in Table 11. Three cutting tests have been executed for each combination of process parameters. The R^2 value of the regression model was higher than 0.95.

Table 11. Data for Taylor's generalized tool life equation.

Cutting Tool	***A***	**1/α**	**1/β**	**1/γ**
RCMT 0803 S05F	789,540	3.88	1.47	2.63

Therefore, the optimum tool life for minimizing SPT, SPC, SER, and SCE indices have been computed to be 346, 623, 437, and 635 s, respectively. The optimum cutting speed $v_{c,\ opt}(i,j)$ was computed by using Equation 4.1 for each pair of a_p and f, and for each optimum tool life criterions.

d. The constraints related to machine tool have been satisfied for all the cutting conditions used during experimental trials. Consequently, the optimum cutting speeds suggested by implementing the proposed methodology are identified. The constraints related to cutting tool are influenced by the tool wear behavior that was observed to change when machining at higher cutting speed [Priarone et al., 2014]. For v_c greater than 35 m/min the cutting tool reached the catastrophic failure instead of being subject to abrasive wear mechanism as observed for lower cutting speed. As a consequence, the range of allowed cutting speed is restricted below 35 m/min. In addition, surface roughness was noted to be affected by the level of feed and depth of cut adopted. Since a better surface quality of the machined workpiece was obtained when cutting at f = 0.1 mm/rev and a_p = 0.3 mm, the lowest value of feed and depth of cut are suggested during finishing operation [Sharman et al., 2001]. The results of $v_{c,\ opt}(i,j)$ computed for the four criteria after these constraints verification are reported in Figure 14.

   The low values of the computed cutting speed seem to be conservative but are not so uncommon when machining of titanium aluminides even when conventional flood cooling is applied [Beranoagirre et al., 2010; Priarone et al., 2013].

   The optimum cutting speeds obtained by considering the four different criteria are similar since the maximum variation observed is around 3 m/min for each value computed for the same pair of feed and depth of cut. Based on the suggested set of a_p, f, and v_c referred to each optimum tool life criterion, the values of MRR are computed and reported in the graphs of Figure 15. The highest values of MRR are obtained when selecting the maximum values of feed and depth of cut accounted for even though the cutting speed (for that pair of a_p and f) is the lowest. The differences between the each MRR (for a given pair of feed and depth of cut) are restricted in the range of 8 mm^3/s among the four optimization criteria.

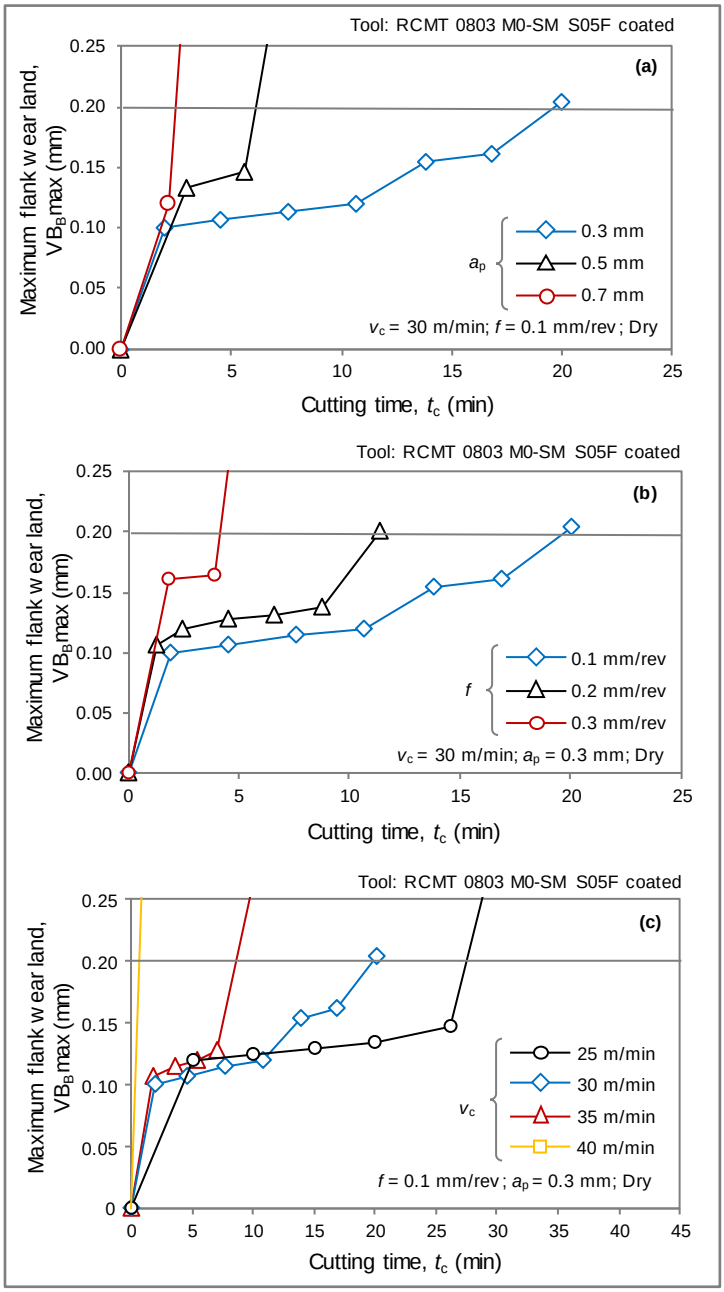

Figure 13. Tool wear curves when dry turning of Ti-48Al-2Cr-2Nb at varying of depth of cut (a), feed (b), and cutting speed (c) [Priarone et al., 2014].

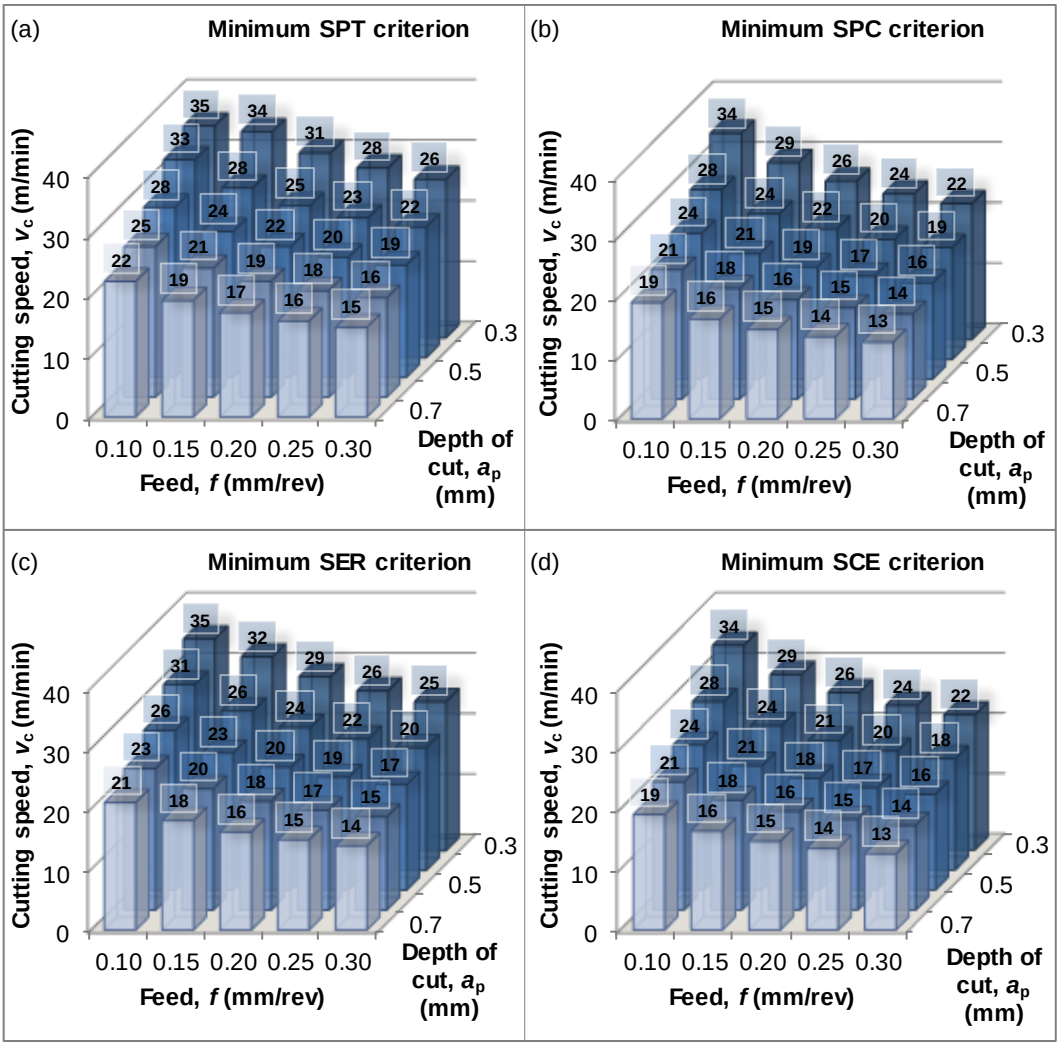

Figure 14. Optimum cutting speeds that satisfy criteria of minimum SPT (a), SPC (b), SER (c), and SCE (d) for each pair of feed and depth of cut.

e. Then, the specific production indicators SPT, SPC, SER, and SCE are computed by using Equations 2.3, 2.13, 2.19, and 2.25, respectively. Each indicator is referred to the respective set of process parameters computed in accordance with its optimization criterion, (e.g., Figure 16-a is referred to Figure 15-a). All the data reported in the inventory section have been used in order to consider time, cost, primary energy demand, and carbon footprint related to the dry turning of Ti-48Al-2Cr-2Nb.

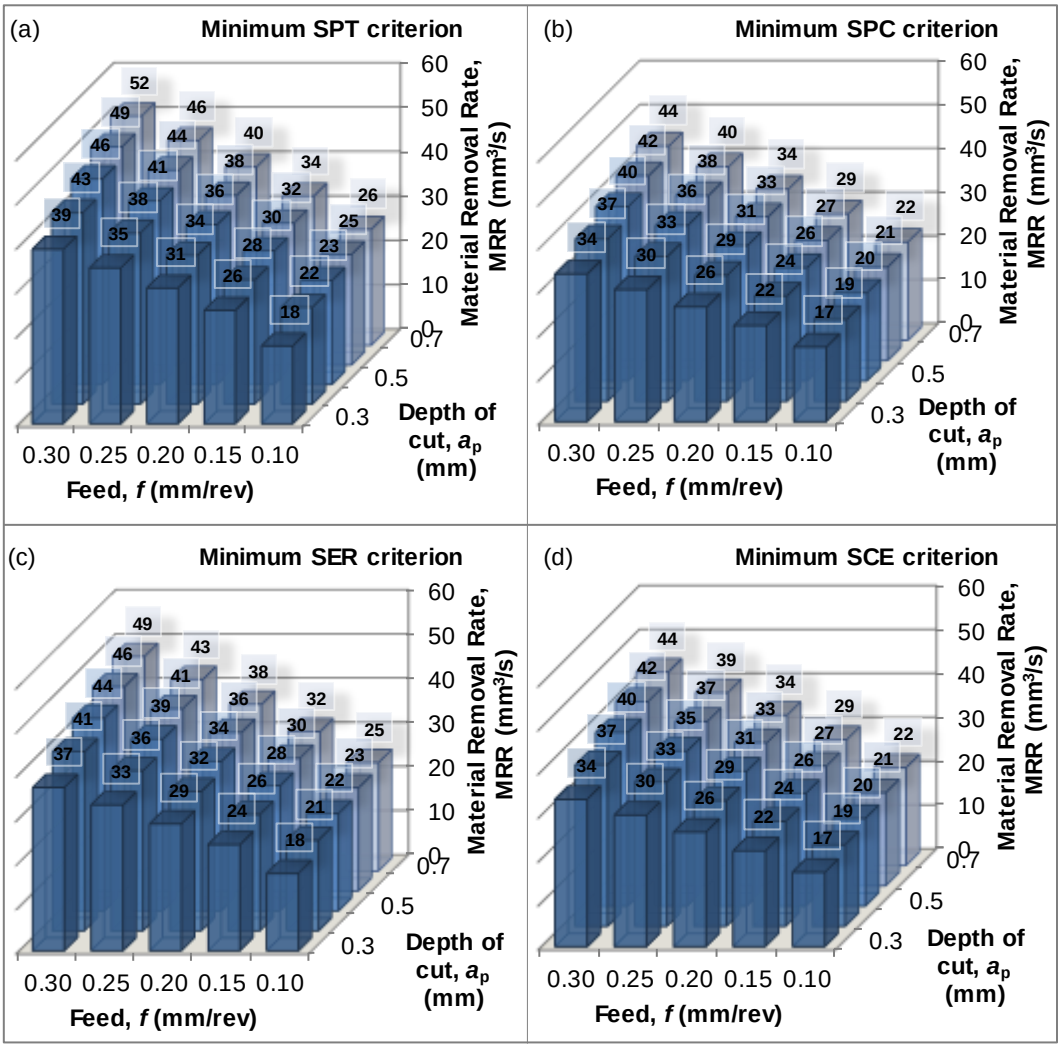

Figure 15. Material removal rate for each set of depth of cut, feed and cutting speed as reported in Figure 14.

The data of k_0, which are needed for the computation of the indicators, are obtained with a different procedure from that explained in Chapter 3 by means of Equation 3.1. This is due to the variation of the tangential cutting force component (F_t) observed when turning at different pair of feed and depth of cut. Therefore, an empirical model (Equation 4.2) is used only for this case study in order to correlate the variation of F_t as a function of k_t (specific cutting force coefficient), f,

and a_p. The adopted model is similar to that used by Arsecularatne et al. [1992].

$$F_t = k_t \cdot f^{p} \cdot a_p{}^{q} \tag{4.2}$$

Regression analysis was used to derive from the experiments the parameters k_t, p, and q used for modelling of F_t as a function of process parameters and tool wear condition. The experimental F_t were continuously acquired by the dynamometer during cutting. The data used in the model refers to the force values when the maximum flank tool wear (VB_Bmax) was approximately equal to 0.0 mm (unworn tool), 0.1 mm, and 0.2 mm (worn tool). Three regression models are computed, i.e. one for each tool wear condition. Three values of F_t (i.e., three repetitions) for each set of cutting speed, feed, and depth of cut are accounted for each regression model. The R^2 values of the regression models were higher than 0.90 for all the three tool wear conditions. The values of k_t, p, and q are reported in Table 12.

Table 12. Values of parameters of the regression model used for the estimation of tangential cutting force (F_t) as a function of process parameters and tool wear progression.

Parameter	Value		
	$VB_Bmax \cong 0.0$ mm	$VB_Bmax \cong 0.1$ mm	$VB_Bmax \cong 0.2$ mm
k_t	1634.6	1437.0	2398.7
p	0.2223	0.1185	0.2804
q	0.8010	0.7750	0.7257

As reported previously, the proposed models of Chapter 2 account for the influence of cutting power by means of the specific cutting energy k_0. The cutting power can be obtained by the product between the tangential cutting force F_t and the cutting speed v_c. Hence, the specific cutting energy k_0 can be finally expressed as function of the parameters k_t, p, and q as shown in Equation 4.3.

$$k_0 = \frac{P_{cut}}{MRR} = \frac{F_t \cdot v_c / 60}{f \cdot a_p \cdot v_c \cdot 1000 / 60} = \\ = \frac{k_t \cdot f^p \cdot a_p{}^q \cdot v_c / 60}{f \cdot a_p \cdot v_c \cdot 1000 / 60} = \frac{k_t \cdot f^{p-1} \cdot a_p{}^{q-1}}{1000} \tag{4.3}$$

Another aspect to be consider when computing the models of Chapter 2 is related to the power demand of spindle motor ($P_{spindle}$). It is worth to remark that $P_{spindle}$ is a function of spindle speed (n), which depends on the cutting speed (v_c) and the average diameter of the workpiece (D_{avg}) as shown in Equation 4.4.

$$n = \frac{1000 \cdot v_c}{\pi \cdot D_{avg}} \tag{4.4}$$

A constant value of the average diameter of the workpiece (D_{avg} = 100 mm) is considered in all the case studies when computing the spindle power required during cutting. Hence, spindle speed and, consequently, spindle power, are varied as a function of the only cutting speed.

Finally, the results of the specific production indicators are reported in the graphs of Figure 16 which are referred to the tool wear condition of $VB_Bmax \cong 0.0$ mm (i.e., unworn tool) except for SPT that is independent by the tool wear condition. The graphs of SER and SCE indices related to $VB_Bmax \cong 0.1$ mm and $VB_Bmax \cong 0.2$ mm are reported in Figure 17. The graphs of SPC for $VB_Bmax \cong 0.1$ mm and $VB_Bmax \cong 0.2$ mm are not reported since the variation of this indicator is negligible with respect to the tool wear condition.

Unanimous conclusions can be made when accounting for the four production indicators at varying of the process parameters: when rough turning the selection of the maximum allowable depth of cut and feed are needed for minimizing all the specific production indicators (SPT, SPC, SER, and SCE). There is a strictly correlation between the MRR and the outcomes of the production indicators. In particular, the maximization of the material removal rate for a given optimum tool life criterion is the best strategy when rough turning in order to reduce all the production indicators.

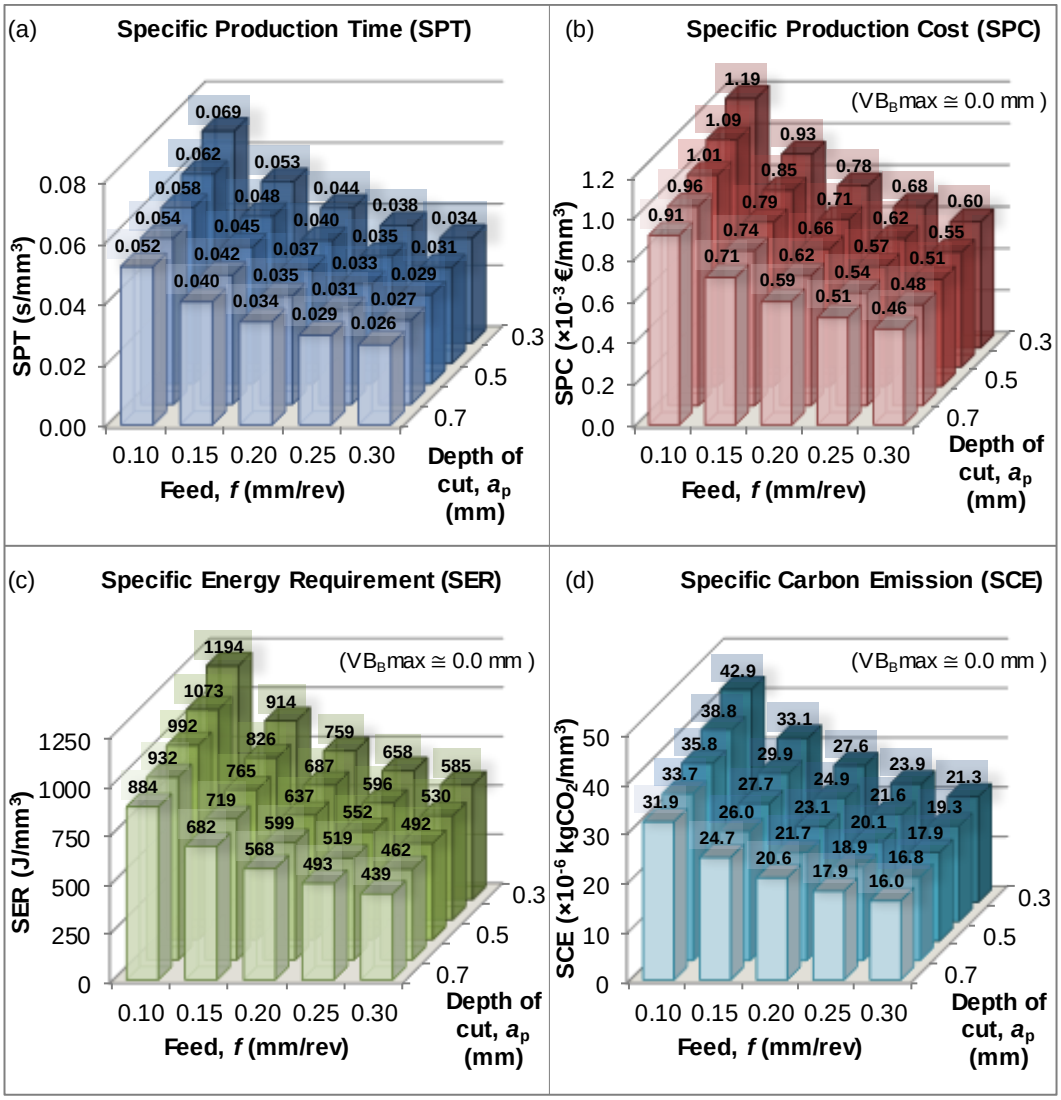

Figure 16. Specific production indicators SPT (a), SPC (b), SER (c), and SCE (d) for each set of depth of cut, feed and cutting speed as reported in Figure 14.

The requirement of setting the maximum allowable feed and depth of cut together with a reduced cutting speed is due to the tool life which is less influenced by the working condition when this combination of process parameters is selected.

The results of SPT and SPC are in accordance with those reported by Meng et al. [2000] when turning of AISI-1045 steel by using a P25 grade carbide tool: the specific production time and the specific

production cost are minimized when selecting the maximum depth of cut and feed. They highlighted that, at a given depth, it is much more economical to machine using a high-feed/low-speed combination than a low-feed/high-speed combination.

The results of SER are confirmed by studies of Velchev et al. [2014] and Yan and Li [2013] which have proposed similar conclusions for the selection of optimal process parameters.

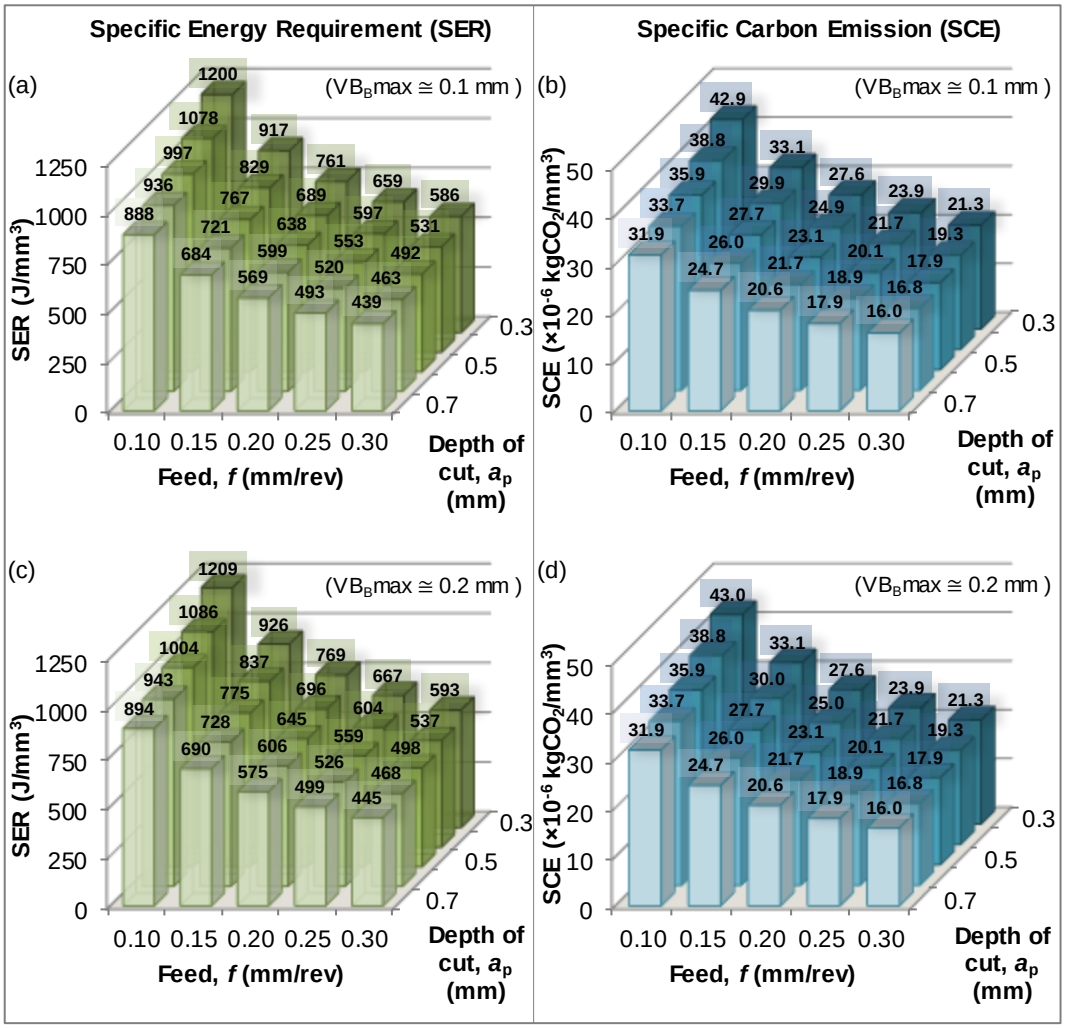

Figure 17. Specific production indicators SER and SCE for $VB_Bmax \cong 0.1$ mm (a, b) and $VB_Bmax \cong 0.2$ mm (c, d).

Furthermore, also Kara and Li [2011] suggested that less energy consumption is achieved at higher MRR (for removing same volume of material). However, their model is focused only on the unit process

energy consumption (i.e., electricity demand of the machine tool), which is not observed to vary for identical values of MRR, even when these values are determined with a different combination of process parameters.

f. Overall, the rough turning of Ti-48Al-2Cr-2Nb by using RCMT 0803 cutting tool is found to be optimized when the depth of cut is equal to 0.7 mm, the feed is 0.3 mm/rev, and the cutting speed is in the range of 13÷15 m/min, according to the production indicator which has to be optimized. However, the process parameters suggested when finish turning are different due to the requirement on surface quality of the workpiece. In this case the node of the grid which cannot satisfied the surface quality constraint are marked as unfeasible and the identification of optimum process parameters is subordinated by this constraint. Hence, a_p = 0.3 mm, f = 0.1 mm/rev and v_c = 34÷35 m/min should be selected.

Since optimum cutting speed varies among the four criteria, the trade-off criteria can be suited to identify a unique value of cutting speed. Hence, the tool life for the trade-off condition has to be used (Equation 2.36), which is equal to 502 s for a common value of weighting factors ($k_{SPT} = k_{SPC} = k_{SER} = k_{SCE} = 0.25$). As a result, the optimum cutting speeds (related to $T_{t\text{-}o}$) are computed for each pair of feed and depth of cut and reported in Figure 18-a. Moreover, the MRR and the four specific production indicators are computed according to these unique cutting speed (for each pair of feed and depth of cut) and are represented on the same Figure 18. Since the variation of specific production indicators with respect to tool wear condition are limited, the graphs of SPC (Figure 18-d), SER (Figure 18-e), and SCE (Figure 18-f) are referred only to the tool wear condition $VB_Bmax \cong 0.0$ mm.

The optimization procedure here developed can be integrated with advance modelling of machining operation such as that of Virtual machining technology [Altintas et al., 2014]. The accuracy and the effectiveness of the optimization procedure can be improved when adopting virtual machining system owing to the implementation of sound mathematical models of metal cutting processes, dynamics of machine kinematics and CNC servo drives, and cutter–part geometry engagement conditions along the tool path.

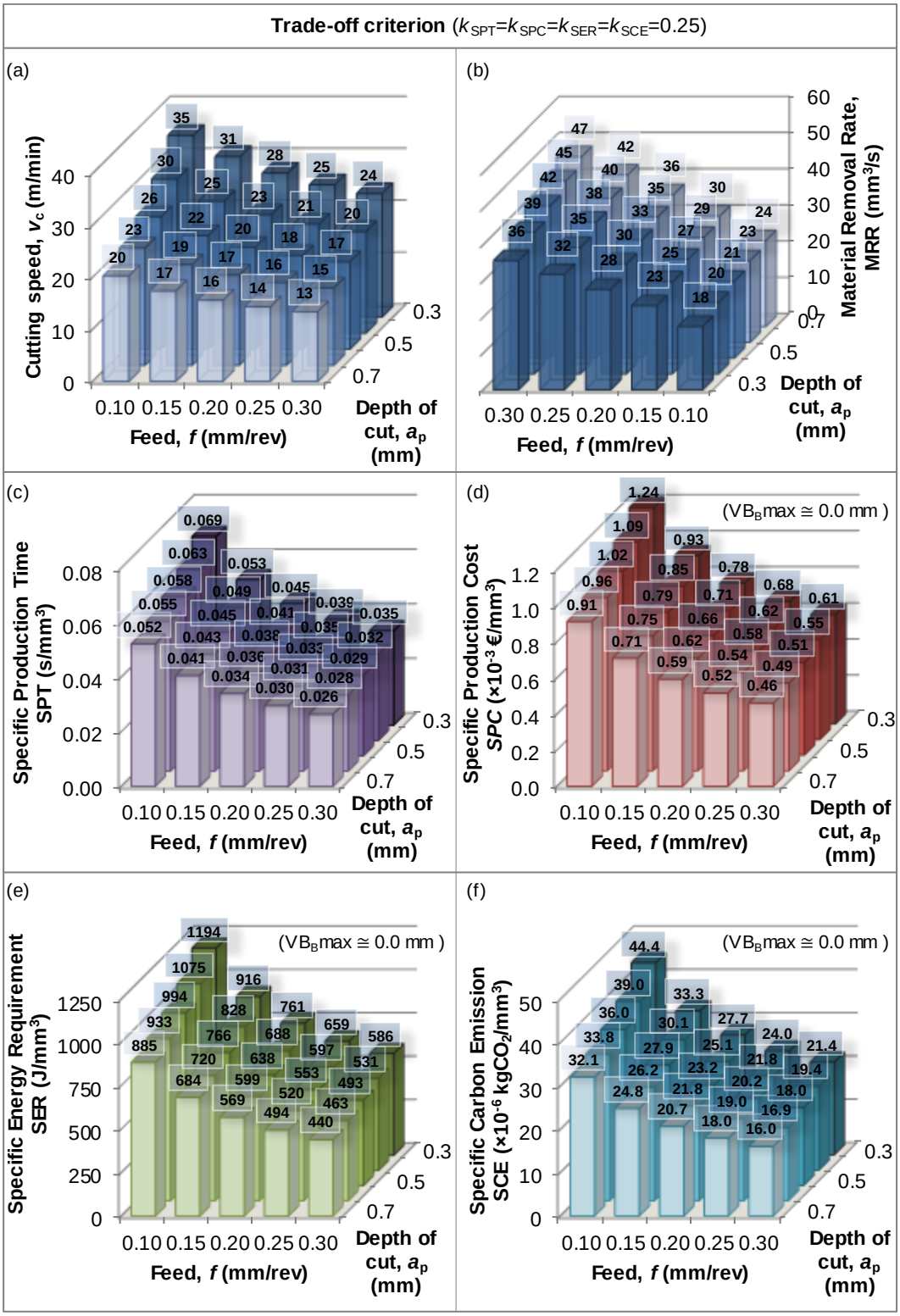

Figure 18. Cutting speed (a), Material Removal Rate (b), SPT (c), SPC (d), SER (e), and SCE (f) for the trade-off criterion.

4.2 Influence of cutting tool

The performance of two cutting tool (RCMT 0803 and RCMT 1204) is analyzed in this section by applying the proposed models. In particular, the purposes of this section are (I) the quantification of the difference in terms of economic and environmental performance and (II) the identification of optimum cutting speeds that minimize the values computed by the developed indicators for each cutting tool.

The two inserts were tested in previous studies [Priarone et al., 2014] in term of tool wear/life within a similar range of variation of cutting speed. Nevertheless, the tests performed with the RCMT 0803 insert at a cutting speed equal or higher than v_c = 40 m/min were interrupted at cutting time lower than 1 minute due to the tool catastrophic failure (Figure 19). Typical tool wear curves when using RCMT 1204 are shown in Figure 20. The 12-mm diameter cutting insert shows a tool life doubled for v_c = 30 and 35 m/min in comparison to that of the 8-mm tool (Figure 13).

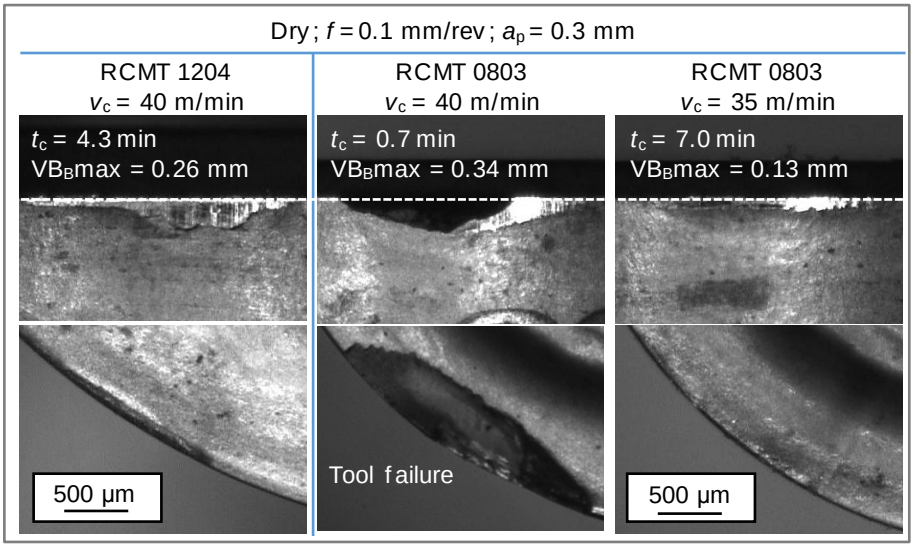

Figure 19. Tool wear observations as a function of cutting time.

The better performance highlighted by the RCMT 1204 cutting tool is owing to the larger corner radius of the main cutting edge which leads to the increase of tool life, to the decrease of cutting forces and to the decrease of surface roughness

indices [Klocke et al., 2013b; Meyer et al., 2012]. Since working conditions are expected to be stable (i.e., without achieving the tool catastrophic failure), the values of cutting speed used during experiments are limited to those reported in Table 13. The adopted process parameters are referred to a finishing operation in which feed (0.1 mm/rev) and depth of cut (0.3 mm) were kept constant.

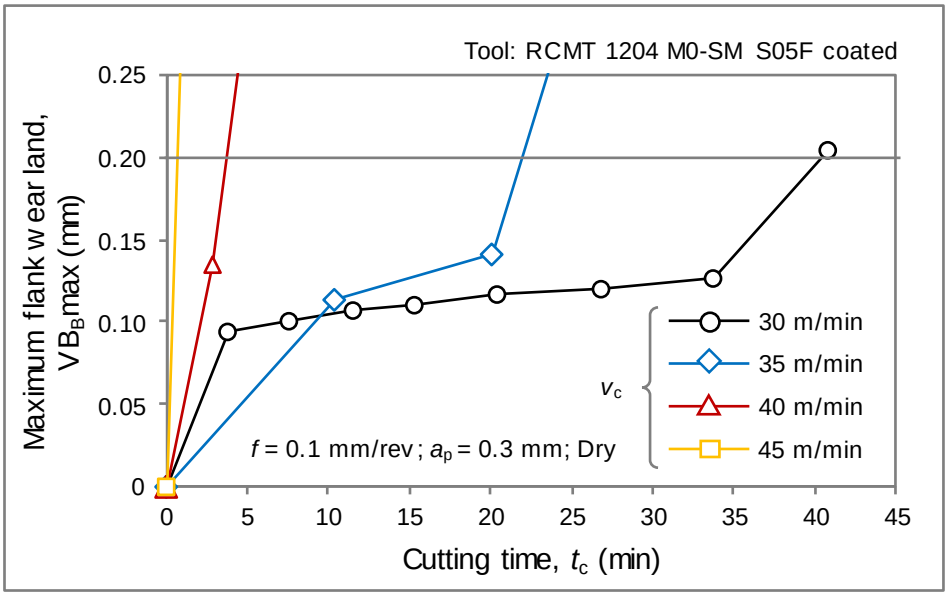

Figure 20. Tool wear curves for dry turning of Ti-48Al-2Cr-2Nb when using RCMT 1204 inserts.

Table 13. Process parameters used when turning of Ti-48Al-2Cr-2Nb as a function of cutting tool.

Cutting Tool	a_p (mm)	f (mm/rev)	v_c (m/min)	MRR (mm^3/s)
RCMT 0803 S05F	0.3	0.1	25-40	12.5-20.0
RCMT 1204 S05F	0.3	0.1	30-45	15.0-22.5

The specific cutting energy has been computed by using Equation 3.1 and the results are reported in Table 14. The values of k_0 related to RCMT 0803 can be also obtained by using Equation 4.3 and the coefficients of Table 11 as described in Section 4.1. The tangential force was found to increase as a function of tool

wear progression for both the cutting inserts. As a consequence, higher values of specific cutting energy were observed when flank tool wear was increased, especially for the insert with 12-mm diameter.

Table 14. k_0 (J/mm^3) as a function of cutting tool and tool wear progression (until reaching the tool wear limit of 0.2 mm for VB_Bmax).

Cutting Tool	VB_Bmax ≅ 0.0 mm	VB_Bmax ≅ 0.1 mm	VB_Bmax ≅ 0.2 mm
RCMT 0803 S05F	12.45	14.34	17.50
RCMT 1204 S05F	15.79	18.29	23.28

For RCMT 1204 tool geometry, the constant and the exponents for Taylor's generalized tool life equation (Table 15) come from the Taylor's curves published in [Priarone et al., 2014]. For RCMT 0803 tool geometry, the constant and the exponents for Taylor's generalized tool life equation (Table 15) are obtained from the experiments reported in Section 4.1. The R^2 values of the regression model were higher than 0.95 for both the cutting inserts. Since the influence of a_p and f were not investigated during the experimental trials when using RCMT 1204 (i.e., only the influence of cutting speed was investigated), their exponents (i.e., $1/\gamma$ and $1/\beta$, respectively) were set to zero in the model.

Table 15. Data for Taylor's generalized tool life equation.

Cutting Tool	A	$1/\alpha$	$1/\beta$	$1/\gamma$
RCMT 0803 S05F	789,540	3.88	1.47	2.63
RCMT 1204 S05F	3.95×10^{15}	8.21	0	0

Since results refers to dry turning operation, the contributes on SPT, SPC, SER, and SCE related to cleaning operations and lubricoolant usage are set to zero. The results are referred to values of $P_{spindle}$ computed for D_{avg} = 100 mm, as accounted for in the case study of Section 4.1.

- Specific Production Time

The results in terms of Specific Production Time (SPT) when turning of Ti-48Al-2Cr-2Nb with the tested cutting tools are presented in Figure 21. The results related to the cutting tool RCMT 0803 are reported within the range of cutting speed and MRR previously reported. It is worth to underline that the results achieved with cutting speed between 35 and 40 m/min are shown with a dashed line due to the change of tool wear behavior, as previously discussed. The maximum cutting speed allowed for RCMT 0803 insert is suggested below 35 m/min in order to prevent the tool catastrophic failure. The specific production time for machining (t_2/V) is inversely proportional to the MRR as well as the specific time for tool change (t_3/T/MRR) is observed to increase when increasing the MRR. The SPT values are deeply influence by the tool change operation since such contribute (t_3/T/MRR) is quantified to be equivalent to that of specific machining time (t_2/V) when MRR is around 20 mm^3/s.

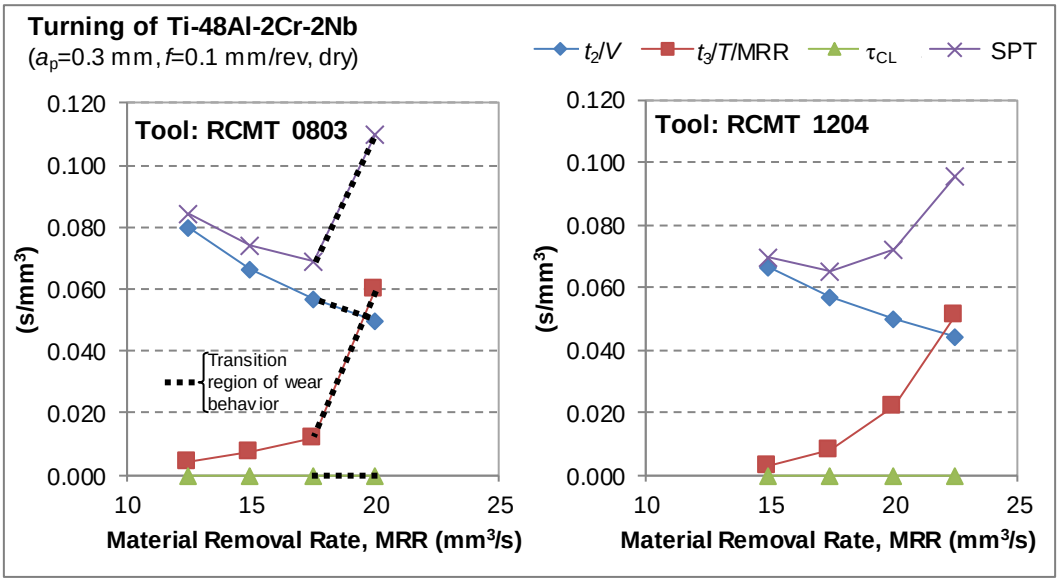

Figure 21. Specific Production Time and its contributions as a function of cutting tool.

- Specific Production Cost

The graphs related to Specific Production Cost (SPC) are presented in Figure 22. The specific cost related to tool change operation (C_3/V) is comparable to the specific cost of the cutting edge itself (C_4/V) especially when considering the tool RCMT 1204. The machining cost (C_2/V) is poorly influenced by the tool wear condition since the curves on the graphs are basically overlapped.

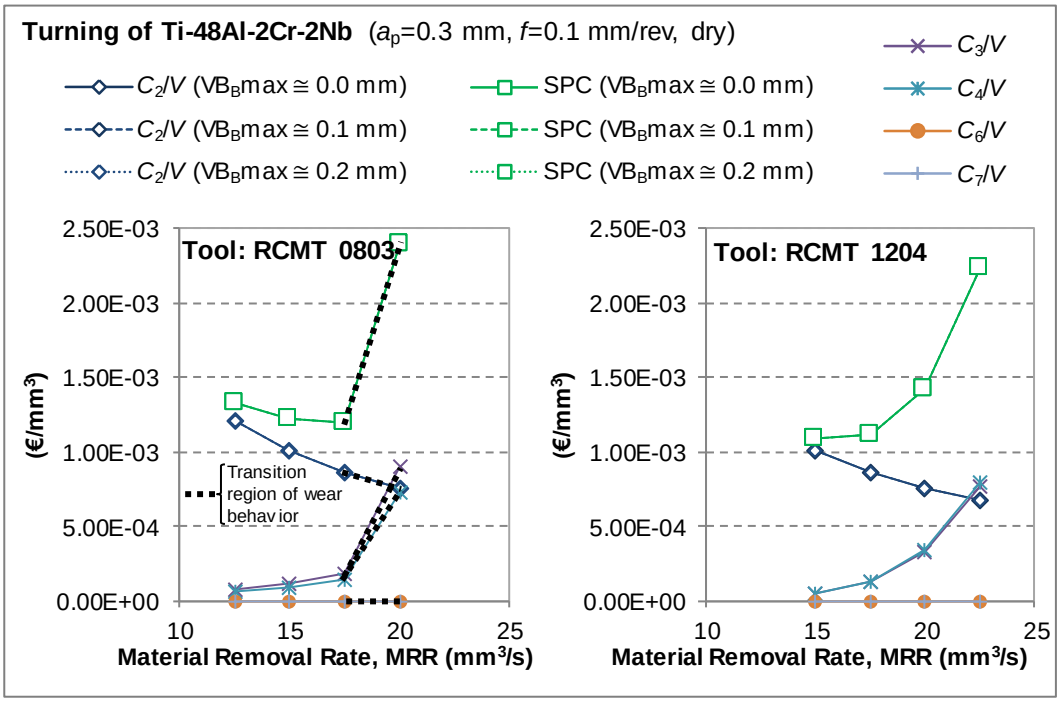

Figure 22. Specific Production Cost and its contributions as a function of cutting tool. Note: the curves for different VB_Bmax are basically overlapped.

- Specific Energy Requirement

Figure 23 represents the SER computed at varying of MRR. The primary energy demand of the machine tool (i.e., E_2/V) is similar for both the inserts and differs among them only due to the different values of k_0 computed. The insert RCMT 1204 has an embodied energy two times greater than that estimated for the RCMT 0803. As a consequence, the contribute E_4/V (together with E_3/V) plays a key role in the SER curve since the differences between the two tools are

noticeable. Slightly variations (around 1%) of SER values can be pointed out when varying the tool wear conditions. This kind of variations has been observed also by Liu et al. [2016] who highlighted that the tool wear progression has a predominant influence on energy consumption at the process level. However, their results of total specific energy are obtained through the estimation of the embodied energy of cutting tool by using the tool wear rate criterion instead of the tool life equation (as accounted for in this thesis).

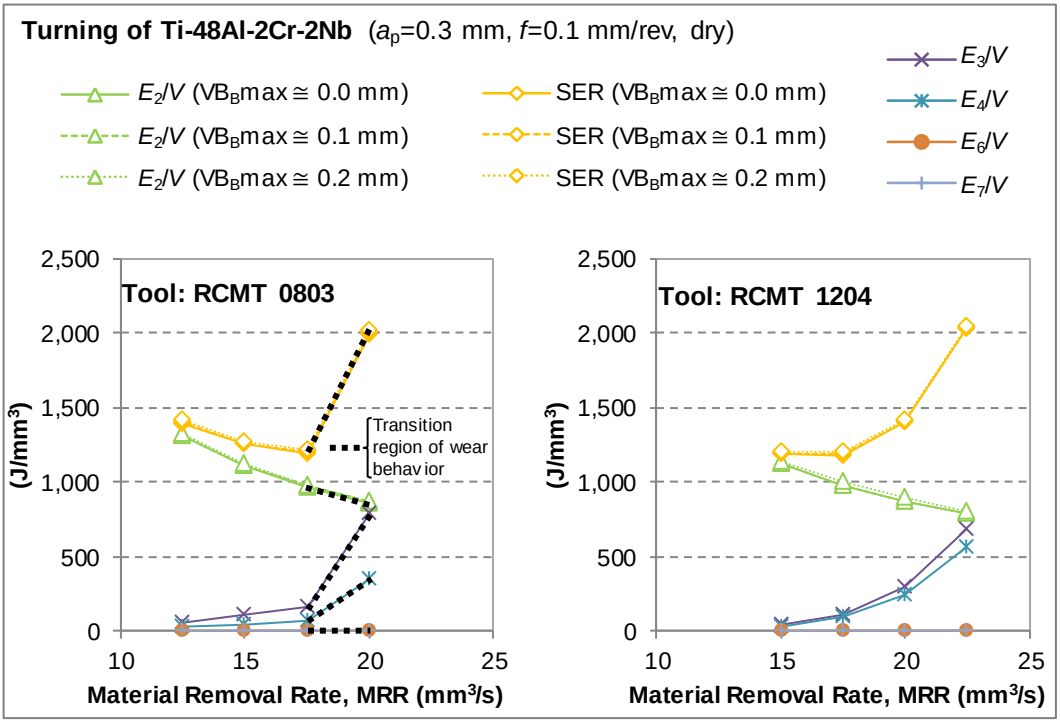

Figure 23. Specific Energy Requirement and its contributions as a function of cutting tool. Note: the curves for different VB_Bmax are basically overlapped.

- Specific Carbon Emission

The graphs related to the two tools in term of SCE index and its contributions are reported in Figure 24. The carbon footprint due to the usage of cutting tool(s) deeply influences the SCE curves especially for higher values of MRR. The term CE_4/V when using RCMT 1208 at MRR higher than 20 mm^3/s outperformed the contribute CE_2/V of the carbon emission due to the electricity consumed by the

machine tool. Therefore, a lower MRR is suggested when turning the investigated intermetallic alloy in order to reduce the total carbon emission related to the whole manufacturing process.

Overall, the four specific production indicators are represented in Figure 25 in order to give a comprehensive evaluation when turning of γ-TiAl by using the two cutting inserts. Both the cutting tools show the minimum values of each specific indicators within the range of MRR tested.

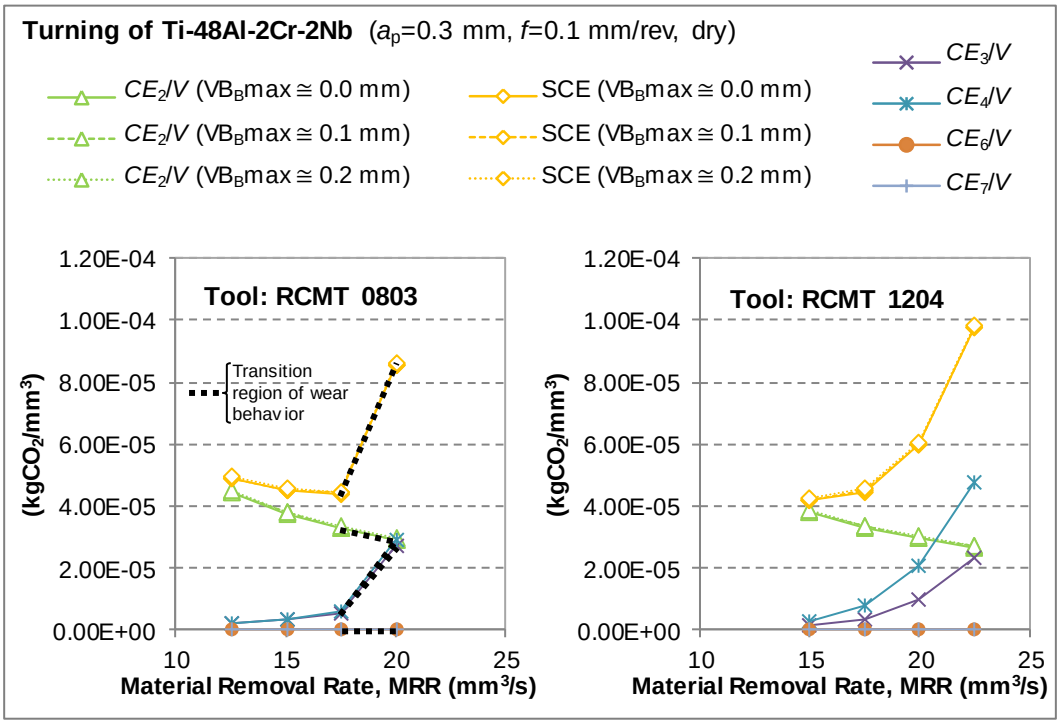

Figure 24. Specific Carbon Emission and its contributions as a function of cutting tool. Note: the curves for different VB_Bmax are basically overlapped.

The tool RCMT 1204 highlights better performance that those of RCMT 0803 in terms of SPT and SPC, while the differences in terms of SER and SCE are unnoticeable, especially around their minimum point. The cutting speeds for minimizing each specific production indicators are computed for both the cutting tool and are reported in the box plot graph of Figure 26. The graph shows the entire range of cutting speed tested for each tool by using a thin horizontal line.

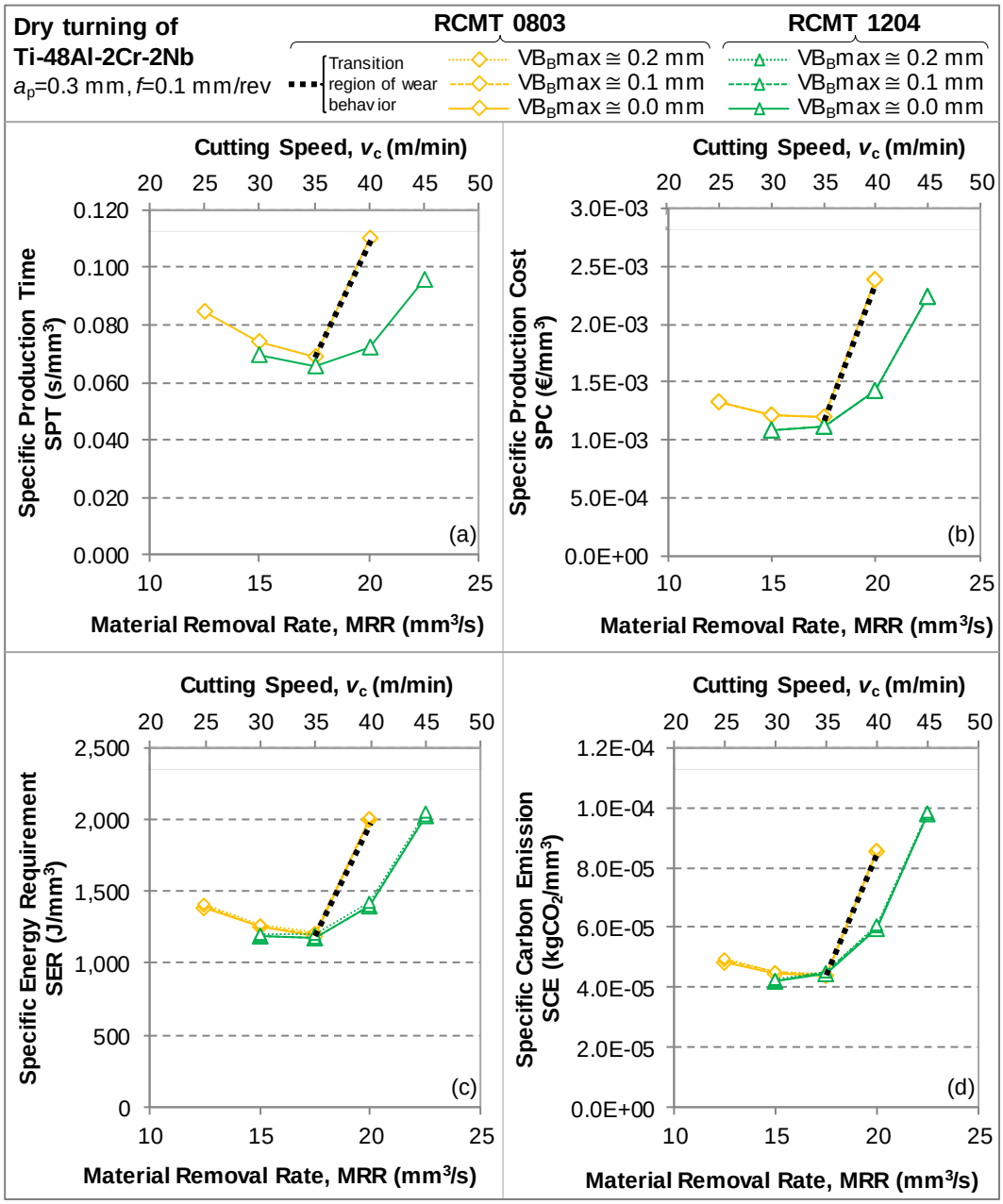

Figure 25. SPT (a), SPC (b), SER (c), and SCE (d) as a function of cutting tool. Note: the curves for different VB_Bmax are basically overlapped.

A box is used to indicate the highest and lowest cutting speed suggested by the four criterions. Each optimum cutting speed is represented by a different colour while the cutting speed for the trade-off criterion is reported with a vertical purple line.

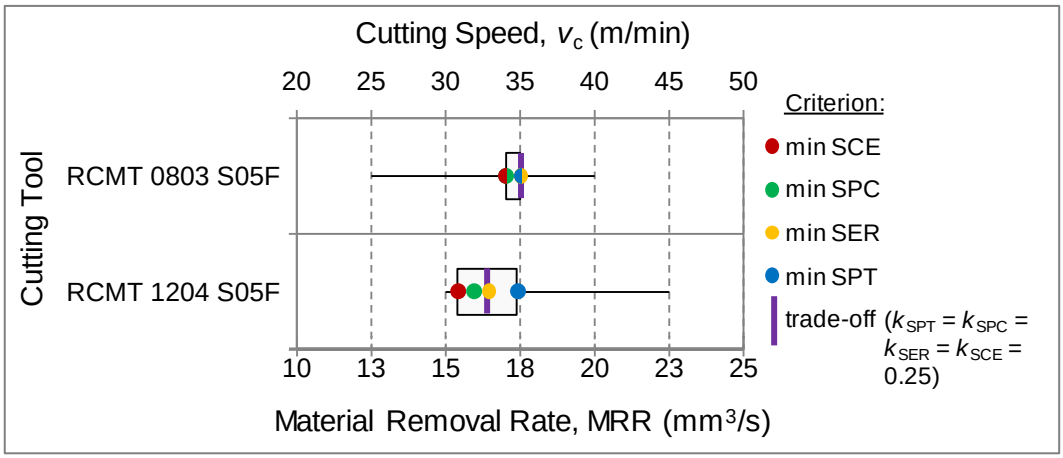

Figure 26. Range of cutting speed for minimizing the four criteria proposed as a function of cutting tool.

The cutting speed range for optimizing each criterion is between 30 and 35 m/min for both the cutting tool. Consequently, the workpiece material can be machined in an effective, economic and environmental sustainable condition by the adoption of a cutting speed enclosed in this range when using both the tool geometries analyzed. In particular, the optimum cutting speeds identified by applying the trade-off criterion ($k_{SPT} = k_{SPC} = k_{SER} = k_{SCE} = 0.25$) are equal to 35 and 32 m/min for RCMT 0803 and 1204, respectively. It is worth to remark that these cutting speeds are suggested only within the range of the tested conditions and in case of the adoption of the selected feed and depth of cut.

4.3 Influence of workpiece material

Titanium alloys such as like alpha, gamma Ti-Al alloy, and burn-resistant Ti alloys like (BuRTi) have different machinability [Pramanik, 2014]. The main issues when machining titanium alloys are caused by high tool wear and chatter due to the variation of chip thickness, high heat stress, and high pressure loads. In addition, the quality of finished products is affected by springback and residual stress. Compared to alpha-beta titanium alloys (e.g., Ti-6Al-4V), gamma TiAl alloys possess higher brittleness and has the tendency of rapid tool wear. Similar

to Ti-6Al-4V, varying shear deformation in the chip flow direction is noted with saw tooth chips composed of angular- and needle-shaped lamellae [Pramanik, 2014]. Therefore, different productivity, manufacturing cost, and environmental impact can be observed when machining different titanium alloys.

The objects of the present case study are (I) the comparison of the machining performance when turning Ti-6Al-4V and Ti-48Al-2Cr-2Nb by using the developed indicators and (II) to identify the optimum cutting speeds which allow the minimization of the aforesaid indicators.

The values of process parameters used when computing the specific production indicators are specifically chosen for each material (according to a finishing turning operation) and are reported in Table 16. Moreover, the selected values are similar to those used by Deiab et al. [2014] when cutting Ti-6Al-4V, and to those suggested by Aspinwall et al. [2005] when machining γ-TiAl. It is worth to remind that the results for Ti-48Al-2Cr-2Nb have been already discussed in Section 4.2, however they are repeated in this section for a better comparison of the result between the two workpiece materials investigated.

Table 16. Process parameters used when turning of Ti-6Al-4V and Ti-48Al-2Cr-2Nb.

Workpiece material	a_p (mm)	f (mm/rev)	v_c (m/min)	MRR (mm^3/s)
Ti-6Al-4V	0.5	0.15	90-130	112.5-162.5
Ti-48Al-2Cr-2Nb	0.3	0.10	30-45	15.0-22.5

The constant and the exponents calculated from the Taylor's curves are listed in Table 17. The Taylor curve for dry turning of Ti-6Al-4V is reported in Figure 27. Each experimental point represents the tool life result of a single cutting test. The coefficients of determination (R^2) was greater than 0.90. The slope of the curve reveals a substantial sensitivity to the cutting speed variation. This can be traced back to the influence of cutting speed on tool wear rate as shown in Figure 28 where typical tool wear curves are reported for dry turning of Ti-6Al-4V. An accelerated wear rate is noticed for cutting speeds higher than 100 m/min [Faga et al., 2017]. However, the tool wear progression for Ti-6Al-4V is lower than that observed for Ti-48Al-2Cr-2Nb (Figure 20).

Table 17. Data for Taylor's generalized tool life equation.

Workpiece material	A	$1/\alpha$	$1/\beta$	$1/\gamma$
Ti-6Al-4V	2.90×10^{13}	5.19	0	0
Ti-48Al-2Cr-2Nb	3.95×10^{15}	8.21	0	0

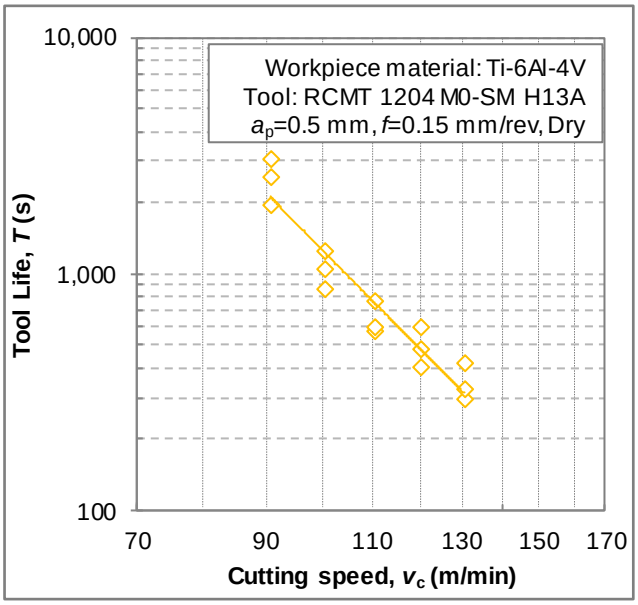

Figure 27. Taylor's curve for dry turning of Ti-6Al-4V.

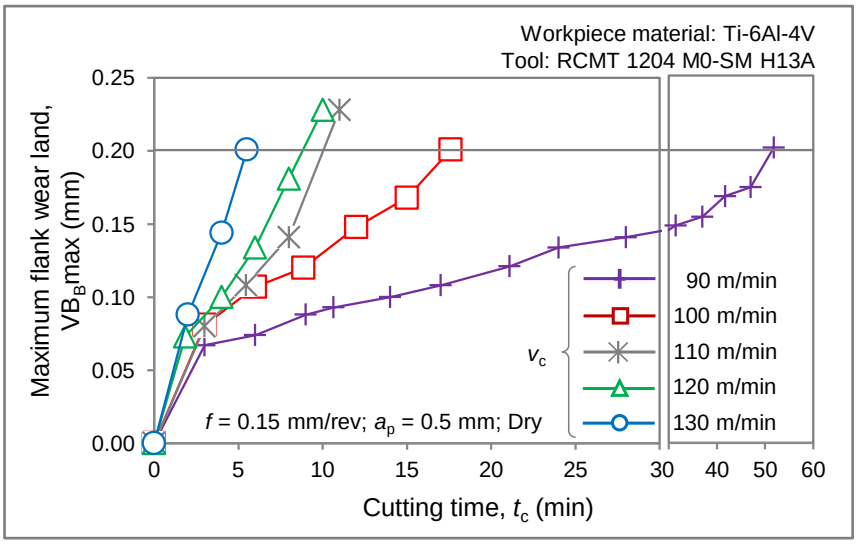

Figure 28. Typical tool wear curves for dry turning of Ti-6Al-4V at varying of cutting speed.

For each workpiece material, the specific cutting energy has been computed by using Equation 3.1 and the results are reported in Table 18. Lower tangential cutting forces were found when machining of Ti-6Al-4V compared to those of Ti-48Al-2Cr-2Nb. For both materials, the tangential cutting force increased as a function of tool wear progression. Moreover, the values of specific cutting energy computed for Ti-48Al-2Cr-2Nb are higher with respect to those of Ti-6Al-4V also due to the different uncut chip section ($a_p \times f$).

Table 18. k_0 (J/mm^3) as a function of workpiece material and tool wear progression (until reaching the tool wear limit of 0.2 mm for VB_Bmax).

Workpiece material	VB_Bmax ≅ 0.0 mm	VB_Bmax ≅ 0.1 mm	VB_Bmax ≅ 0.2 mm
Ti-6Al-4V	2.69	3.07	3.70
Ti-48Al-2Cr-2Nb	15.79	18.29	23.28

The models described in Chapter 2 were applied for computing the specific production indicators (SPT, SPC, SER, and SCE) for the finish turning of Ti-6Al-4V and Ti-48Al-2Cr-2Nb at varying of MRR. All the data listed in the inventory section related to time, cost, energy demand, and carbon emission have been used. Since the results for Ti-48Al-2Cr-2Nb are the same presented in the previous case study of Section 4.2 (see graphs for tool RCMT 1204), only the results for Ti-6Al-4V are shown in detail in the next paragraphs. Nevertheless, a comparison of the results for both the workpiece material is given and discussed with new graphs reported at the end of this section.

- Specific Production Time

Machining of Ti-6Al-4V requires a Specific Production Time (Figure 29) one order of magnitude lower than that needed when cutting Ti-48Al-2Cr-2Nb (Figure 21). A slightly variation of SPT at varying of MRR is noticed when turning Ti-6Al-4V, therefore the differences between each test performed are enclosed in a small interval (0.001 s/mm^3) compared to that observed for Ti-48Al-2Cr-2Nb (0.03 s/mm^3). The specific time required for tool change operation (t_3/T/MRR) is low compared to the specific time for cutting (t_2/V). However, this contribute on SPT becomes greater when MRR increases.

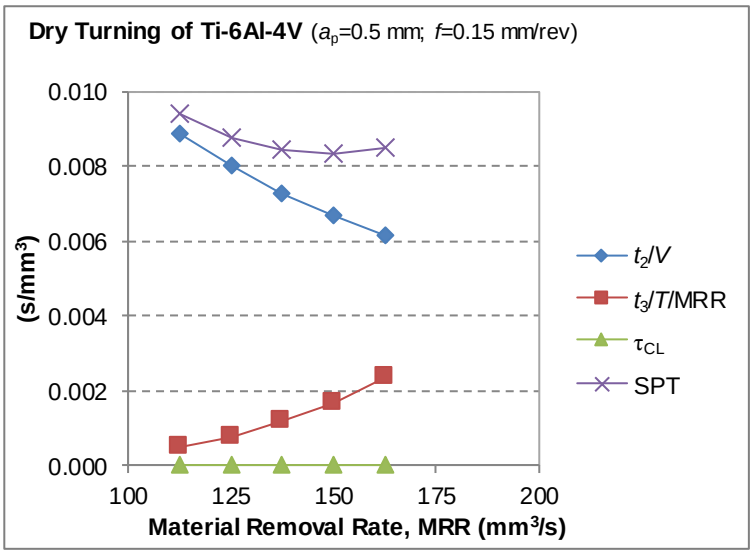

Figure 29. Specific Production Time and its contributions for dry cutting of Ti-6Al-4V.

- Specific Production Cost

The results of Specific Production Cost computed for Ti-6Al-4V alloy are represented in Figure 28 together with its contributes. The cost contributes related to the cutting tool (C_3/V and C_4/V) are lower than the contribute owing to machine tool usage (C_2/V) even for the highest values of MRR tested. The minimum specific cost when machining Ti-6Al-4V is one order of magnitude lower than that required for TiAl intermetallic alloy, and this consideration is according to the value of specific production time previously discussed. The influence of tool wear state on C_2/V and SPC is negligible since the curves at varying of VB_Bmax are basically overlapped.

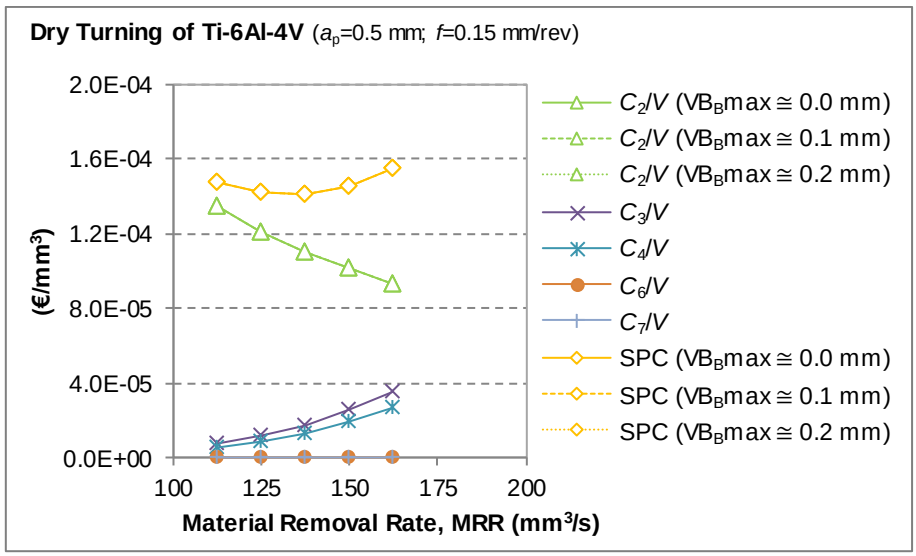

Figure 30. Specific Production Cost and its contributions for dry cutting of Ti-6Al-4V. Note: the curves for different VB_Bmax are basically overlapped.

- Specific Energy Requirement

The curves of SER and its contributions for Ti-6Al-4V are plotted in Figure 31. Each contribute remarks the trend previously observed in terms of specific production time/cost. Therefore, the Specific Energy Requirement index is deeply influenced by the contribute related to machine tool usage (E_2/V), whereas the contributes owing to cutting tool usage and replacing (E_3/V and E_4/V) become relevant only at higher values of MRR. The minimum value of SER for Ti-6Al-4V is 15 % of that observed for Ti-48Al-2Cr-2Nb. The influence of tool wear behavior on SER is marginal even if is more evident than that observed in term of cost. This fact be traced back to the electricity demand which is higher when tool wear increases. Hence, primary energy demand is more sensitive to the variation of the specific cutting energy (k_0) with respect to machining cost, which is mainly influenced by the overall machining cost rate. An increase in electricity consumption is less significant in terms of cost with respect to the effect in terms of environmental impact (i.e., primary energy demand).

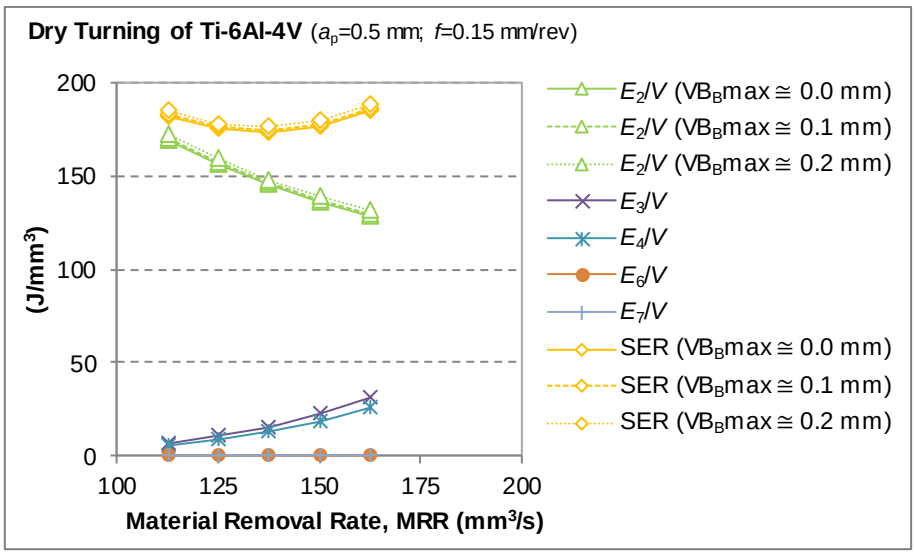

Figure 31. Specific Energy Requirement and its contributions for dry cutting of Ti-6Al-4V.

- Specific Carbon Emission

Figure 32 shows the curves of Specific Carbon Emission indicator and its contributions for Ti-6Al-4V. Similar considerations can be repeated for the composition of the SCE curve with respect to those discussed in terms of SER. However, the contribute of carbon emission due to tool usage (CE_4/V) is greater than that for tool change operation (CE_3/V). This can be traced back to the production phases used for the production of carbide cutter, in which high amounts of heat and electricity are required [Katiyar et al., 2014]. The minimum carbon footprint when machining Ti-6Al-4V is 15 % of that for Ti-48Al-2Cr-2Nb.

Overall, Figure 33 is presented in order to plot four graphs in which the results of each specific production indicator are computed for both the workpiece material taken into account. The differences between Ti-6Al-4V and Ti-48Al-2Cr-2Nb are noticeable since the curves of the two materials are placed in different areas of each graph. Ti-48Al-2Cr-2Nb highlights high values of SPT, SPC, SER and SCE as well as requires low MRRs. By contrast, curves of specific production indicators for Ti-6Al-4V are defined for higher values of MRR and each indicator is one order of magnitude lower that those observed for Ti-48Al-2Cr-2Nb.

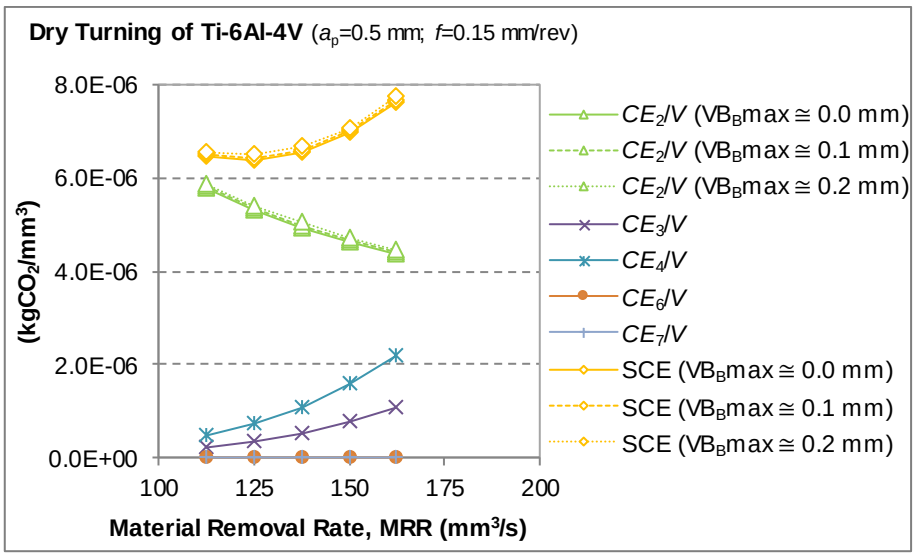

Figure 32. Specific Carbon Emission and its contributions for dry cutting of Ti-6Al-4V.

Moreover, the variation of process parameters when machining Ti-6Al-4V led to a negligible variation on specific production indices when compared to the variation observed when machining γ-TiAl intermetallic alloy. The productivity when dry cutting of titanium aluminides is extremely reduced due to the high tool wear caused by the rapid grow of temperature in the cutting zone. However, several techniques such as the application of coolant and the usage of high conductive cutting tool and tool holder have been applied in some researches in order to limit this problem [Pramanik et al., 2014]. Nevertheless, the minimization of SPT, SPC, SER and SCE is suggested for both the workpiece material by the adoption of optimal cutting speeds.

The values of each cutting speed that allow to minimize each indicators are represented in the box plot graph of Figure 34. The horizontal axis used for MRR is discontinuous due to the different values of feed and depth of cut used for the two workpiece materials. In particular, the portion of axis between 10 and 25 mm^3/s is valid for TiAl while the axis portion between 113 and 175 mm^3/s is valid for Ti-6Al-4V. The range of cutting speed which should be adopted for an efficient and sustainable machining of both materials is comprised between the cutting speed for minimum carbon emission and the cutting speed for minimum production time. The range of optimum cutting speed for Ti-6Al-4V is between 98 and 119 m/min. In particular, a cutting speed of 107 m/min is suggested when

adopting the trade-off criterion ($k_{SPT} = k_{SPC} = k_{SER} = k_{SCE} = 0.25$) as a tool for decision. It is worth to point out that this range of cutting speed is valid for the tested condition and for the selected values of feed and depth of cut.

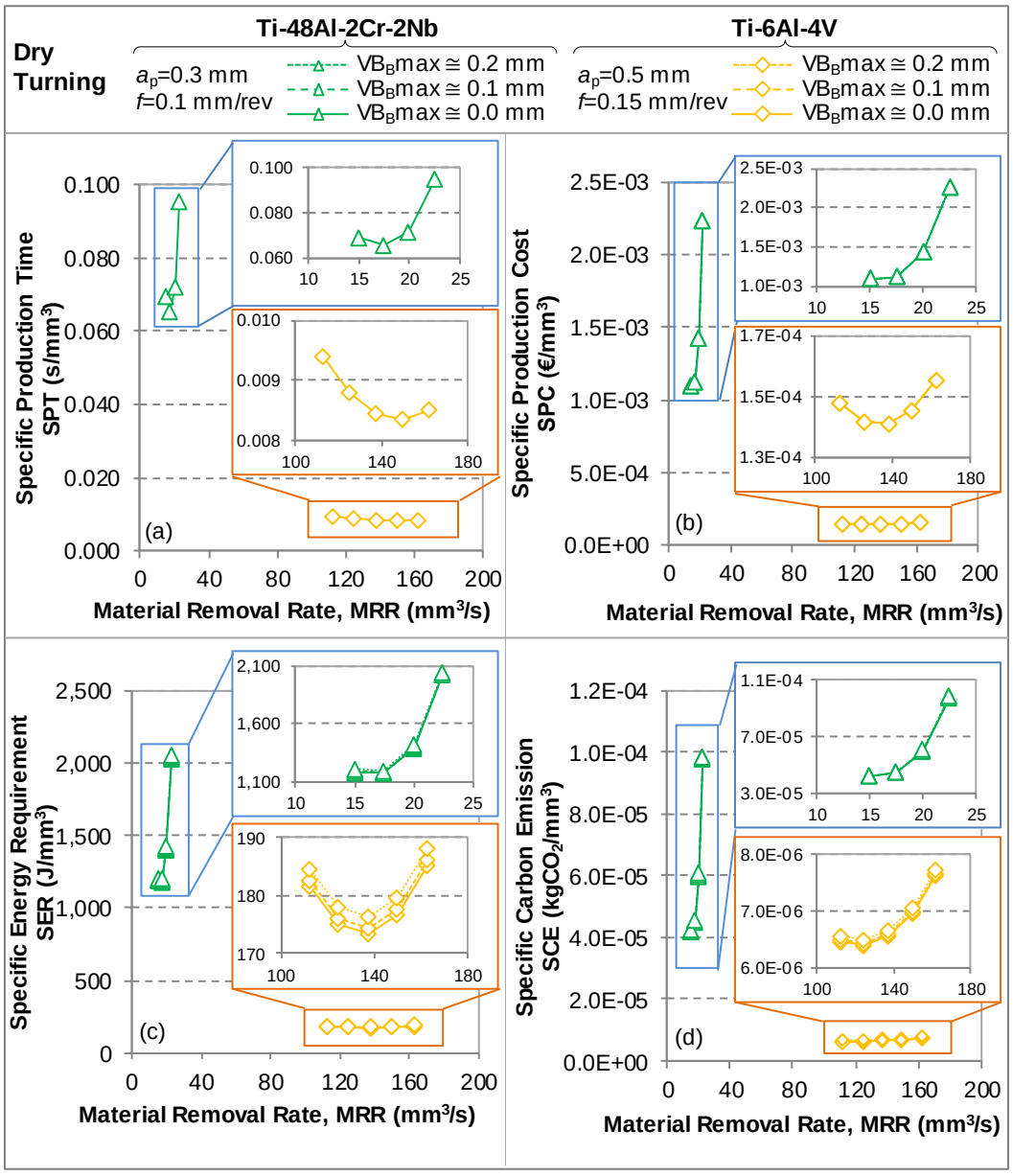

Figure 33. SPT (a), SPC (b), SER (c), and SCE (d) as a function of workpiece material. Note: the curves for SPC at different VB_Bmax are basically overlapped.

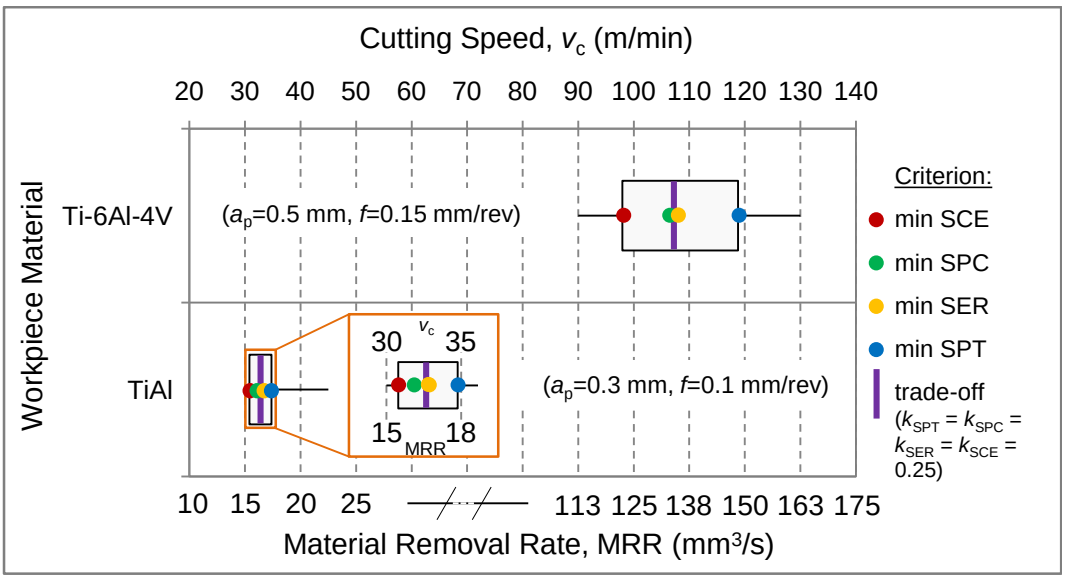

Figure 34. Range of cutting speed for minimizing the four criteria as a function of workpiece material. Note: The values of MRR between 10 and 25 mm^3/s are valid for TiAl. The values of MRR between 113 and 175 mm^3/s are valid for Ti-6Al-4V.

4.3.1. Contribute of the workpiece on total cost, energy demand, and carbon emission

This subsection is introduced in order to consider the influence of the workpiece on total cost, energy demand, and carbon emission since this contribute has been omitted in the computation of specific production indicators. The material is expected to play a key role in the determination of cost, primary energy demand, and carbon emission, especially when difficult-to-cut materials are taken into account. Hence, this subsection is aimed at providing a complete overview of the cradle-to-gate LCA described in Section 1.2 which comprises the phases related to the material production and the product manufacture.

When workpiece material is accounted for the computation of total production cost, energy, and carbon footprint some hypotheses have to be apply regarding the volume (or the mass) of the part produced as well as the volume of material removed from the initial workpiece. The Buy-to-Fly (BtF) ratio can be suited to analyze the influence of the material onto the whole manufacturing process. The Buy-to-Fly (BtF) ratio is defined as the ratio of the mass (or volume) of the starting bar/billet of material (i.e., workpiece) to the mass (or volume) of the final

machined part [Watson and Taminger, 2016] The form of BtF used in this thesis is reported in Equation 4.5.

$$\mathrm{BtF} = \frac{V_W}{V_P} \tag{4.5}$$

BtF ratios of 10-to-1 or even higher are common in aerospace applications and this implies that most of the initial volume of the workpiece is removed and discarded when using machining processes to manufacture a product. As a consequence, the economic and environmental sustainability of material removal processes is deeply influence by the BtF ratio to be satisfied.

The total production cost (*C*), the total energy requirement (*E*), and the total carbon emission (*CE*) can be computed as the sum of the contribute due to the material production plus the contribute related to the machining phase (Equations 4.6, 4.7, and 4.8). The volume of the material removed during machining (*V*) and the volume of the initial workpiece (V_W) can be expressed as a function of the buy-to-fly ratio and the volume of the final part (V_P).

$$\begin{aligned} C &= \overbrace{\mathrm{SPC}\cdot V}^{machining} + \overbrace{x_W \cdot V_W}^{material} = \overbrace{\mathrm{SPC}\cdot\frac{V_W - V_P}{V_P}\cdot V_P}^{machining} + \overbrace{x_W \cdot \frac{V_W}{V_P}\cdot V_P}^{material} = \\ &= \underbrace{\mathrm{SPC}\cdot(\mathrm{BtF}-1)\cdot V_P}_{machining} + \underbrace{x_W \cdot \mathrm{BtF}\cdot V_P}_{material} \end{aligned} \tag{4.6}$$

$$\begin{aligned} E &= \overbrace{\mathrm{SER}\cdot V}^{machining} + \overbrace{y_W \cdot V_W}^{material} = \overbrace{\mathrm{SER}\cdot\frac{V_W - V_P}{V_P}\cdot V_P}^{machining} + \overbrace{y_W \cdot \frac{V_W}{V_P}\cdot V_P}^{material} = \\ &= \underbrace{\mathrm{SER}\cdot(\mathrm{BtF}-1)\cdot V_P}_{machining} + \underbrace{y_W \cdot \mathrm{BtF}\cdot V_P}_{material} \end{aligned} \tag{4.7}$$

$$\begin{aligned} CE &= \overbrace{\mathrm{SCE}\cdot V}^{machining} + \overbrace{z_W \cdot V_W}^{material} = \overbrace{\mathrm{SCE}\cdot\frac{V_W - V_P}{V_P}\cdot V_P}^{machining} + \overbrace{z_W \cdot \frac{V_W}{V_P}\cdot V_P}^{material} = \\ &= \underbrace{\mathrm{SCE}\cdot(\mathrm{BtF}-1)\cdot V_P}_{machining} + \underbrace{z_W \cdot \mathrm{BtF}\cdot V_P}_{material} \end{aligned} \tag{4.8}$$

Hence, even the total production cost (*C*), the total energy requirement (*E*), and the total carbon emission (*CE*) are a function of the buy-to-fly ratio and the

volume of final part. Figure 35 has been prepared in order to evaluate the contributes of cost, primary energy, and carbon emission due to material and machining of Ti-6Al-4V and Ti-48Al-2Cr-2Nb at varying of BtF. V_P is assumed equal to 1 dm^3 while the machining costs of Ti-6Al-4V and Ti-48Al-2Cr-2Nb are computed selecting their minimum SPC values (see Figure 33-b). For each type of material, the trend of both cost contributes (machining and material) is linear with respect to BtF (Figure 33-a). However, the curves show a different slope with the presence of a breakeven point in which the two contributes are equal. This point is verified when the buy-to-fly ratio is equal to SPC/(SPC - x_W). Since the cost curves (machining and material) for Ti-6Al-4V show a similar slope, the BtF for their breakeven point (~17) is higher than that for Ti-48Al-2Cr-2Nb (~1.5). Below the BtF for the breakeven condition the cost contribute due to the workpiece prevails on that owing to machining. Hence, the machining cost of Ti-48Al-2Cr-2Nb plays a key role in the total production cost and the optimization of the machining phase is crucial.

The contributes on primary energy demand (Figure 35-b) and on carbon footprint (Figure 35-c) highlight a different behaviour with respect to those observed in terms of costs. The minimum values of SER and SCE (see graphs c and d of Figure 33) related to each workpiece material have been accounted for the computation of the energy demand and carbon emission, respectively, due to the machining contribute. The environmental impact due to material production is higher than that of machining for both the titanium alloys. As a consequence, the breakeven point of the material and machining curves does not exist.

Overall, when the system boundary of the LCA refers to a cradle-to-gate approach, in which the material production is accounted for together with the manufacturing phase, contrasting conclusion can be defined with respect to targets of cost and environmental sustainability. For difficult-to-cut materials, which are machined at higher buy-to-fly ratio, the total production cost can be more influenced by the contribute related to the product manufacture phase compared to that of the material production phase. On the other hand, both the primary energy requirement and carbon emission are more affected by the material production phase. Materials which are obtained by secondary production (i.e., with recycled material) can represent a sustainable alternative in order to reduce the environmental impact [Ingarao, 2017].

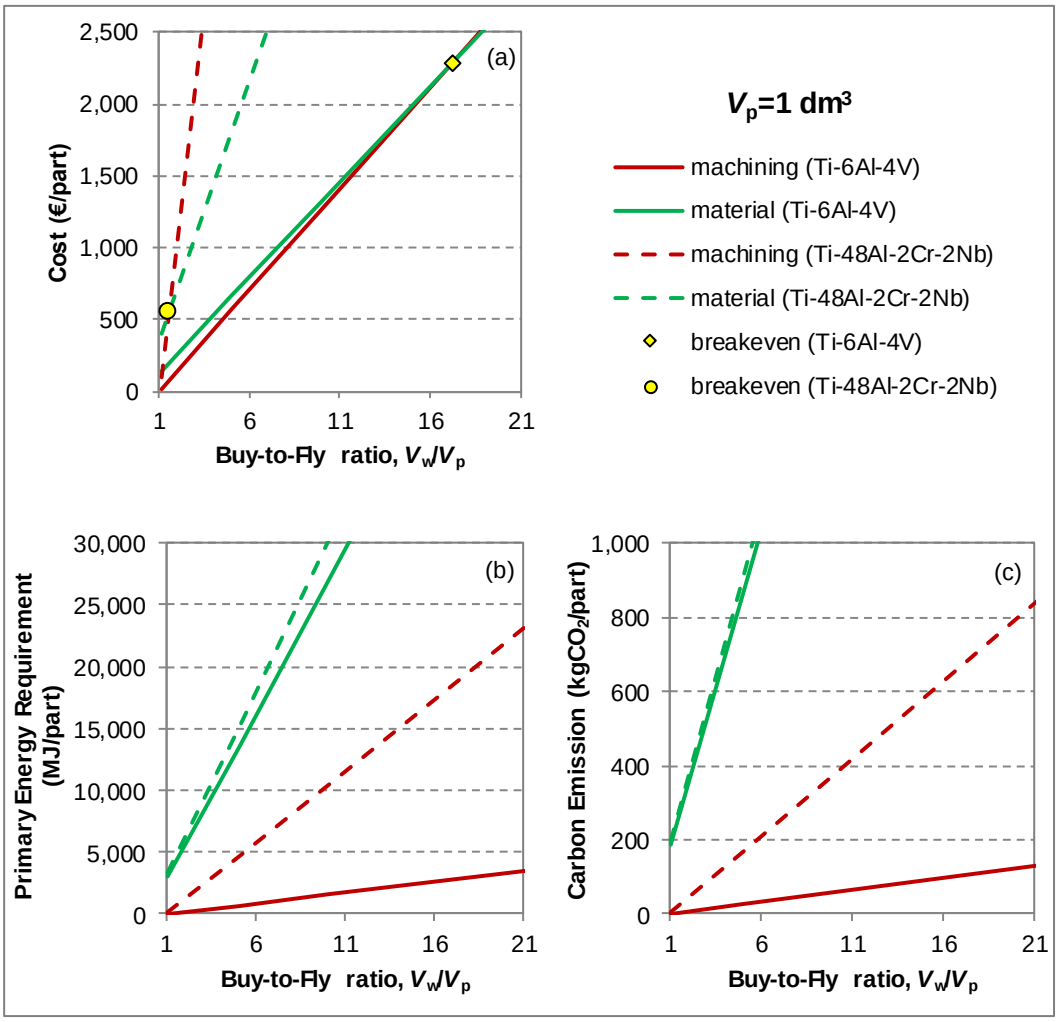

Figure 35. Production costs (a), primary energy demands (b) and carbon footprints (c) versus buy-to-fly ratio when machining of Ti-6Al-4V and Ti-48Al-2Cr-2Nb.

4.4 Influence of lubrication/cooling conditions

The application of metalworking fluids can improve the process productivity ensuring workpiece quality as well as reducing tool wear [Brinksmeier et al., 2015]. However, the consumption of cutting fluids represents an additional productive cost and causes environmental issues which are dependent on the specific chemical composition of the metalworking fluid used. Therefore, the

evaluation of the influence of lubrication/cooling condition should be performed accounting for either economic aspects or environmental issues. The application of alternative lubrication/cooling strategies such as those represented by Minimum Quantity Cooling Lubrication (MQCL) systems has to be assessed with respect to conventional flood cooling by considering an integrated approach that accounts for all the aspects related to cutting fluid consumption, power demand for auxiliary systems, and additional costs for buying and maintaining the specific supply system.

The aim of the present case study is (I) to exploit the developed models for quantify the difference in terms of production time/cost/energy demand/CO_2 emission when turning of Ti-6Al-4V under various lubrication/cooling conditions (i.e., Dry, Wet, MQL, EMCL); (II) to provide optimum working conditions (i.e., cutting speeds) which lead the minimum values computable by the proposed indices with respect to a specific target or for the trade-off condition.

A conventional finishing operation was considered at which the feed and the depth of cut were kept constant to 0.15 mm/rev and 0.5 mm, respectively. Cutting speed and, as a consequence, MRR were varied within a range specifically chosen for each lubrication/cooling condition, as reported in Table 19. The data related to dry cutting condition has been already presented in Section 4.3, however they are reported again in the following as benchmark for the comparison with other lubrication/cooling conditions.

Table 19. Process parameters used when turning of Ti-6Al-4V under various lubrication conditions.

Lubrication	a_p (mm)	f (mm/rev)	v_c (m/min)	MRR (mm^3/s)
Dry	0.5	0.15	90-130	112.5-162.5
Wet	0.5	0.15	100-150	125.0-187.5
MQL	0.5	0.15	110-140	137.5-175.0
EMCL	0.5	0.15	120-150	150.0-187.5

The data for Taylor's tool life equation are obtained from experimental tests in which each lubrication/cooling system was used during machining. The data refer to cutting tests aimed at assessing the tool wear progression at varying of cutting speed. The tool wear observations revealed that the flank wear was

progressively increased until reaching the tool wear limit of $VB_B max = 0.2$ mm for all the applied lubrication/cooling conditions [Faga et al., 2017]. The occurrence of catastrophic tool failure or breakage/chipping of the cutting edge was not detected. Typical tool wear curves when turning of Ti-6Al-4V under wet, MQL, and EMCL conditions are plotted in Figure 36.

Higher cutting speeds (up to 150 m/min) can be allowed when machining by using water-based cutting fluids such as those used for wet or EMCL lubrication/cooling conditions. Moreover, the results achieved with the EMCL were proved to be even better, in terms of tool wear, than those obtained with the conventional flood cooling (wet cutting). Such evidence can be traced back to the different kind of cutting fluid used and to the delivery system that was used to apply the lubricoolant to the cutting area. In particular, the setup for EMCL has been assessed to allow a higher penetration of the cutting fluid into the chip/tool wedge [Priarone et al., 2015]. By contrast, the application of MQL, which provides only a lubricating effect of the vegetable-based oil, achieved intermediate results in terms of tool wear between those of dry (Figure 28) and wet cutting (Figure 36-b).

The constant and the exponents calculated from the Taylor's curves (Figure 27 and Figure 37) are listed in Table 20. The R^2 values of the regression models were higher than 0.95 for all the lubrication conditions. Each experimental point represents the tool life result of a single cutting test. The slope of the curves of Figure 35 reveals a substantial sensitivity to the variation of cutting speed as noticed in case of dry cutting (Figure 25). Since a_p and f were fixed, their exponents were set to zero in the model.

Table 20. Data for Taylor's generalized tool life equation [Priarone et al., 2016].

Lubrication	A	$1/\alpha$	$1/\beta$	$1/\gamma$
Dry	2.90×10^{13}	5.19	0	0
Wet	5.25×10^{14}	5.63	0	0
MQL	1.83×10^{13}	5.02	0	0
EMCL	3.97×10^{16}	6.45	0	0

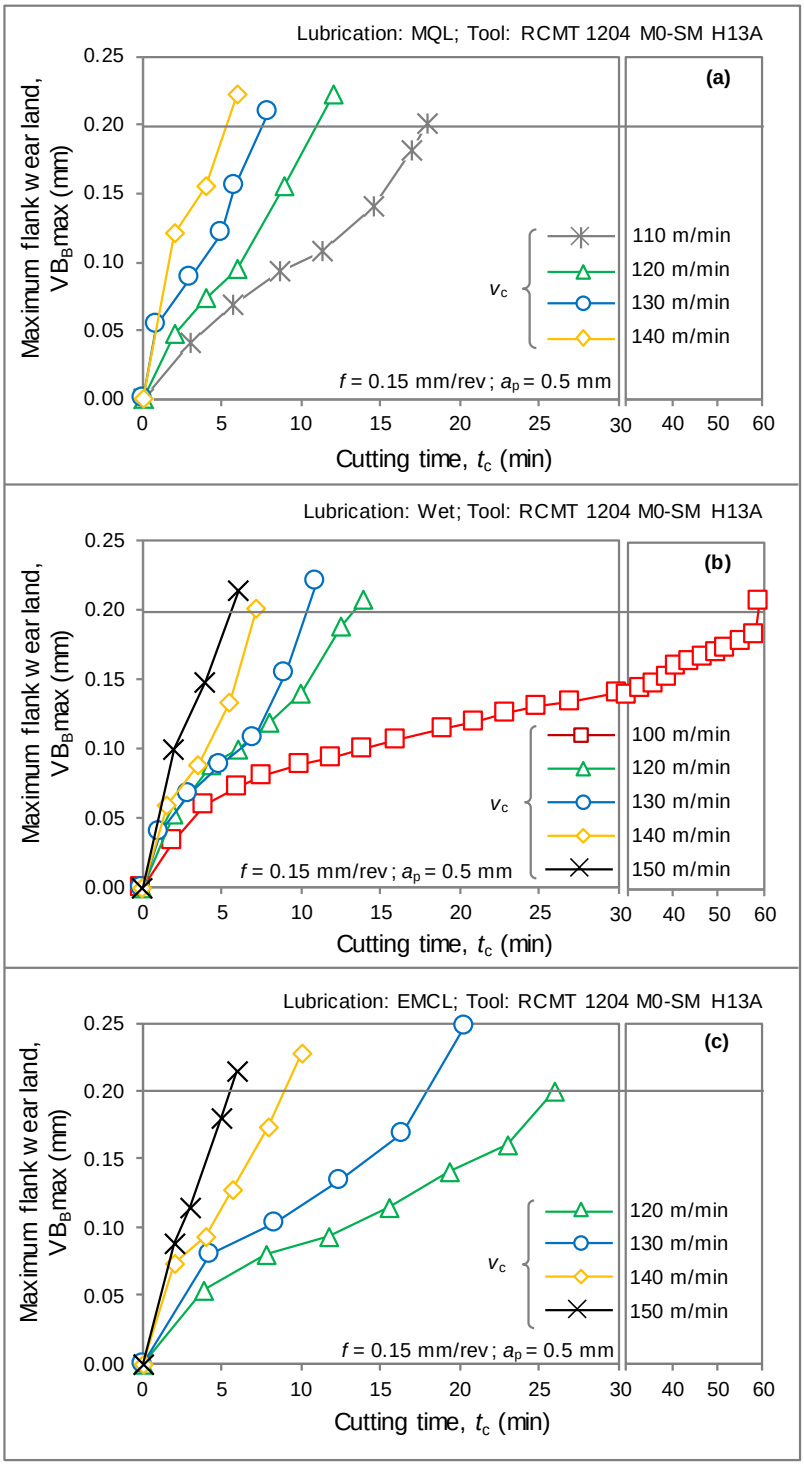

Figure 36. Typical tool wear curves for different lubrication/cooling conditions (MQL (a), Wet (b), EMCL (c)) when turning of Ti-6Al-4V at varying of cutting speed.

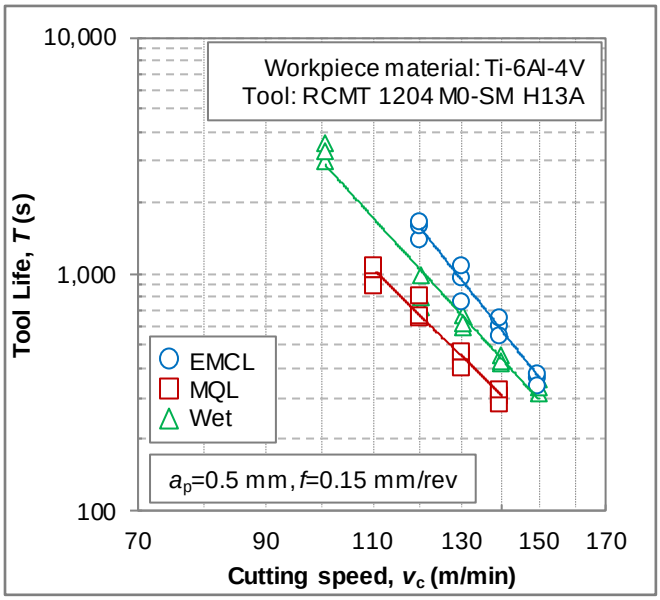

Figure 37. Taylor's curves when turning of Ti-6Al-4V under various lubrication conditions.

A constant value of k_0 was observed when turning of Ti-6Al-4V within the chosen range of cutting speeds and for each lubrication condition [Faga et al., 2017; Priarone et al., 2016]. This evidence is consistent with the results of Denkena et al. [2015], and Cotterell and Byrne [2008]. Nevertheless, k_0 was found to be higher when tool wear increased (Table 21). Values of k_0 vary between 3 and 5 J/mm^3 and are in agreement with those reported by Jeswiet and Kara [2008].

Table 21. k_0 (J/mm^3) as a function of tool wear progression (until reaching the tool wear limit of 0.2 mm for VB_Bmax) and lubrication condition [Priarone et al., 2016].

Lubrication	VB_Bmax ≅ 0.0 mm	VB_Bmax ≅ 0.1 mm	VB_Bmax ≅ 0.2 mm
Dry	2.69	3.07	3.70
Wet	2.59	3.30	4.10
MQL	2.70	3.06	3.72
EMCL	2.62	3.01	3.73

The models described in Chapter 2 were applied for computing the specific production indicators (SPT, SPC, SER, and SCE) for finish turning of Ti-6Al-4V at varying the MRR. All the data related to time, cost, energy, and carbon dioxide emission, which are listed in the inventory sections, have been used. Since the results of specific production indicators for dry turning of Ti-6Al-4V have been already presented in the previous case study (Section 4.3), in this section they are used only for the final comparison with the results of the other lubrication/cooling conditions (wet, MQL, and EMCL).

- Specific Production Time

The results of SPT for wet, MQL, and EMCL lubrication/cooling conditions are plotted in Figure 38. The three considered contributions (t_2/V, t_3/T/MRR, and τ_{CL}) are shown together with the SPT curve. The graphs are characterized by same trend observed for dry condition (Figure 29). In addition, the specific time required to cleaning operation (τ_{CL}) has been added for wet and EMCL lubrication/cooling conditions. This contribute shows a constant value that is almost negligible.

- Specific Production Cost

The results of SPC indicator are presented in Figure 39. The contributes C_2, C_3, C_4, C_6, and C_7 of the SPC indicator are plotted divided by the volume of material removed V. In addition, C_2 and SPC are shown for three different values of tool wear condition. However, the influence of tool wear condition on cost is negligible since the curves of C_2 and SPC for the three VB_Bmax conditions are overlapped. The costs related to cutting tool (either in term of the electricity cost due to tool change operation, or for the cost of the tool insert itself) become relevant when MRR increases. Cost related cutting fluid usage (C_6) is negligible, and also the cost for cleaning operation (C_7) is low compared to other contributes. However, part of the cost related to cutting fluids usage is inclusive in C_2 contribute due to the cost of amortization of the lubrication/cooling equipment and the cost for electricity demand of the same apparatus. Overall, the results are according to those reported by Klocke and Eisenblätter [1997] who estimated the cost for cooling lubricant in the range 7-17 % of the total manufacturing costs.

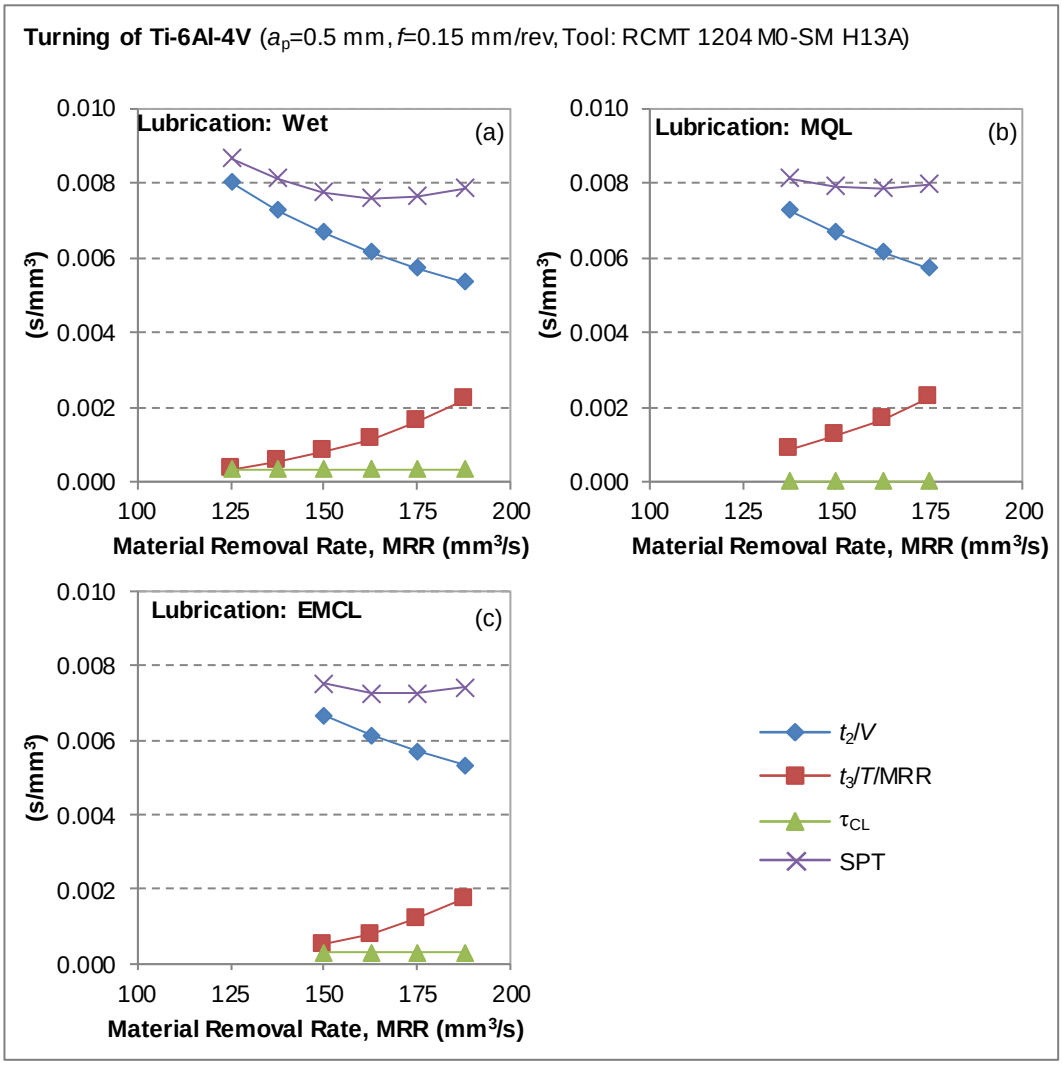

Figure 38. Specific Production Time and its contributions when turning of Ti-6Al-4V under different lubrication/cooling conditions: Wet (a), MQL (b), and EMCL (c).

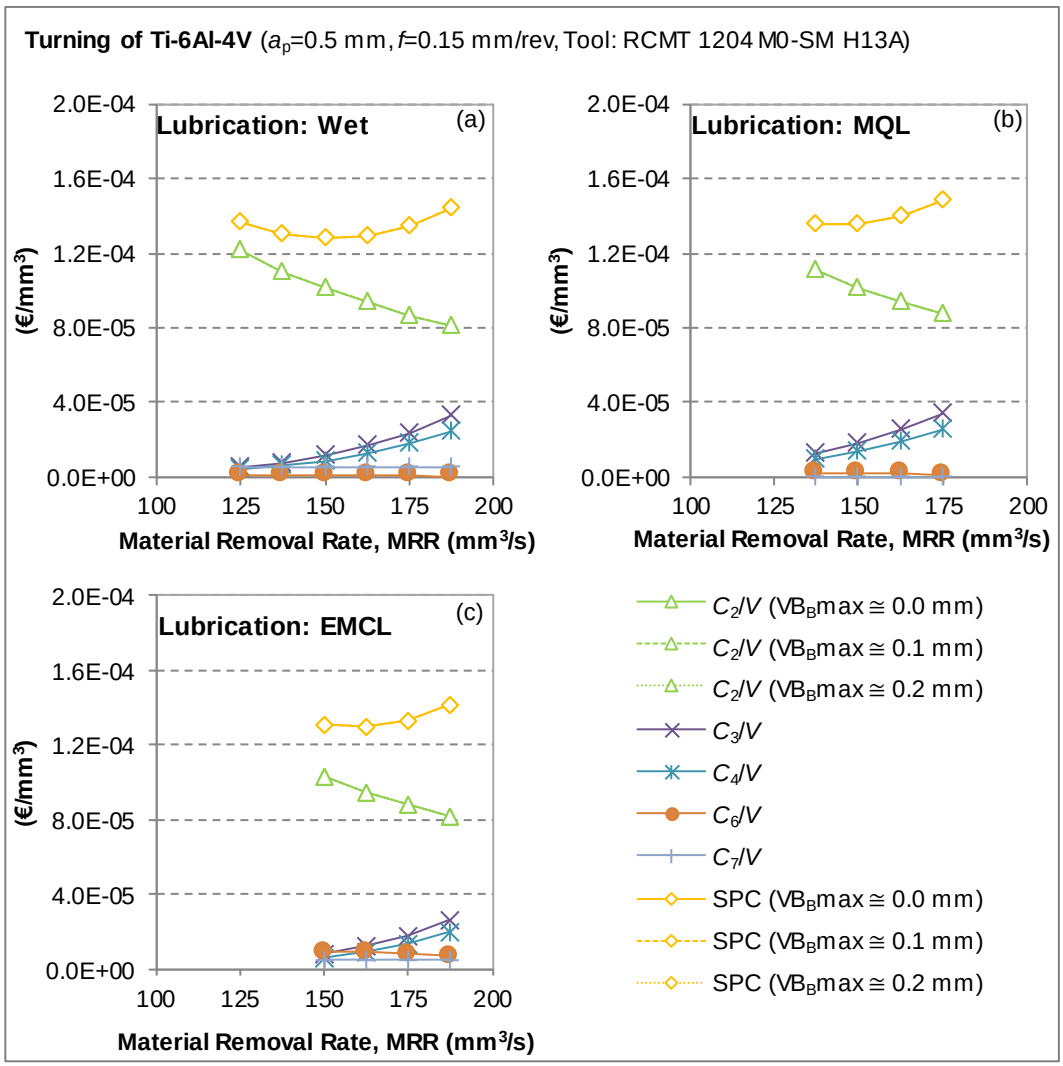

Figure 39. Specific Production Cost and its contributions when turning of Ti-6Al-4V under various lubrication/cooling conditions: Wet (a), MQL (b), and EMCL (c). Note: the curves for different $VB_B max$ are basically overlapped.

- Specific Energy Requirement

The Specific Energy Requirement indicator and its contributes are plotted in Figure 40. The primary energy demand due to electricity consumption (E_2/V) has the largest impact on SER especially at lower values of MRR. The specific energy requirement due to tool change operation (E_3/V) and cutting insert production (E_4/V) are comparable, while the contribute due to cutting fluid usage (E_6/V) shows a negligible influence on SER.

On the other hand, cleaning operation (E_7/V) represents an important contribute on the total energy demand. E_2/V and then SER are slightly influenced by the tool wear progression since the values for $VB_Bmax \cong 0.2$ mm are higher than those observed when using an unworn tool ($VB_Bmax \cong 0.0$ mm).

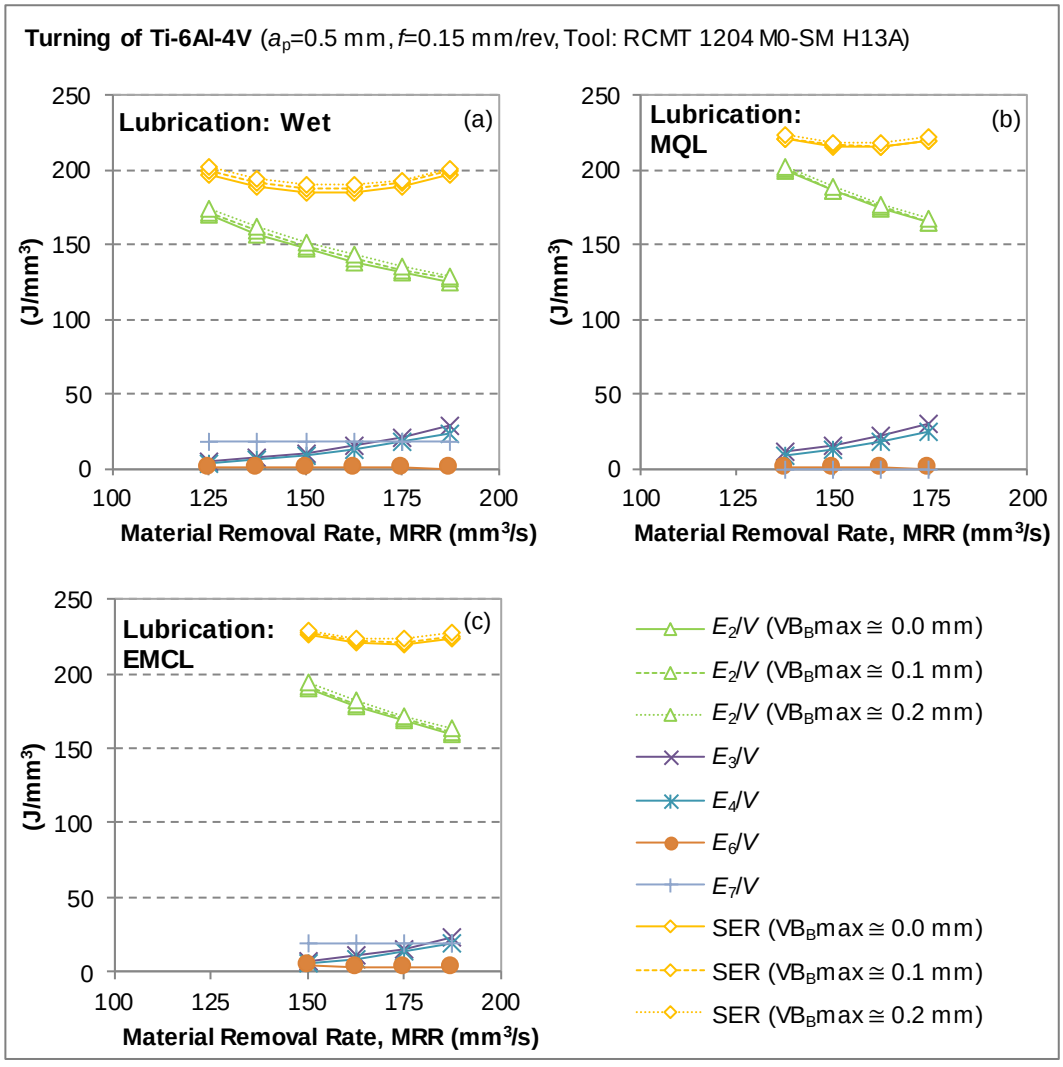

Figure 40. Specific Energy Requirement indicator and its contributions when turning of Ti-6Al-4V under various lubrication/cooling conditions: Wet (a), MQL (b), and EMCL (c).

- Specific Carbon Emission

The curves of Specific Carbon Emission (SCE) related to turning of Ti-6Al-4V under wet, MQL, and EMCL conditions are reported in the graphs of Figure 41. The results are similar to those of Specific Energy Requirement due to the correlation between primary energy demand and carbon footprint. However, the term (CE_4/V) related to carbon emission owing to the production of cutting tool shows a higher contribute on the total carbon emission with respect to that showed in term of primary energy. The increased influence of cutting tool on the total carbon emission implies the shift to the left of the minimum point of each SCE curve. Consequently, a reduced value of material removal rate is suggested for minimizing carbon footprint of the manufacturing phase.

Overall, Figure 42 is presented in order to compare the four lubrication/cooling conditions (including dry cutting) when turning of Ti-6Al-4V. Each specific production indicator is shown on a dedicated graph. EMCL lubrication condition highlights the best performance in terms of SPT (Figure 42-a) due to the highest allowed values of MRR and extended tool life when turning under this lubrication/cooling environment. Dry cutting shows the worst results in terms of SPT while MQL and wet conditions reach intermediate results.

Figure 42-b represents the comparison of SPC values. Wet cutting is estimated to be the cheapest solution immediately followed by EMCL. Dry cutting does not offer advantages in term of cost reduction even if cutting fluids are neglected. MQL leads to intermediate values of specific production cost.

Figure 42-c shows the results in terms of Specific Energy Requirement. Dry cutting lead to the lower primary energy demand due to the absence of cutting fluid which have to be applied to the cutting zone by an ancillary system. Therefore, both the reduced power consumption when machining and the absence of primary energy demand for the production of metalworking fluid enhanced the choice of dry cutting for reducing global energy requirements.

MQL and EMCL conditions appear to be the highest energy intensive strategies due to the air compressor consumption, which is estimated to be one of the most expensive utilities in an industrial facility [Dindorf, 2012]. The results of SER for wet cutting can be classified in an intermediate position with respect to those of dry, MQL and EMCL conditions.

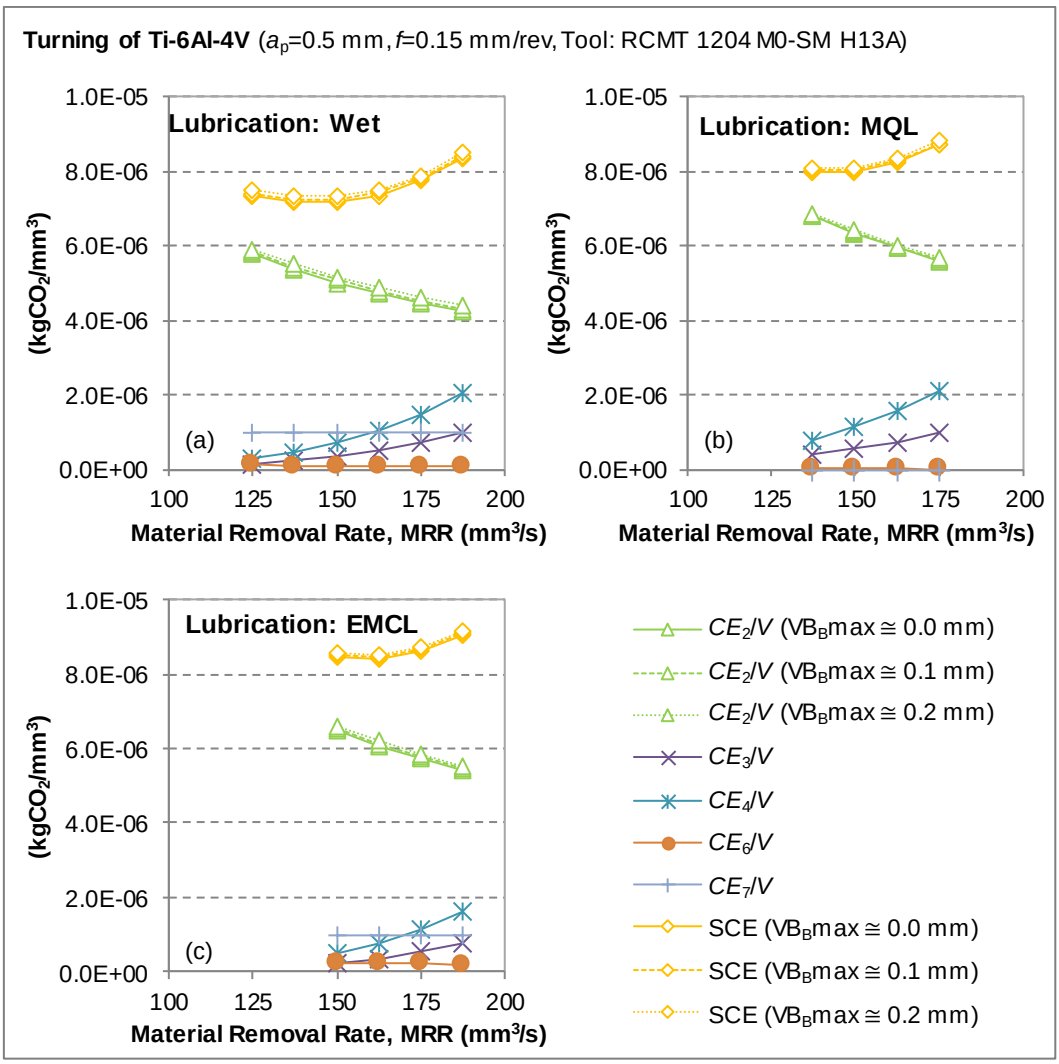

Figure 41. Specific Carbon Emission and its contributions when turning of Ti-6Al-4V under various lubrication/cooling condition: Wet (a), MQL (b), and EMCL (c).

The curves related to SCE for different cooling/lubrication conditions (Figure 42-d) show the same trend than those of SER, therefore the same conclusions can be made. However, the minimum of all curves is positioned at lower values of MRR for the reason discussed above regarding the carbon emission of cutting tools.

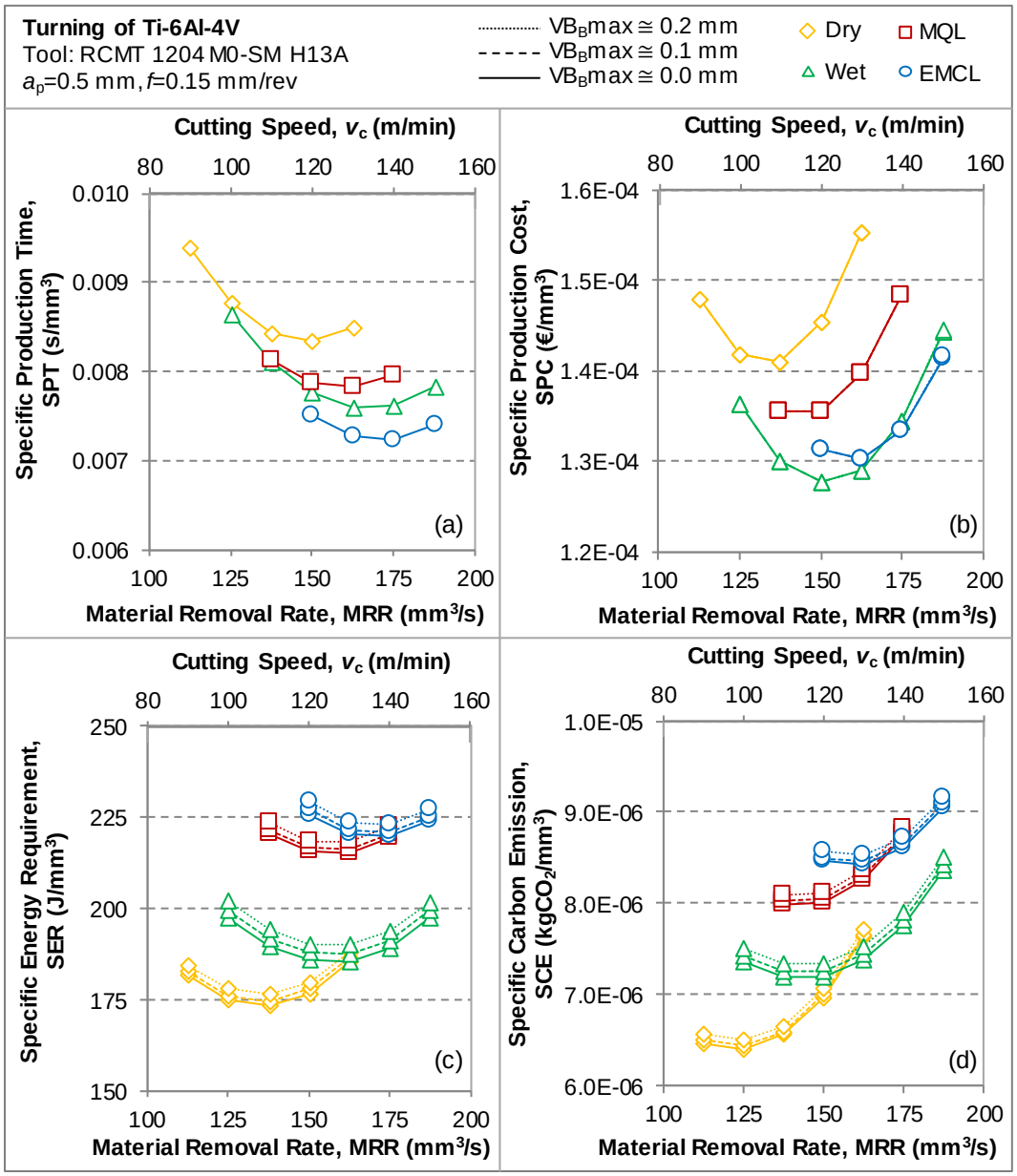

Figure 42. Specific production indicators (SPT (a), SPC (b), SER (c), and SCE (d)) when turning of Ti-6Al-4V under various lubrication/cooling condition. Note: the curves for SPC at different VB_Bmax are basically overlapped.

The curves of specific production indicators versus MRR show a minimum, therefore optimum cutting conditions can be identified for all the criteria and lubrication strategies. The box plots of Figure 43 reported each value of optimum cutting speed, for a specific lubrication/cooling condition, that allows to minimize

a single target among SPT, SPC, SER, and SCE. The range of optimum cutting speed identified for each lubrication strategy are represented in the box plot. This range falls inside the interval of cutting speeds tested during preliminary experiments (represented by a horizontal thin line). Each optimized range is enclosed between the optimal cutting speed identified by the minimum SCE criterion (lower limit) and the optimal cutting speed identified by the minimum SPT criterion (upper limit). The highest difference between SCE and SPT criterions in term of optimal cutting speed is around 20 %. In addition, the cutting speeds for trade-off criterion have been computed (by using Equation 2.37) for all the lubrication conditions when considering $k_{SPT} = k_{SPC} = k_{SER} = k_{SCE} = 0.25$, and are represented by a vertical purple line.

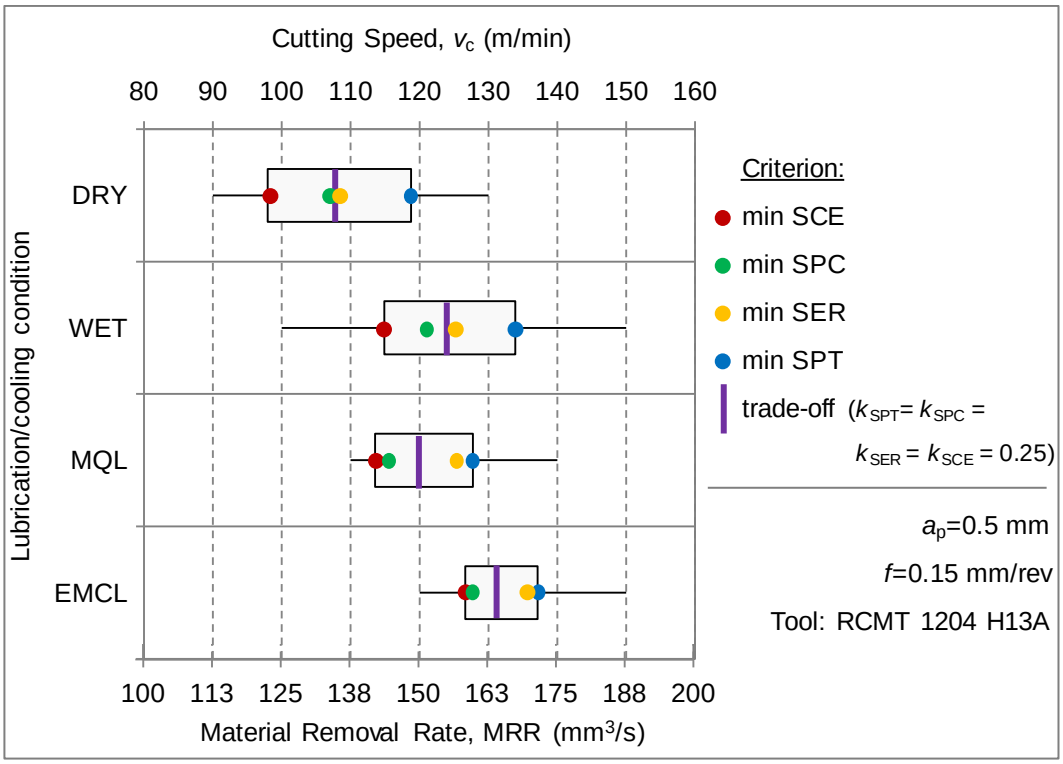

Figure 43. Identification of optimum values of MRR and cutting speed for various criteria and lubrication conditions.

Overall, the influence of lubricating/cooling condition on the process performance can be summarized by using the graphs of Figure 44 and Figure 45.

The graphs are prepared in order to consider simultaneously all the four specific production indicators (SPT, SPC, SER, and SCE) since they can be used as metric for the evaluation of the global process performance in term of productivity, cost, and environmental sustainability. The first graph (Figure 44) is prepared under the assumption that each point represented refers to the minimum value of the specific production indicator taken into account. In particular, the cutting speed used for the computation of each point is referred to the correspondent point showed in Figure 43 (with the colored points) according to the specific lubrication/cooling condition and optimization target accounted for. Therefore, each of the sixteen points represented in Figure 44 is computed with a specific value of cutting speed, which is a function of the considered lubrication/cooling condition and optimization target. On the other hand, the second graph (Figure 45) is obtained by considering the values of the specific production indicators computed with the trade-off cutting speed proper of each lubrication/cooling condition. In this way, the four indicators (SPT, SPC, SER, and SCE) computed for a single lubrication condition are referred to the same levels of process parameters. Therefore, the sixteen point represented are referred to only four different values of cutting speed, i.e. one for each lubricating/cooling condition.

Finally, the results reported in the two graphs are comparable and the same conclusion can be summarized as follows:

- Emulsion Mist Cooling Lubrication (EMCL) condition can be adopted when turning of Ti-6Al-4V for maximizing productivity since a lower specific production time is allowed. This result can be traced back to the better penetration of the cutting fluid into the wedge between tool and chip provided by the EMCL system. This lubrication/cooling condition was evaluated to give the best results in terms of tool life compared to other cutting conditions [Priarone et al., 2015]. The cutting fluid flow rate of the EMCL system is 115 ml/min which is two order of magnitude lower than that for wet cutting (10,000 ml/min). Nevertheless, the application of the emulsion in the form of mist environment is more effective than flood cooling (wet) lubrication.

- Wet cutting represents the cheapest strategy for minimizing the total manufacturing cost and this observation can be viewed as one of the reasons why conventional flood cooling is the *de facto* a standard for industrial production.

- Dry cutting is assessed as the most environmental sustainable choice due to the absence of metalworking fluids. On the contrary, MQL and EMCL do not appear to be advantageous solutions mainly due to the energy demand for compressed air usage. In addition, the consumption of cutting fluid of the EMCL system is 115 ml/min, which is the highest among the lubrication/conditions tested since the MQL equipment requires a cutting oil consumption of 0.3 ml/min, while the conventional (Wet) system needs an equivalent emulsion usage estimated equal to 7.9 ml/min (i.e., 1000 l per 2112 h).

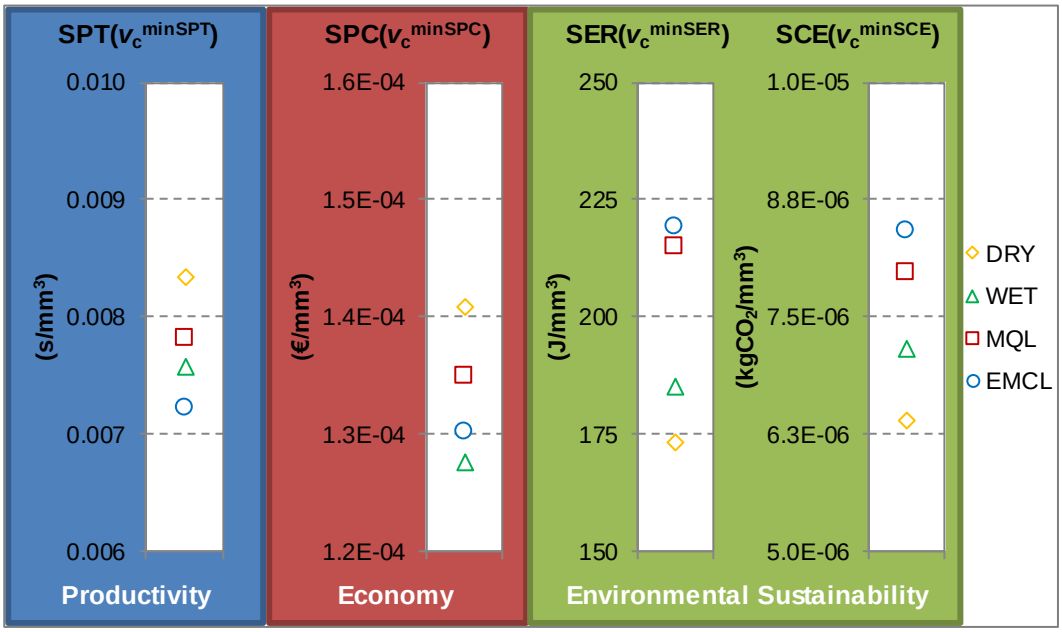

Figure 44. Influence of lubricating/cooling condition on productivity, economy, and environmental sustainability when turning Ti-6Al-4V at the cutting speed identified for each optimization criterion.

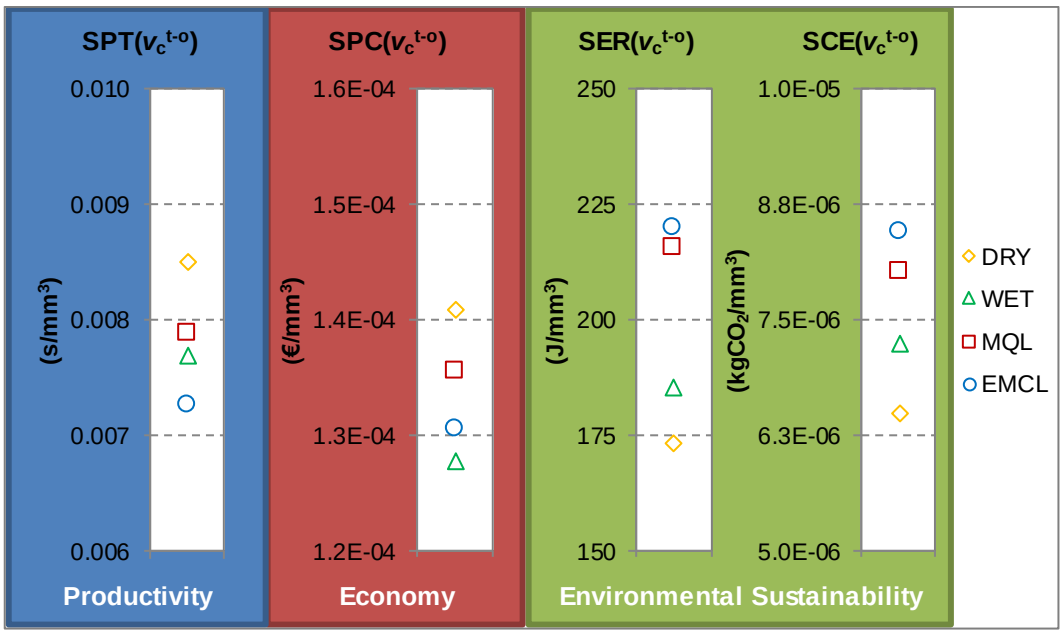

Figure 45. Influence of lubricating/cooling condition on productivity, economy, and environmental sustainability when turning Ti-6Al-4V at the cutting speed for trade-off criterion.

4.5. Conclusions of the case studies

Four case studies have been assessed by means of the developed models of specific production time, specific production cost, specific energy requirement, and specific carbon emission. The models can be considered as tools for decision making when several alternatives of machining are available. The case studies refer to the evaluation of machining performance when different (1) process parameters, (2) cutting tools, (3) workpiece materials, and (4) lubrication/cooling strategies are used. The machining performance, either in terms of economic or environmental sustainability, have been observed to be influenced by the four variables accounted for in each case study. Therefore, the optimization of a machining process, such as the single pass turning operation adopted in this thesis, is needed to improve its efficiency, which can be easily achieved by the correct tuning of the process variables as well as the proper selection of auxiliary systems and materials.

The first case study concerns the dry turning of Ti-48Al-2Cr-2Nb with RCMT 0803 cutting tool. The selection of process parameters such as depth of cut, feed, and cutting speed has been evaluated according to technological and quality targets, by means of an improved optimization method supported by the developed models. The result highlighted that, for a rough turning operation, improvements of productivity, economy, and environmental sustainability can be achieved at the same time by adopting the set of allowable process parameters which maximize the material removal rate without affecting too much the tool life. In particular, the maximum allowable feed and depth of cut, together with a lower cutting speed are needed to determine the best combination of process variables which satisfies a given tool life proper of a specific optimization target. However, lower feed and depth of cut, together with a higher cutting speed are the parameters suggested when finish machining due to the compliance of surface quality of the machined part.

The second case study compare the performance exhibited by two cutting tool having different diameters when dry turning of Ti-48Al-2Cr-2Nb. The indicators are computed at varying of the cutting speed and, therefore, of the material removal rate. The tool with the greatest diameter (RCMT 1204) is found to achieve the best performance. However, the results provided by the indicators highlighted slight differences compared to those achieved by the smaller tool (RCMT 0803) especially when the optimum cutting speed proper of each tool is selected.

The third case study focuses on the assessment of two workpiece materials (Ti-6Al-4V and Ti-48Al-2Cr-2Nb) when using RCMT 1204 cutting tool under dry condition. The indicators are computed at varying of the cutting speed and material removal rate. The results are deeply influenced by the workpiece material since this factor is proved to be a key factor in manufacturing. As a consequence, productivity, costs, and environmental impact become relevant when difficult-to-cut materials are accounted for. In particular, the machinability offered by titanium aluminides such as Ti-48Al-2Cr-2Nb is lower compared to that of conventional titanium alloys (Ti-6Al-4V) and this implies to work with reduced material removal rate in order to limit the tool wear. It is proved that the cost related to machining is dominant on the total manufacturing cost even when small amount of material has to be removed from a workpiece (i.e., in case of low buy-to-fly ratio). On the contrary, workpiece material plays a key role in the primary energy demand and carbon footprint due to its production phase before machining.

The fourth case study is aimed at the evaluation of four lubrication/cooling conditions (dry, wet, MQL, and EMCL) when turning of Ti-6Al-4V by using RCMT 1204 cutting tool at varying of cutting speed. The application of a lubrication/cooling method enables to machine with higher process parameters but requires the consumption of cutting fluids and additional power due to the presence of auxiliary systems. Emulsion Mist Cooling Lubrication (EMCL) is proved to represent the best strategy for maximizing productivity due to its positive influence on the tool life. Wet cutting seems to be the most economic condition, while dry cutting is assessed as the most environmental sustainable choice due to the absence of the issues related to the consumption of metalworking fluids and the usage of auxiliary systems.

Conclusions and outlooks

In recent years, the increase in energy demand and constraints in carbon emissions have forced policy makers to put pressure on industry sector in order to improve their process efficiency with respect to environmental sustainability. Therefore, energy saving has become not only an added value, but also a real priority for manufacturing sector in the era of Industry 4.0. Life-Cycle Assessment is a common practice for estimating the environmental impact of products during their life-cycle and it can be used more widely and easily if specific models are available and are focused on each life-cycle phase. In this thesis, the manufacturing phase of products, which are typically machined through material removal processes, is modelled by the development of several production indicators by enhancing bottom-up approaches. Both the economic efficiency and the environmental sustainability are accounted for when modelling the manufacturing phase. The Specific Production Time (SPT) is proposed as indicator of the manufacturing productivity; the Specific Production Cost (SPC) indicator is developed in order to quantify the direct and indirect costs related to the manufacturing process; finally, the Specific Energy Requirement (SER) and the Specific Carbon Emission (SCE) indices are proposed in order to assess the environmental sustainability of the manufacturing phases in terms of primary energy demand and carbon dioxide footprint, respectively. Energy demand, especially in the form of electricity energy vector, is an aspect of primary importance in the analysis of machining processes since machine tools are expected to require the largest portion of the total energy consumed for manufacturing a product. As a consequence, energy and CO_2 footprint are two metrics conventionally adopted for assessing the environmental stress due to machining processes. Moreover, they are related and are easy understandable. Energy is easy to be monitored since it can be measured with relative precision and can be suited as a proxy for the estimation of carbon dioxide footprint.

The proposed models are developed in order to be valid for conventional machining processes in which cutting tools with defined cutting edge are used. The models are tuned in order to express their output measures per unit of volume of material removed.

The Specific Production Time (SPT) index is composed by four contributes which account for the times needed for (1) the setup of the machine tool, (2) the machining operation, (3) the tool change operation(s), and (4) the activities related to swarf and part cleaning. The Specific Production Cost (SPC), the Specific Energy Requirement (SER), and the Specific Carbon Emission (SCE) indices are obtained as the sum of seven contributes. The first four contributes are linked to those accounted for by the SPT index, while the remaining three contributes concern the usage and consumption of cutting tool(s), metalworking fluid(s), and workpiece material. These last three contributes are usually omitted in most of the studied presented in literature. For this reason, the models proposed in this thesis are aimed to bridge this gap by implementing a comprehensive and well-structured approach for the evaluation of machining processes.

More in detail, the SPC index estimates the costs related to the usage of the machine tool and auxiliary systems including their amortization cost, the cost due to the electricity consumption during all the operations considered, and the hourly cost for the machine tool operator. In addition, the cost for buying cutting tool(s), metalworking fluid(s), and workpiece material are quantified. The SER index provides the estimation of the primary energy demand due to the electricity required by the machine tool and auxiliary systems, as well as the embodied energy owing to the production of cutting tool(s), metalworking fluid(s), and workpiece material. The SCE index is strictly related to the SER index since energy is a proxy for carbon dioxide footprint.

A peculiar aspect of the models is represented by the fact that they can be suited for the identification of optimum process parameters which allow to minimize a specific target among productivity (SPT), economic (SPT) and environmental sustainability (SER and SCE). In particular, an optimum tool life value can be computed for each optimization criterion as a function of constant values assumed by the characterization of the machine tool, the cutting tool, the metalworking fluid, and the workpiece material accounted for. As a consequence, optimum process parameters such as cutting speed can be selected with respect to respective optimum tool life.

The high-efficiency machining range is known in literature as the interval in which process parameters should be selected when considering the optimization in term of economic targets, i.e. related to the minimization of productive cost or production time. The development of the additional two models concerning the environmental sustainability is aimed at the redefinition of the conventional high-

efficiency machining range by including all the four optimization targets. As a consequence, the improved range is bounded by the identification of the four optimal cutting speeds (or material removal rates) that allow to minimize each production indicator. The obtainment of four different optimum cutting speed/tool life gave rise to the need to introduce a function for a rapid selection of the compromise among the different optimization criterions of time, cost, and environmental sustainability. Hence, a trade-off criterion is proposed and developed by the implementation of an innovative holistic function aimed at identifying a unique value of optimum cutting speed (or optimum tool life). This advanced optimization method is tuned also by the introduction of weighting factors which can assign different weights on each optimization target.

A deep analysis and collection of inventory data has been conducted in order to apply the developed models on four case studies. In particular, the case studies are referred to single pass turning operations and are presented in order to assess the influence of (1) process parameters, (2) cutting tool geometries, (3) workpiece materials, and (4) lubrication/cooling conditions onto the machining performance. The collected data concern the inventory of time, cost, primary energy demand, and carbon dioxide emission referred to each process, equipment, and consumable accounted for in the case studies. By means of the developed models, the two purposes outlined for each case study are (I) the quantification of the machining performance (in terms of SPC, SPC, SER, and SCE) between the examined factor of influence, and (II) the direct identification of process parameters which lead to the minimization of each production indicators.

The first case study investigates the influence of process parameters such as depth of cut, feed, and cutting speed on machining performance. The results refer to dry turning of Ti-48Al-2Cr-2Nb intermetallic alloy by using a RCMT 0803 carbide cutting tool. A method for identifying optimum cutting parameters is developed with respect to constraints related to machine tool, cutting tool, and workpiece surface quality/integrity. The selection of the maximum allowable depth of cut and feed is found to be an efficient strategy to minimize all the production indicators (SPT, SPC, SER, and SCE) when rough turning.

The second case study refers to the comparison of two tool geometries (RCMT 0803 and RCMT 1204) having different cutting diameters. The results concern the dry turning of Ti-48Al-2Cr-2Nb at varying of cutting speed and, as a consequence, of material removal rate within a range selected according to each tool geometry. The results of the production indicators highlighted by the 12-mm

tool are slightly better than those of 8-mm tool. Despite these differences, the minimum values of SPT, SPC, SER, and SCE indices are identified to be achieved when a similar cutting speed is used for both the tools.

The third case study concerns the comparison of two different titanium alloys (Ti-6Al-4V and Ti-48Al-2Cr-2Nb) which are known as difficult-to-cut materials. The results are referred to dry turning operations by using the RCMT 1204 tool geometry and are presented at varying of cutting speed/material removal rate within a range specifically chosen for each workpiece material. The results in terms of SPT, SPC, SER, and SCE reveal that the values computed for Ti-6Al-4V are one order of magnitude lower than those of Ti-48Al-2Cr-2Nb when comparing the best machining condition of both materials. Therefore, a proper selection of cutting speed is needed when turning of titanium alloys, especially in case of titanium aluminides which have to be machined at reduced production rates.

The fourth case study is focused onto the comparison of four different lubrication/cooling conditions such as dry, wet, Minimum Quantity Lubrication (MQL), and Emulsion Mist Cooling Lubrication (EMCL). The results are related to the turning of Ti-6Al-4V by using the RCMT 1204 tool geometry at varying of cutting speed/material removal rate within a range specifically chosen for each lubrication/cooling condition. The outcomes revealed that a lubrication/cooling condition that offers simultaneously the best performance measured by all the indicators does not exist. In particular, the best results of SPT index are achieved by the EMCL, the wet cooling condition provides the best results in terms of SPC, while the environmental stress measured by SER and SCE indices is minimized under dry cutting condition. The identification of optimum cutting speed is given for all the lubrication/cooling conditions.

In conclusion, in this thesis, a methodology for the assessment of the manufacturing phase of products is proposed by the development of production indicators. Productivity as well as economic and environmental sustainability are considered as metrics for the process assessment. The developed models are implemented as decision-support tools for the direct identification of optimized machining parameters. Future research activities should be oriented on the comparison, in terms of Life-Cycle Assessment, of products obtained by different manufacturing strategies such as those offered by additive processes or advanced hybrid systems. The presented machining optimization could be also integrated with advance simulation of part cutting operations in virtual environments.

References

Alvarez MEP, Bárcena MM, González FA. On the sustainability of machining processes. Proposal for a unified framework through the triple bottom-line from an understanding review. Journal of Cleaner Production (In press) pp. 15, dx.doi.org/10.1016/j.jclepro.2016.10.071.

Altintas Y, Kersting P, Biermann D, Budak E, Denkena B, Lazoglu I. Virtual process systems for part machining operations. CIRP Annals - Manufacturing Technology 63 (2014) 585-605.

Anderberg E, Kara S, Beno T. Impact of energy efficiency on computer numerically controlled machining. Proceedings of the Institution of Mechanical Engineers, Part B: Journal of Engineering Manufacture 224/4 (2010) 531-541.

Anderson J, Shier D, Steele K. The Green Guide to Specification - An Environmental Profiling System for Building Materials and Components. Blackwell Science Publishing (2009) fourth edition, Oxford, UK.

Aramcharoen A, Mativenga PT. Critical factors in energy demand modelling for CNC milling and impact of toolpath strategy. Journal of Cleaner Production 78 (2014) 63-74.

Arvidsson R, Svanström M. A Framework for Energy Use Indicators and Their Reporting in Life Cycle Assessment. Integrated Environmental Assessment and Management 12/3 (2015) 429-436.

Arrazola PJ, Özel T, Umbrello D, Davies M, Jawahir IS. Recent advances in modelling of metal machining processes. CIRP Annals - Manufacturing Technology 62 (2013) 695-718.

Arsecularatne JA, Hinduja S, Barrow G. Optimum cutting conditions for turned components. Proceedings of Institution of Mechanical Engineers 206/B2 (1992) 15-31.

Ashby MF. Materials and the Environment (Second Edition)- Eco-Informed Material Choice. Butterworth Heinemann (2013) ISBN 978-0-12-385971-6.

Aspinwall DK, Dewes RC, Mantle AL. The Machining of γ-TiAl Intermetallic Alloys. CIRP Annals - Manufacturing Technology 54/1 (2005) 99-104.

Aurich JC, Linke B, Hauschild M, Carrella M, Kirsch B. Sustainability of abrasive processes. CIRP Annals - Manufacturing Technology 62/2 (2013) 653-672.

Azkarate A, Ricondo I, Pérez A, Martínez P. An assessment method and design support system for designing sustainable machine tools. Journal of Engineering Design 22/3 (2011) 165-179, dx.doi.org/10.1080/09544820903153570.

Balogun VA, Mativenga PT. Modelling of direct energy requirements in mechanical machining processes. Journal of Cleaner Production 41 (2013) 179-186.

Baykasoğlu A, Ozsoydan FB. Minimizing tool switching and indexing times with tool duplications in automatic machines. International Journal of Advance Manufacturing Technology (2016) pp. 15, dx.doi.org/10.1007/s00170-016-9194-z.

Behrendt T, Zein A, Min S. Development of an energy consumption monitoring procedure for machine tools. CIRP Annals - Manufacturing Technology 61 (2012) 43-46.

Beranoagirre A, Olvera D, Urbicain G, López de Lacalle LN, Lamikiz A. Hole making in gamma TiAl. Chapter 32 in DAAAM International Scientific Book 2010, pp. 337-346, B. Katalinic (Ed.).

Brander M, Sood A, Wylie C, Haughton A, Lovell J. Electricity-specific emission factors for grid electricity. Ecometrica Technical Paper (2011) pp.22.

Brinksmeier E, Meyer D, Huesmann-Cordes AG, Herrmann C. Metalworking fluids—Mechanisms and performance. CIRP Annals - Manufacturing Technology 64/2 (2015) 605-628.

Calvanese ML, Albertelli P, Matta A, Taisch M. Analysis of Energy Consumption in CNC Machining Centers and Determination of Optimal Cutting

Conditions. Proceeding of 20th CIRP International Conference on Life Cycle Engineering, Singapore 2013, pp. 227-232.

Campatelli G, Lorenzini L, Scippa A. Optimization of process parameters using a Response Surface Method for minimizing power consumption in the milling of carbon steel. Journal of Cleaner Production 66 (2014) 309-316.

Cao H, Li H, Cheng H, Luo Y, Yin R, Chen Y. A carbon efficiency approach for life-cycle carbon emission characteristics of machine tools. Journal of Cleaner Production 37 (2012) 19-28.

Childs T, Maekawa K, Obikawa T, Yamane Y. Metal Machining - Theory and Applications. 2000 Arnold - Hodder Headline Group, London, 2000.

Cotterell M, Byrne G. Dynamics of chip formation during orthogonal cutting of titanium alloy Ti-6Al-4V. CIRP Annals - Manufacturing Technology 57 (2008) 93-96.

Dahmus JB, Gutowski TG. An Environmental Analysis of Machining. Proceedings of IMECE2004 (2004) ASME International Mechanical Engineering Congress and RD&D Expo November 13-19, 2004, Anaheim, California USA, pp. 10.

Deiab I, Raza SW, Pervaiz S. Analysis of Lubrication Strategies for Sustainable Machining during Turning of Titanium Ti-6Al-4V alloy. Procedia CIRP 17 (2014) 766-771.

Denkena B, Helmecke P, Hülsemeyer L. Energy efficient machining of Ti-6Al-4V. CIRP Annals - Manufacturing Technology 64 (2015) 61-64.

Diaz N, Choi S, Helu M, Chen Y, Jayanathan S, Yasui Y, Kong D, Pavanaskar S, Dornfeld D. Machine Tool Design and Operation Strategies for Green Manufacturing. Proceedings of 4th CIRP International Conference on High Performance Cutting (2010) pp.10.

Diaz N, Redelsheimer E, Dornfeld D. Energy Consumption Characterization and Reduction Strategies for Milling Machine Tool Use. Glocalized Solutions for Sustainability in Manufacturing: Proceedings of the 18th CIRP International Conference on Life Cycle Engineering, Technische Universität

Braunschweig, Braunschweig, Germany, May 2nd - 4th, 2011, DOI 10.1007/978-3-642-19692-8.

Dindorf R. Estimating Potential Energy Savings in Compressed Air Systems. Procedia Engineering 39 (2012) 204-211.

Dornfeld DA, Green Manufacturing - Fundamentals and Applications. Springer, New York (2013).

Draganescu F, Gheorghe M, Doicin CV. Models of machine tool efficiency and specific consumed energy. Journal of Materials Processing Technology 141 (2003) 9-15.

Duflou JR, Sutherland JW, Dornfeld D, Herrmann C, Jeswiet J, Kara S, Hauschild M, Kellens K. Towards energy and resource efficient manufacturing: A processes and systems approach. CIRP Annals - Manufacturing Technology 61 (2012) 587–609.

Eskicioğlu AM, Eskicioğlu H. Application of three non-linear programming techniques in optimizing machining conditions. Proceedings of the Institution of Mechanical Engineers, Part B: Journal of Engineering Manufacture 206/3 (1992) 183-189.

Eurostat database (2016) table of electricity prices by type of user: medium size industries, http://ec.europa.eu/eurostat/tgm/table.do?tab=table&init=1&plugin=1&language=en&pcode=ten00117 (accessed on January 22, 2016).

Fluke 430 Series II - Technical data sheet, http://media.fluke.com/documents/2643006_6112_ENG_D_W.PDF (accessed on December 7, 2016).

Frischknecht R, Wyss F, Knöpfel SB, Lützkendorf T, Balouktsi M. Cumulative energy demand in LCA: the energy harvested approach. International Journal of Life Cycle Assessment 20 (2015) 957-969.

Gabriel M, Pessl E. Industry 4.0 and Sustainability Impacts: Critical Discussion of Sustainability Aspects with a Special Focus on Future of Work and Ecological Consequences. Annals of the Faculty of Engineering Hunedoara14/2 (2016) 131-136.

Garbie I. Sustainability in Manufacturing Enterprises - Concepts, Analyses and Assessments for Industry 4.0. Green Energy and Technology, Springer, Switzerland (2016).

Gonzalez A. Machine Tool Utilisation Phase: Costs and Environmental Impacts with a Life Cycle View. Master of Science Thesis presented at the Industrial Ecology Royal Institute of Technology, Stockholm (2007).

Guo Y, Duflou JR, Qian J, Tang H, Lauwers B. An operation-mode based simulation approach to enhance the energy conservation of machine tools. Journal of Cleaner Production 101 (2015) 348-359.

Guo Y, Loenders J, Duflou J, Lauwers B. Optimization of energy consumption and surface quality in finish turning. Procedia CIRP 1 (2012) 512-517.

Gutowski T, Dahmus J, Thiriez A. Electrical Energy Requirements for Manufacturing Processes. Proceeding of 13th CIRP International Conference of Life Cycle Engineering, Lueven, May 31st - June 2nd, 2006, pp. 5.

He Y, Li Y, Wu T, Sutherland JW. An energy-responsive optimization method for machine tool selection and operation sequence in flexible machining job shops. Journal of Cleaner Production 87 (2015) 245-254.

Hinduja S, Petty DJ, Tester M, Barrow G. Calculation of optimum cutting conditions for turning operations. Proceedings of Institution of Mechanical Engineers 199/B2 (1985) 81-92.

Ingarao G. Manufacturing strategies for efficiency in energy and resources use: The role of metal shaping processes. Journal of Cleaner Production 142 (2017) 2872-2886.

Ingarao G, Priarone PC, Gagliardi F, Di Lorenzo R, Settineri L. Subtractive versus mass conserving metal shaping technologies: an environmental impact comparison. Journal of Cleaner Production 87 (2015) 862-873.

IPCC, 2014: Climate Change 2014: Synthesis Report. Contribution of Working Groups I, II and III to the Fifth Assessment Report of the Intergovernmental Panel on Climate Change [Core Writing Team, R.K. Pachauri and L.A. Meyer (eds.)]. IPCC, Geneva, Switzerland, 151 pp.

ISO 14040:2006, Environmental management - Life cycle assessment - Principles and framework.

ISO 14044:2006, Environmental management - Life cycle assessment - Requirements and guidelines.

Jayal AD, Badurdeen F, Dillon Jr OW, Jawahir IS. Sustainable manufacturing: Modeling and optimization challenges at the product, process and system levels. CIRP Journal of Manufacturing Science and Technology 2 (2010) 144-152.

Jeswiet J, Kara S. Carbon emissions and CES^{TM} in manufacturing. CIRP Annals - Manufacturing Technology 57 (2008) 17-20.

Kalpakjian, S, Schmid, SR. Manufacturing Engineering and Technology. Pearson, sixth ed. (2009).

Kara S, Li W. Unit process energy consumption models for material removal processes. CIRP Annals - Manufacturing Technology 60/1 (2011) 37-40.

Katiyar PK, Randhawa NS, Hait J, Jana RK, Singh KK, Mankhand TR. An overview on different processes for recovery of valuable metals from tungsten carbide scrap. International Conference on Nonferrous Materials and Metals (ICNFMM), Jul 2014, Nagpur.

Kellens K. Energy and Resource Efficient Manufacturing - Unit process analysis and optimisation. PhD thesis, KU Leuven, December 2013, pp. 249, ISBN 978-94-6018-765-0.

Klocke F, Döbbeler B, Binder M, Kramer N, Grüter R, Lung D. Ecological evaluation of PVD and CVD coating systems in metal cutting processes. Proceedings of the 11th Global Conference on Sustainable Manufacturing (GCSM) - Innovative Solutions, September 23-25, 2013, Berlin, (2013a) 381-386.

Klocke F, Eisenblätter G. Dry Cutting. CIRP Annals - Manufacturing Technology 46/2 (1997) 519-526.

Klocke F, Lung D, Arft M, Priarone PC, Settineri L. On high-speed turning of a third-generation gamma titanium aluminide. The International Journal of Advanced Manufacturing Technology 65 (2013b) 155-163.

Kong D, Choi S, Yasui Y, Pavanaskar S, Dornfeld D, Wright P. Software-based tool path evaluation for environmental sustainability. Journal of Manufacturing Systems 30 (2011) 241-247.

Kwon Y, Fischer GW. A novel approach to quantifying tool wear and tool life measurements for optimal tool management. International Journal of Machine Tools & Manufacture 43 (2003) 359-368.

Li C, Tang Y, Cui L, Li P. A quantitative approach to analyze carbon emissions of CNC-based machining systems. Journal of Intelligent Manufacturing 26 (2015) 911-922.

Li L, Yan J, Xing Z. Energy requirements evaluation of milling machines based on thermal equilibrium and empirical modelling. Journal of Cleaner Production 52 (2013) 113-121.

Li W, Kara S. An empirical model for predicting energy consumption of manufacturing processes: a case of turning process. Proceedings of the Institution of Mechanical Engineers, Part B: Journal of Engineering Manufacture 225/9 (2011) 1636-1646.

Lin W, Yu DY, Wang S, Zhang C, Zhang S, Tian H, Luo M, Liu S. Multi-objective teaching–learning-based optimization algorithm for reducing carbon emissions and operation time in turning operations. Engineering Optimization 47/7 (2015) 994-1007, dx.doi.org/10.1080/0305215X.2014.928818.

Lin W, Yu D, Zhang C, Zhang S, Tian Y, Liu S, Luo M. Multi-objective optimization of machining parameters in multi-pass turning operations for low-carbon manufacturing. Proceedings of the Institution of Mechanical Engineers, Part B: Journal of Engineering Manufacture (2016) pp.12, http://dx.doi.org/10.1177/0954405416629098.

Liu F, Xie J, Liu S. A method for predicting the energy consumption of the main driving system of a machine tool in a machining process. Journal of Cleaner Production 105 (2015) 171-177.

Liu N, Zhang YF, Lu WF. A hybrid approach to energy consumption modelling based on cutting power: a milling case. Journal of Cleaner Production 104 (2015) 264-272.

Liu ZY, Guo YB, Sealy MP, Liu ZQ. Energy consumption and process sustainability of hard milling with tool wear progression. Journal of Materials Processing Technology 229 (2016) 305-312.

Manyika J, Chui M, Bughin J, Dobbs R, Bisson P, Marrs A. Disruptive technologies: Advances that will transform life, business, and the global economy. McKinsey Global Institute, May 2013.

Mativenga PT, Rajemi MF. Calculation of optimum cutting parameters based on minimum energy footprint. CIRP Annals - Manufacturing Technology 60 (2011) 149-152.

McManus MC, Hammond GP, Burrows CR. Life-Cycle Assessment of Mineral and Rapeseed Oil in Mobile Hydraulic Systems. Journal of Industrial Ecology 7 (2003) 163-177.

Meng Q, Arsecularatne JA, Mathew P. Calculation of optimum cutting conditions for turning operations using a machining theory. International Journal of Machine Tools & Manufacture 40 (2000) 1709-1733.

Meyer R, Kohler J, Denkena B. Influence of the tool corner radius on the tool wear and process forces during hard turning. The International Journal of Advanced Manufacturing Technology 58 (2012) 933-940.

Moradnazhad M, Unver HO. Energy efficiency of machining operations: A review. Proc IMechE Part B: J Engineering Manufacture (2016) 1-19, DOI: 10.1177/0954405415619345.

Mori M, Fujishima M, Inamasu Y, Oda Y. A study on energy efficiency improvement for machine tools. CIRP Annals - Manufacturing Technology 60 (2011) 145-148.

Patel M. Cumulative energy demand (CED) and cumulative CO_2 emissions for products of the organic chemical industry. Energy 28 (2003) 721-740.

Pramanik A. Problems and solutions in machining of titanium alloys. International Journal of Advance Manufacturing Technology 70 (2014) 919-928.

Priarone PC, Rizzuti S, Ruffa S, Settineri L. Drilling experiments on a gamma titanium aluminide obtained via electron beam melting. International Journal of Advance Manufacturing Technology 69 (2013) 483-490.

Pusavec F, Kramar D, Krajnik P, Kopac J. Transitioning to sustainable production - part II: evaluation of sustainable machining technologies. Journal of Cleaner Production 18 (2010a) 1211-1221.

Pusavec F, Kramar D, Krajnik P, Kopac J. Transitioning to sustainable production - part I: Application on machining technologies. Journal of Cleaner Production 18 (2010b) 174-184.

Qian M, Froes FHS. Titanium Powder Metallurgy: Science, Technology and Applications. First edition, 2015, Butterworth-Heinemann (Elsevier).

Rajemi MF, Mativenga PT, Aramcharoen A. Sustainable machining: selection of optimum turning conditions based on minimum energy considerations. Journal of Cleaner Production 18 (2010) 1059-1065.

Sala S, Vasta A, Mancini L, Dewulf J, Rosenbaum E. Social Life Cycle Assessment - State of the art and challenges for supporting product policies. European Commission, Joint Research Centre, Institute for Environment and Sustainability, Publications Office of the European Union, Luxemburg, 2015.

Santos JP, Oliveira M, Almeida FG, Pereira JP, Reis A. Improving the environmental performance of machine-tools: influence of technology and throughput on the electrical energy consumption of a press-brake. Journal of Cleaner Production 19 (2011) 356-364.

Schultheiss F, Hägglund S, Ståhl J-E. Modeling the cost of varying surface finish demands during longitudinal turning operations. International Journal of Advance Manufacturing Technology 84 (2016) 1103-1114.

Seow Y, Goffin N, Rahimifard S, Woolley E. A 'Design for Energy Minimization' approach to reduce energy consumption during the manufacturing phase. Energy 109 (2016) 894-905.

Sharman ARC, Aspinwall DK, Dewes RC, Bowen P. Workpiece surface integrity considerations when finish turning gamma titanium aluminide. Wear 249 (2001) 473-481.

Shashidhara YM, Jayaram SR. Vegetable oils as a potential cutting fluid-An evolution. Tribology International 43/5-6 (2010) 1073-1081.

Stock T, Seliger G. Opportunities of Sustainable Manufacturing in Industry 4.0. Procedia CIRP 40 (2016) 536-541.

Sutherland JW, Richter JS, Hutchins MJ, Dornfeld D, Dzombak R, Mangold J, Robinson S, Hauschild MZ, Bonou A, Schoensleben P, Friemann F. The role of manufacturing in affecting the social dimension of sustainability. CIRP Annals - Manufacturing Technology 65 (2016) 689-712.

Tang Y, Mak K, Zhao YF. A framework to reduce product environmental impact through design optimization for additive manufacturing. Journal of Cleaner Production (2016) pp. 13, http://dx.doi.org/10.1016/j.jclepro.2016.06.037.

Terna. Synthesis Report (in Italian) - Nota di sintesi "Dati statistici sull'energia elettrica in Italia - 2014" (2015) pp. 5.

Trentesaux D, Borangiu T, Thomas A. Emerging ICT concepts for smart, safe and sustainable industrial systems. Computers in Industry 81 (2016) 1-10.

Velchev S, Kolev I, Ivanov K, Gechevski S. Empirical models for specific energy consumption and optimization of cutting parameters for minimizing energy consumption during turning. Journal of Cleaner Production 80 (2014) 139-149.

Wang Q, Liu F, Li C. An integrated method for assessing the energy efficiency of machining workshop. Journal of Cleaner Production 52 (2013) 122-133.

Watson JK, Taminger KMB. A decision-support model for selecting additive manufacturing versus subtractive manufacturing based on energy consumption. Journal of Cleaner Production (2016), doi:10.1016/j.jclepro.2015.12.009.

Weinert N, Chiotellis S, Seliger G. Methodology for planning and operating energy-efficient production systems. CIRP Annals - Manufacturing Technology 60 (2011) 41-44.

Yi Q, Tang Y, Li C, Li P. Optimization of CNC Machine Processing Parameters for Low Carbon Manufacturing. 2013 IEEE International Conference on Automation Science and Engineering (CASE), pp. 498-503, dx.doi.org/10.1109/CoASE.2013.6654011.

Yan J, Li L. Multi-objective optimization of milling parameters - the trade-offs between energy, production rate and cutting quality. Journal of Cleaner Production 52 (2013) 462-471.

Yoon H-S, Moon J-S, Pham M-Q, Lee G-B, Ahn S-H. Control of machining parameters for energy and cost savings in micro-scale drilling of PCBs. Journal of Cleaner Production 54 (2013) 41-48.

Yoon H-S, Lee J-Y, Kim M-S, Ahn S-H. Empirical power-consumption model for material removal in three-axis milling. Journal of Cleaner Production 78 (2014) 54-62.

Yoon H-S, Kim E-S, Kim M-S, Lee J-Y, Lee G-B, Ahn S-H. Towards greener machine tools - A review on energy saving strategies and technologies. Renewable and Sustainable Energy Reviews 48 (2015) 870-891.

Zhong Q., Tang R., Lv J., Jia S., Jin M. Evaluation on models of calculating energy consumption in metal cutting processes: a case of external turning process. Int. J. Adv. Manuf. Technol. 82 (2016) 2087-2099.

Zhou L, Li J, Li F, Meng Q, Li J, Xu X. Energy consumption model and energy efficiency of machine tools: a comprehensive literature review. Journal of Cleaner Production 112 (2016) 3721-3734.

Paper published by the Author

Faga MG, Priarone PC, **Robiglio M**, Settineri L, Tebaldo V. Technological and sustainability implications of dry, near-dry, and wet turning of Ti-6Al-4V alloy. International Journal of Precision Engineering and Manufacturing - Green Technology 4/2 (2017) 129-139.

Loglisci G, **Robiglio M**, Priarone PC, Settineri L. La sostenibilità di un processo produttivo. Utensili e Attrezzature (Ed. Tecniche Nuove) Vol. 6 (2014a) 18-21.

Loglisci G, **Robiglio M**, Priarone PC, Settineri L. Sostenibilità: metodi di analisi e indicatori. Utensili e Attrezzature (Ed. Tecniche Nuove) Vol. 4 (2014b) 16-19.

Priarone PC, **Robiglio M**, Ingarao G, Settineri L. Assessment of cost and energy requirements of Electron Beam Melting (EBM) and machining processes. G. Campana et al. (eds.), Sustainable Design and Manufacturing 2017, Smart Innovation, Systems and Technologies 68, Springer International Publishing AG 2017, pp. 723-735, DOI 10.1007/978-3-319-57078-5_65.

Priarone PC, **Robiglio M**, Settineri L, Tebaldo V. Effectiveness of minimizing cutting fluid use when turning difficult-to-cut alloys. Procedia CIRP 29 (2015) 341-346.

Priarone PC, **Robiglio M**, Settineri L, Tebaldo V. Milling and turning of titanium aluminides by using minimum quantity lubrication. Procedia CIRP 24 (2014) 62-67.

Priarone PC, **Robiglio M**, Settineri L, Tebaldo V. Modelling of specific energy requirements in machining as a function of tool and lubricoolant usage. CIRP Annals - Manufacturing Technology 65 (2016b) 25-28.